IOWA STATE UNIVERSITY
Digital Repository

2015

Development of gold nanoparticle-based antigen delivery platform for vaccines against HIV-1

Feng Lin
Iowa State University

Follow this and additional works at: https://lib.dr.iastate.edu/etd

Part of the Allergy and Immunology Commons, Immunology and Infectious Disease Commons, Medical Immunology Commons, Nanoscience and Nanotechnology Commons, and the Virology Commons

Development of gold nanoparticle-based antigen delivery platform for vaccines against HIV-1

by

Feng Lin

A dissertation submitted to the graduate faculty

in partial fulfillment of the requirements for the degree of

DOCTOR OF PHILOSOPHY

Major: Genetics

Program of Study Committee:
Michael Cho, Major Professor
Diane Birt
Drena Dobbs
Lisa Nolan
Qijing Zhang

Iowa State University

Ames, Iowa

2015

TABLE OF CONTENTS

LIST OF FIGURES

LIST OF TABLES

ACKNOWLEDGMENTS

I would like to thank my mentor, Michael Cho, for introducing me into such an amazing research field. I cannot make to this step without his continuous support and guidance. I would also like to thank my committee members, Diane Birt, Drena Dobbs, Lisa Nolan and Qijing Zhang, for their critiques and advises on my research projects. I would like to express my gratitude to all my lab members. They all make my research life more colorful and joyful. My special thanks are given to the senior members of the lab, Yali Qin, Habtom Habte and Marisa Banasik. I have learned a lot from them, and their achievements and successes have always been my motivation to fight for a brighter future.

My deepest gratitude is to my Mother and Father, Honglan Yang and Ligui Lin. As the only child of the family, I can always feel their unconditional love no matter where I am in the world. I would like to dedicate all my work to them for their selfless support from the other side of Pacific Ocean.

ABSTRACT

As one of the world's most devastating viruses, HIV-1 has killed more than 39 million people, and around two million cases of newly infected individuals are recorded every year. However, no effective vaccine has been developed to stop this pandemic since its onset in the 1980s. Since vaccine development is moving slowly, delivery platforms as an essential element to enhance both the efficiency and efficacy of vaccines have drawn increased attention. Gold nanoparticles (GNPs) as a novel delivery platform has been studied in drug and vaccine delivery. My research goal is to apply this delivery platform in the AIDS vaccine development field for HIV-1 envelope protein-based subunit antigens.

We studied different conjugation methods to load antigens on GNPs. First, we tried to directly link an antigen onto GNPs through an introduced cysteine mutation in the antigen, since the thiol group of cysteine can form a covalent bond with GNP. In this direct-linking study, we made several antigen variants with cysteine introduced in different positions of the original antigen. All cysteine variants can be successfully loaded on GNPs, with neutralizing epitopes exposed after bond on GNPs. We found that the terminal cysteine variants (with the cysteine mutation on either end of the antigen) can elicit high antibody response in rabbits; however, the antibody responses from the internal cysteine variants (with the cysteine mutation inside of the antigen) are exceptionally low. We suspected that the antigens loaded on GNPs trough the internal linkage might be too close to the GNP surface, therefore, it might be difficult to cleave these

protein antigens from the GNPs in vivo by the protease in the endosome, which could result a low immune response.

To further enhance the antibody response, we hypothesized that a spacer between the GNP and antigen might be needed instead of direct linkage. We speculated that a linker between the antigen and GNP might promote antigen processing in the immune system after the antigen-loaded GNPs have been taken by the antigen presenting cells (APCs), which could assist in eliciting high immune responses. Therefore, we examined two linkers for our antigens to attach onto the GNPs. Again, our antigen can be successfully loaded on the GNPs through these linkers, with the critical neutralizing epitope exposed even after loading on the GNPs. After the pilot animal experiment, we chose the N-[Nα,Nα-Bis(carboxymethyl)-L-lysine]-12-mercaptododecanamide (SH-NTA) linker to continue our immunization studies in both mice and rabbits. As expected, compared to the protein-only immunized group, the protein-on-GNP group exhibited a much higher antibody titer reaching 10^7 after only three immunizations in two animal models. Neutralizing activity was also detected in rabbits. Our result suggests that the GNP-NTA system as a delivery platform could preserve the critical epitopes of the loaded antigen as well as elevate their antibody responses. Since our GNP-NTA platform was designed to deliver any protein-based antigen, the positive results from our study indicate that our GNP-NTA delivery system has great potential to be applied in protein-based vaccine development.

CHAPTER 1   GENERAL INTRODUCTION

1.1   Dissertation Organization

Chapter 1 is the General Introduction, which covers the basic information for both Human Immunodeficiency Virus type 1(HIV-1) and vaccine delivery platforms. An overview is provided that includes the HIV-1 pandemic's history, HIV-1 subtypes, and HIV-1 genome proteins, with an emphasis on the envelope protein. This is followed by information on the current strategies for developing HIV-1 vaccines and clinical trials. Gold nanoparticles (GNPs) are used in my thesis for vaccine delivery; therefore, an overview is given to several popular delivery platforms, then a detailed review is given to GNP synthesis, different coating agents and linkers on the GNP surface, and a summary of its application in vaccine delivery.

Chapter 2 is a manuscript in preparation, "Assessing the immune response of HIV-1 gp41-based antigens delivered on gold nanoparticles," which describes the immune responses elicited in rabbits using GNPs to a deliver HIV-1 gp41 based antigen, using different orientations of the protein on GNPs as determined by the inclusion of a cysteine amino acid. Different responses were identified using different cysteine variants. The contributions of each author to the paper are as follows: Habtom Habte and I carried out immunization studies, Habtom Habte generated the terminal mutants, I generated the internal mutants and conducted the antigenicity and immunogenicity tests for all mutants, Keiji

Takamoto helped with the GNPs binding protocol, and Michael Cho and I wrote and revised the manuscript.

Chapter 3 is a manuscript in preparation, "Development of a novel antigen delivery platform based on gold nanoparticles to induce potent antibody responses," which describes using the N-[Nα,Nα-Bis(carboxymethyl)-L-lysine]-12-mercaptododecanamide (SH-NTA) linker to deliver a gp120 based antigen, ODx3, on GNPs. Animal experiments were carried out in both mice and rabbits, with strong antibody responses elicited in both animal models. Neutralizing activity was detected in rabbit sera after the third immunization. The contributions of each author to the paper are as follows: I carried out all the immunization studies, Habtom Habte helped to establish the protocol for linker binding, Yali Qin provided the antigen, Kari Rohl helped to run the agarose gel and antigenicity tests of the antigen loaded on GNPs, Feng Jiao helped with the neutralizing assay, Keiji Takamoto designed the SH-NTA linker, and Michael Cho, Kari Rohl and I wrote and revised the manuscript.

Chapter 4 is the Conclusion chapter that states general conclusions as well as implications for future work.

1.2   HIV and Vaccine Research

1.2.1 History of The HIV Pandemic

Acquired Immunodeficiency Syndrome (AIDS) was first recognized in Los Angeles in 1981 [1,2]. Two years later, the responsible retrovirus was isolated at the Pasteur Institute in France [3]. This virus was later named Human

Immunodeficiency Virus (HIV) by the International Committee on Taxonomy of Viruses in 1986 [4]. HIV is a devastating virus, which has claimed more than 39 million lives since the start of the epidemic. In the most resent global report from the Joint United Nations Program on HIV/AIDS (UNAIDS), there were 35 million people living with HIV with 2.1 million people becoming newly infected in 2013 (http://www.unaids.org/en/resources/campaigns/2014/2014gapreport/factsheet).

1.2.2 HIV Subtypes and Global Pandemic

HIV is subdivided into HIV-1 and HIV-2. Compared to HIV-1, HIV-2 is much less virulent [5] and mostly confined in western Africa [6]. Therefore, HIV-1 is the major research target in the efforts to cure AIDS. HIV-1 can be further divided into groups: M (major), O (outlier), N (non-M, non-O) [7] and P (putative) [8,9]. Group M causes over 95% of infections worldwide and accounts for the vast majority of the global pandemic [10]. This group has 9 clades (A, B, C, D, F, G, H, J, and K), 51 circulating recombinant forms (CRFs, hybrid viruses that have genetic material from two or more clades and infect more than one person), and many unique recombinant forms (URFs, hybrid viruses only exist in one individual patient) [11]. These clades show geographically evident distribution patterns. For example, Clade B is prevalent in North America and Europe, while clade C is prevalent in South Africa and South Asia (Figure 1.1).

The HIV-1 group M subtypes were originally divided according to their phylogenetic relationships [12]. The distribution locations of each subtype is shown according to the 2003-2007 global distribution [13] (Figure 1.1). Clade C

viruses are the most prevalent subtype, which accounts for 48% of total infections. Clade A and clade B are the other two dominant clades, which each account for more than 10% of infections (12% and 11%, respectively). Other clades are less prevalent, and they are generally found only in Africa. CRFs are also a growing threat, including AE, which makes up 5% of infections and is found mainly in East Asia.
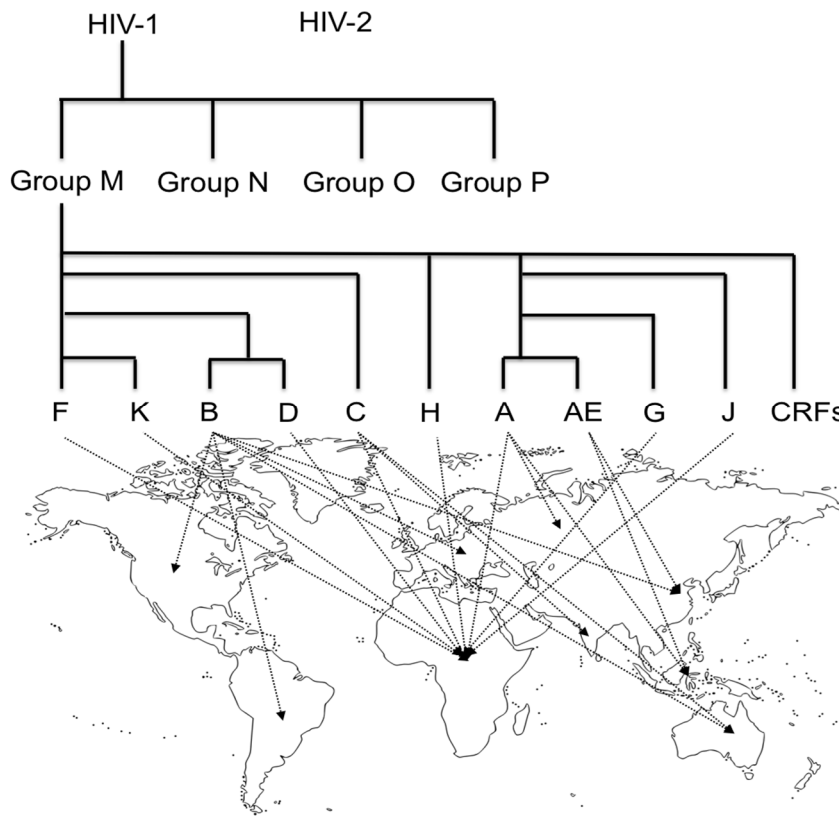
Figure 1.1: HIV-1 subtypes and distribution

Schematic representation of the phylogenetic relationship between the subtypes in M group and their major distribution regions worldwide.

1.2.3 Course of Infection

Unlike other viruses, HIV-1 cannot be eliminated by our own immune system following infection, because this lethal virus directly destroys the human immune system by infecting helper T cells (CD4 T cells) [14], macrophages [15], and dendritic cells [16], which all have the CD4 receptor required for HIV-1 infection. HIV-1 virus infection typically results in the depletion of helper T cells [17] that play a crucial role in regulating immune responses by releasing T cell cytokines. These cytokines are responsible for mediating both humoral immunity and cellular immunity by activating leukocytes like B cells, cytotoxic T cells (CD8 T cell) and macrophages [18]. Therefore, after the CD4+ lymphocyte cell number drops under 200 per mm^3 in the blood following prolonged HIV-1 infection [19], the patients become more susceptible to opportunistic infections because of the collapse of the immune system [20]. This leads to the final stage of HIV-1 infection known as AIDS, which finally results in the patient's death (Figure 1.2).
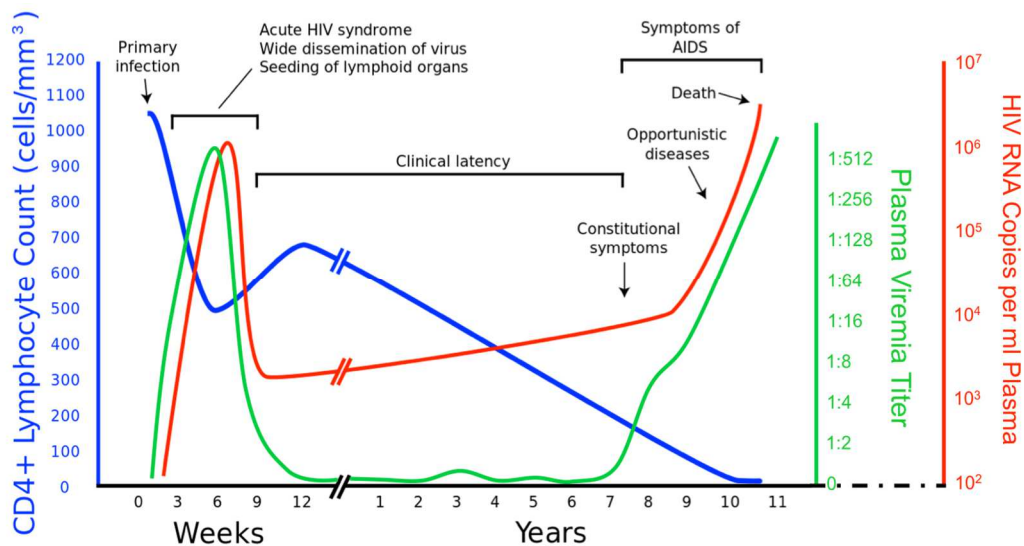
Figure 1.2: Typical course of HIV-1 infection

The blue line indicates the CD4 T cell count (cells per mm^3), the red line indicates the HIV-1 RNA copies per ml of plasma, and the green line indicates the detectable viremia. Adapted from [21].

1.2.4 HIV-1 Genome

The HIV-1 genome is RNA-based with a size around 10kb, which encodes 15 different proteins [22] (Table 1.1).

Gag and Env are basically structure components of the viral core and the outer membrane envelope. Pol provides necessary enzymatic function. Other regulatory and accessory proteins also assist the virus function in many different ways [23] as shown in Table 1.1.

Table 1.1: Proteins encoded by HIV-1 genome

Name	Subunits/ Size	Function
Gag (Group specific antigen/p55)	MA (matrix)/p17	Stabilizes viral particles; escorts viral DNA to the nucleus [24]
	CA (capsid)/p24	Conical core of viral particles; essential for viral replication [25]
	NC (nucleocapsid)/p7	Packages viral RNA [26]; facilitates reverse transcription [27]
	P6	Helps Vpr incorporate into assembling virions [28]
Env (envelope/ gp160)	GP120 and GP41	Explained in Section 1.2.5 below
Pol (polymerase)	PR (protease) /p10 [29]	Cleaves of the Gag and Gag-Pol polyprotein precursors [30]
	RT (reverse transcriptase) /p51 and p66 (with the RNase H domain/p15) [31]	Polymerase activity of reverse transcription; Rnase H removes the viral RNA templates [32]
	IN (integrase)/ p31	Mediates the insertion of the HIV-1 proviral DNA to infected cell genome [33]

Table 1.1 continued

Regulatory proteins	Tat (transcriptional transactivatitor)/p14 and p16	Essential for HIV-1 replication [34]
	Rev (regulator of virion gene expression)/p19	Regulates HIV-1 gene expression [35]
Accessory proteins	Nef (negative effector)/p25-p27	Down regulation of CD4 [36] and class I MHC [37]
	Vif (viral infectivity factor) /p23	Affects virus infectivity [38]
	Vpr (viral protein r) /p10-p15	Influences the nuclear localization of viral genome in non-dividing cells [39]; blocks cell division [40]
	Vpu (viral protein u) /p16	Induces CD4 degradation and enhances virus release from cell [41]

1.2.5 HIV-1 Envelope

Of all these different proteins, Env is the main target for antibodies because it is the only HIV-1 genome encoded protein located outside the viral membrane [42], and thus is accessible to the immune system. The *env* gene encodes for a precursor glycoprotein called gp160, which is later processed by a host cell protease into the surface subunit (SU) gp120 and the trans-membrane subunit (TM) gp41 [22,43] (Figure 1.3).
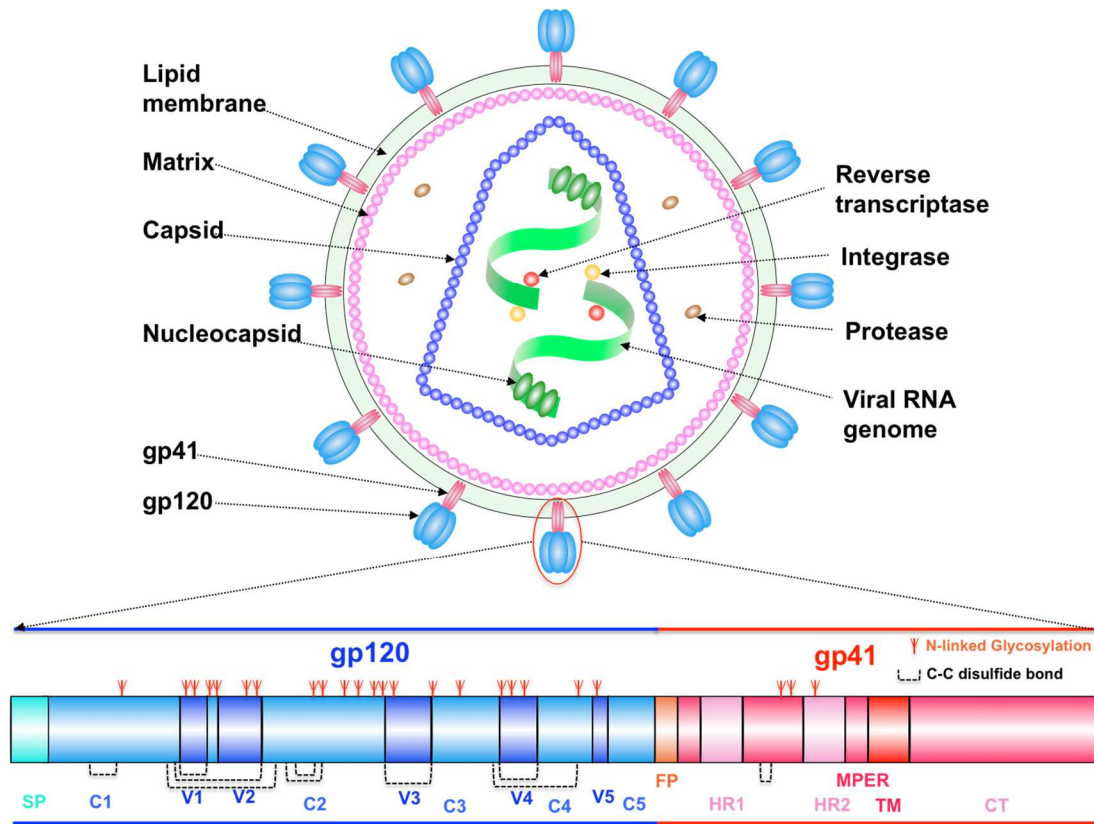
Figure 1.3: HIV-1 virus structure and schematic map of the Env protein

HIV-1 Env is composed of gp120 and gp41. Gp120 is made of five constant regions (C1-C5) and five variable regions (V1-V5). SP stands for signal peptide, FP stands for fusion peptide, HR1 and HR2 are the heptad repeat region 1 and 2, MPER stands for membrane proximal external region, TM stands for trans-membrane domain, and CT is the cytoplasmic tail.

On the HIV-1 surface, gp120 forms a trimer, which is non-covalently linked to the trimeric gp41 to form hetero-oligomeric spikes. The binding of gp120 to the receptors on cell surface initiates the viral entry. The major receptor is CD4, and there are two main co-receptors: C-C chemokine receptor type 5 (CCR5) and C-X-C chemokine receptor type 4 (CXCR4). HIV-1 can be classified into three different tropisms, R5 (use CCR5 for cell entry), X4 (use CXCR4 for cell entry),

and R5X4 (use both R5 and X4 for cell entry) [44]. Gp120 can be divided into three structural domains: the outer domain (OD), the inner domain, and the bridging sheet. It also contains five variable regions (V1-V5) and five constant regions (C1-C5) (Figures 1.3 and 1.4).
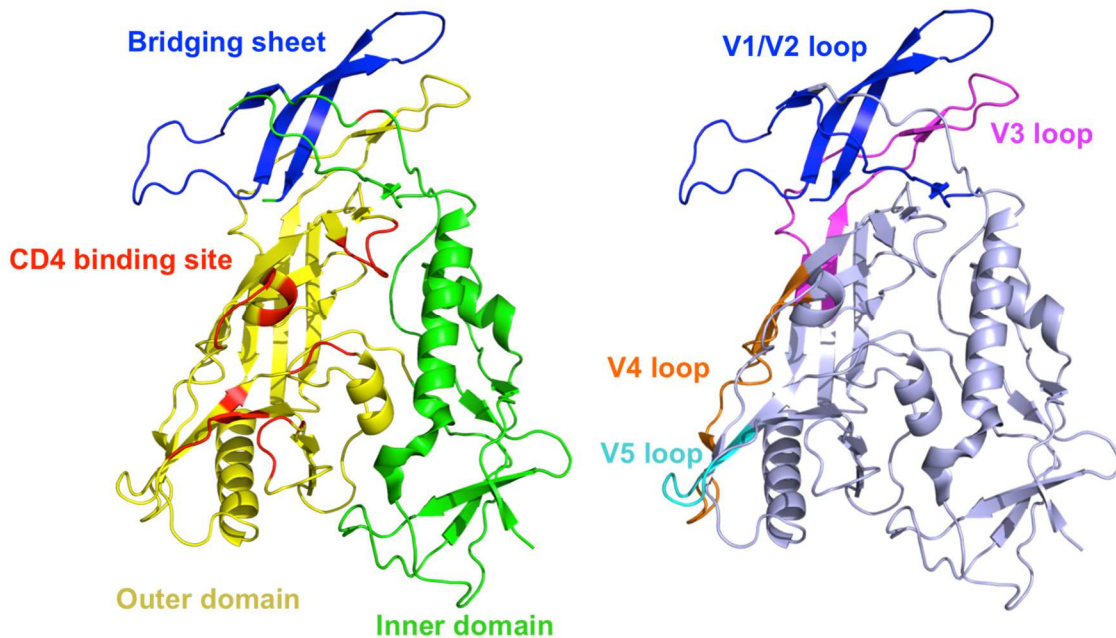
Figure 1.4: Structure of gp120

The two identical gp120 structures are colored to differentiate the labeled functional regions. These two structures are based on the crystal structure in Protein Data Bank (PDB: 4NCO).

Although around 50% of gp120 is covered by a glycan shield [45], there are still many exposed portions that can be targeted by broadly neutralizing antibodies bnAbs (Table 1.2).

Table 1.2: Regions in gp120 targeted by bnAbs

Region name	Representative Binding bnAbs	Comments [46-48]
CD4 binding site (CD4bs)	HJ16, 3BNC117/60, NIH45-46, VHH J3, VRC01, b12 [46-49]	Binding pocket for CD4 receptor; the most potent and broad neutralizing antibodies target this area.
CD4-induced site (CD4i)	3BC176 [50], 17b [51]	Once the envelope binds to CD4, induced epitopes will appear due to conformational changes.
V1/V2 loop	PG9/PG16 [52]	Highly variable and immunogenic; tends to shield the CD4bs.
V3 loop	447-52D [53], 257-D [53]	A semi-conserved region, it can interact with the chemokine receptors on the target cell surface.
Carbohydrate motif	2G12 [54]	Glycan shied is poorly immunogenic; only one bnAb has been isolated.
N332 supersite	PGT121 [55], PGT135 [56]	Antibodies target epitopes on both the protein and glycan site N332
gp120-gp41 interface	8ANC195 [57], 35O22 [58]	Antibodies target epitopes on both gp120 and gp41

Another component of the Env is gp41. Gp41 is composed of a fusion peptide (FP), fusion peptide proximal region (FPPR), two heptad repeats (HR1 and HR2), membrane proximal external region (MPER) and the trans-membrane region (TM), and the cytoplasmic tail (CT) [59,60] (Figure 1.3). This glycoprotein plays an essential role in the fusion step of the virus cell entry [61]. During the HIV-1 fusion process, the structure of glycoproteins changes. Gp41 will go through three major different stages: pre-fusion, fusion intermediate, and post-fusion (see Figure 1.5). The fusion intermediate state is the most vulnerable state, which can be more easily targeted by bnAbs than the other two states [62]. Currently, there are four bnAbs (4E10 [63], 2F5 [64], Z13e1 [65] and 10E8 [66]) isolated against gp41, and they all target the MPER. However, this stage is highly transient, and gp41 can quickly move to the post-fusion state, in which

HR1 and HR2 fold together and form the six-helix bundle [67]. The HIV-1 virus is resistant to the bnAbs attack after the post-fusion state, since the virus genome will be inside the target cell when the fusion process completes. The fusion step is a crucial step of the HIV-1 life cycle, after the fusion, the viral RNA will be reverse-transcribed into DNA and integrated into the host cell genome with the help of the viral reverse transcriptase and integrase. The integrated viral genome (called provirus) can produce more viral proteins to make more viruses and infect other healthy CD4+ cells to spread the infection.
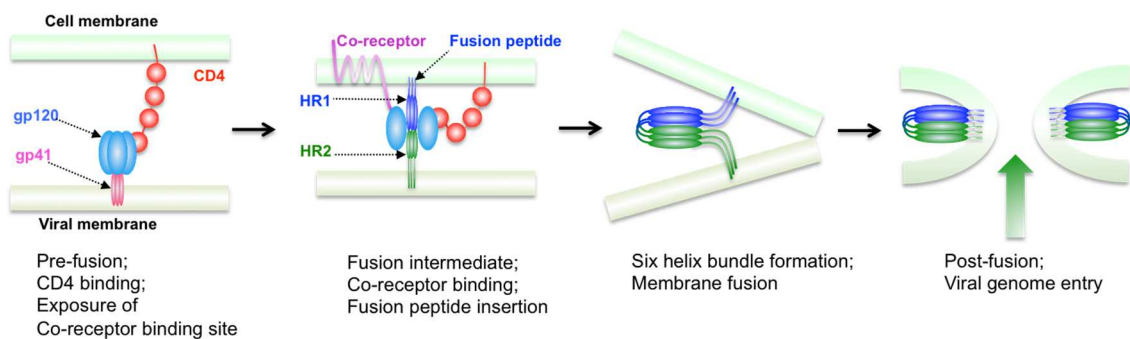
Figure 1.5: HIV-1 fusion process

HIV-1 fusion occurs with the assistance of receptors on the host cell surface. Adapted from [68].

1.2.6 HIV Vaccine

HIV-1 is lethal because it directly destroys the immune system. Significantly, the virus has extensive genetic variations caused by a dramatic mutation rate [69], which means that HIV-1 can quickly grow resistant to medical treatments, resulting in the current global pandemic. To try and stop the

pandemic, HIV-1 has been studied extensively during the past three decades [70]. The introduction of highly active antiretroviral therapy (HAART) is a significant milestone during history of the fight against HIV. While patients do survive longer under the HAART treatment [71,72], there is still no way to eradicate the virus through drugs alone. Vaccines, however, as "one of the greatest achievements of modern medicine" [73], can completely eradicate the prevailing diseases caused by viruses. There are some successful vaccines against viruses like smallpox and polio [74], however, vaccine research in the HIV-1 field is still proceeding slowly and with only limited success in human trials [75]. Nevertheless, as the only hope to prevent virus spread before infection, vaccine research against HIV-1 continues.

The concept of vaccination is best described as a prophylaxis to prepare the body for virus infection. After vaccination, a small portion of effector B and T cells can develop into memory B and T cells that can "remember" the vaccine as the corresponding virus [76]. Thus, when infection occurs later, those memory cells can be quickly activated to launch immune responses, such as secreting neutralizing antibodies (nAbs), to eliminate the foreign viruses. As mentioned earlier, the HIV-1 Env protein is the sole component exposed on the virion surface, and is therefore the only target for vaccine elicited nAbs [77]. Thus, the Env protein is widely used in HIV-1 vaccine development to elicit bnAbs [47].

To elicit neutralizing antibodies, many studies have designed antigens, which included a variety of bnAb epitopes. Zhang et al. [78] used synthetic HIV-1 MPER peptides containing the epitopes of 4E10 and 2F5 to immunize guinea

pigs, and they observed broad neutralizing activity against several tier 1 viruses and three tier 2 viruses after four times of immunizations. Bhattacharyya et al. [79] designed two antigens, which were derived from small fragments of HIV-1 gp120 that covered about 70% of b12 epitope. These two antigens were produced in *E. coli* with very high yield (20mg/L), and although only partially folded, could still bind to b12 but not the CD4bs-directed non-neutralizing antibody b6. Surprisingly, although sera antibody tier only reached to 10^5 after four immunizations with either antigen, broad and potent neutralizing activity against nine tier 2 and tier 3 viruses, and many other tier 1 viruses were elicited in rabbits.

Since HIV-1 has multiple subtypes and a highly variable genome, other strategies to elicit cross-clade neutralizing activity are to design antigens using a consensus sequence derived from many different clades, or to develop a cocktail vaccine that includes many different antigens together. Qin et al. [80] designed two gp120 outer domain antigens (OD and ODx3) based on an M-group consensus sequence. While still maintaining strong binding to most gp120 targeting bnAbs, these antigens could also elicit strong antibody responses with a titer over 10^6 after only two immunizations in rabbits. BnAbs against multi-clade tier 1 viruses were also elicited. Bricault et al. [81] designed several clade C HIV-1 gp140 trimers with different antigenic properties. They found that a quadrivalent cocktail of the trimers could elicit better neutralizing activity than any single trimer in guinea pigs.

Although the results from animal models are inspiring, we have yet to

achieve any significant success in human clinical trials. From over 200 trials, only five advanced to phase IIb and III clinical trials. To date, only one trial, the RV144 demonstrated limited efficacy [82]. This phase III trial used a recombinant HIV-1 (env-gag-protease) carnarypox vector vaccine to prime four times followed by boosting twice with a gp120 protein subunit vaccine [83]. After three years of testing 16,402 subjects, this trial demonstrated a modest 31.2% efficacy in preventing HIV-1 infection.

While HIV-1 vaccine development continues to move slowly, attentions have also been drawn to novel vaccine delivery platform development. My thesis work focuses on developing a GNP-based delivery platform for HIV-1 vaccines. Therefore, several common delivery platforms for vaccines, especially the GNP delivery platform is overviewed in the following section.

1.3   Vaccine Delivery Platform

1.3.1 Delivery Platform Overview

Delivery platform choice is of crucial importance to improve the efficiency and efficacy of a candidate vaccine. Currently there are several popular delivery platforms including biological platforms such as DNA plasmid and recombinant viral vectors; and organic/inorganic materials such as immunostimulating complexes (ISCOMs), polymer, lipid and metal-based delivery platforms (see Figure 1.6).

A DNA vaccine **B Recombinant viral vector** **C ISCOM**

D Polymer **E Liposome** **F Non-degradable particle**
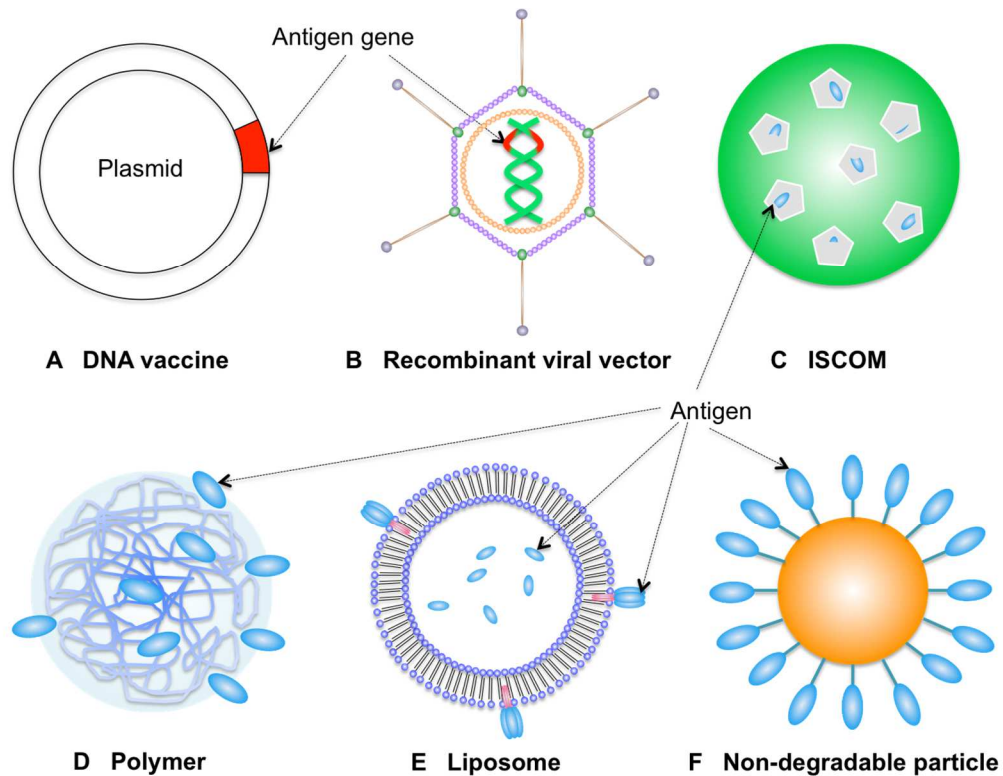
Figure 1.6: Schematic view of different nanoparticle delivery systems

Commonly used delivery platform for vaccine antigens. Antigens can be either loaded on the surface of the platform (Polymer, Liposome and Non-degradable particles) or inside the platform (ISCOM, Polymer and liposome), DNA vaccine and recombinant vial vectors also provide antigen expression in vivo. Adapted from [84].

1.3.1.1   DNA Vaccine

Antigen gene delivered by DNA plasmid was first found could elicit immune response in vivo back in 1992 [85]. Compare to the traditional live attenuate vaccine, DNA vaccine is quite safe for *in vivo* immunization, thus has been used extensively for HIV-1 vaccine development (reviewed in [86]). Besides safety, DNA vaccine is very easy to design and manufacture, however, the immunogenicity of DNA vaccine is very low although both T and B cell responses

could be elicited (reviewed in [87]). Researchers have been using different delivering methods such as gene gun[88] or electroporation[89,90] to facilitate the gene delivery therefore enhance the immune response. Currently, the DNA vaccine has been used together with protein-based vaccine. The DNA prime, protein boost strategy is a very effective approach to induce strong B/T cell immune responses[91-93].

1.3.1.2   Recombinant viral vectors

Recombinant viral vectors have been used to deliver foreign genes since the 1970s [94]. Nowadays, these platforms have been extensively used to induce robust cytotoxic T lymphocyte (CTL) immune responses [95]. Famous vectors like adenovirus [96] and vaccinia virus [97,98] vectors are widely used for HIV-1 antigen delivery. These recombinant viral vectors can be used to generate viruses *in vitro*, which later could be used for *in vivo* immunizations. Notably, the only positive human clinical trial RV144 used a recombinant carnarypox vector (ALVAC) containing HIV-1 genes [83]. In this study, the recombinant viruses were produced in chicken embryo fibroblasts, and they were used to prime the patients while AIDSVAX B/E (gp120) boosts were used later [99]. However, the use of the viral vector as a delivery vehicle may cause safety issues such as induction of an antiviral immune response [100], and depending on the vector used, integration of the viral DNA in chromosomal DNA could result in unwanted side effects [101].

1.3.1.3   ISCOMs

ISCOMs are around 40 nm in diameter with a cage-like structure [102]. ISCOM nanostructure can be formed spontaneously when *Quillaja* saponins, cholesterol and phospholipids are mixed under controlled conditions. ISCOMs are well known for their adjuvant capability, along with their delivery features for many viral antigens including HIV-1 [103-105]. One group recently evaluated the effect of ISCOMs together with 11 other adjuvants in HIV-1 gp140 trimer immunized guinea pigs and non-human primates [106]. They found that unlike the oil-in-water emulsions (GLA-emulsion, Ribi, Emulsigen) that resulted in aggregation and disruption of antigen structural integrity, ISCOMs together with alum (GLA-alum, Adju-phos, Alhydrogel), TLR (GLA-aqueous, CpG, MPLA) or liposomes (GLA-liposomes, virosomes) preserved the trimer integrity. However, in term of eliciting antibody responses, ISCOMs did not demonstrate better results as compared to other adjuvants.

1.3.1.4   Polymers

Synthetic polymers like poly lactic acid (PLA) [107,108] or Poly Lactide-co-Glycolic acid (PLGA) [109-111] are used for the development of drug and vaccine delivery systems because of their excellent biocompatibility and biodegradability. Natural polymers like chitosan, gelatin and sodium alginate are also frequently used for delivery purposes since they are not associated with toxicological problems as with synthetic polymers [112]. Chitosan is a natural polymer often chosen as an agent delivery platform and vaccine adjuvant [113-115]. It is derived from de-acetylation of chitin [116], which is the structural

element in the exoskeleton of crustaceans (e.g. crab shells). My lab also uses chitosan as a vaccine delivery platform and obtains a significant immune response from mice, rabbits [80] and macaques (unpublished data).

1.3.1.5 *Liposomes*

Liposomes were first described in 1964 [117], and are currently widely applied in biomedical delivery [22,118-121]. The simplest liposome is made of lipid bilayers, which can carry hydrophilic molecules inside the aqueous core and hydrophobic molecules among the bilayers [122]. Today, liposomes have become a multifunctional delivery platform for a wide range of different targets [122]. Since the cell membrane is also made of lipid bilayers, lipid-based delivery platforms are very biocompatible and can easily fuse with the cell membrane to complete delivery. However, there are also some drawbacks, such as fast elimination from blood circulation, a lack of structural integrity that results in content leakage and instability during storage [123]. Researchers have been working to overcome those drawbacks with lipid-polymer hybrid nanoparticles [124].

1.3.2 Gold Nanoparticle Delivery Platform

Metal is one of the most used non-degradable materials for delivery purposes. Noble metals such as gold or sliver, or metal sulfides like AuS and CuS have been demonstrating great potential as nano-carriers [125]. GNPs among all other metal-based nano-carriers are the most popular and extensively explored delivery platform.

1.3.2.1 Synthesis of GNPs

GNPs can be easily generated by reducing tetrachloroauric acid ($HAuCl_4$), a method was first introduced in 1951 [126]. The synthesis reaction can be summarized as:

$2HAuCl_4 + 3C_6H_8O_7$(citric acid) $\rightarrow$ $2Au + 3C_5H_6O_5$(3-ketoglutaric acid) + $8HCl + 3CO_2$ [127]
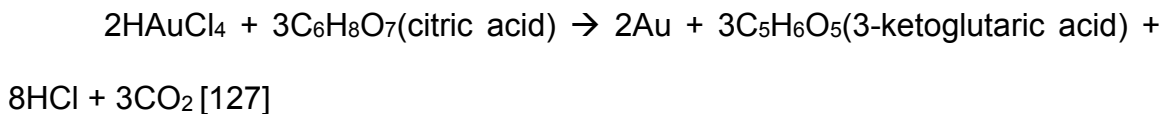
The size of the gold nanoparticles can be controlled from 16 to 150 nm by adjusting the gold to citrate concentration ratio [128]. The citrate acts as both a reducing agent and stabilizer (Figure 1.7)
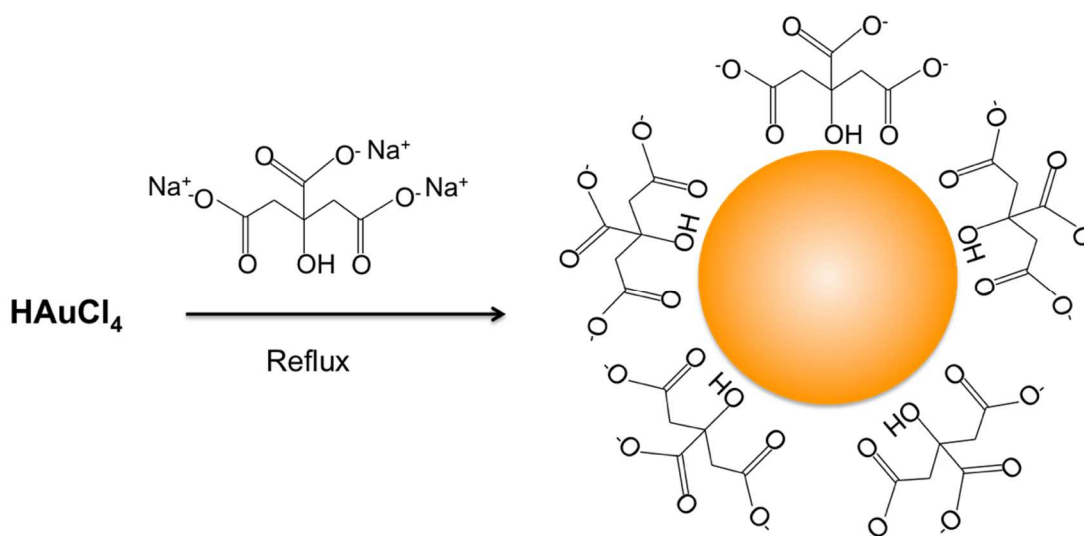
Figure 1.7: Schematic presentation of preparation of citrate stabilized GNP in water

The citrate reduces the gold salt into GNPs and then caps the surface of GNPs. Adapted from [129]

1.3.2.2 *From sphere to rod*

The shape of GNPs can also be controlled. Chen et al. [130] made five different GNP shapes including nano-spheres, nano-cubes, nano-branches, nano-rods, and nano-bipyramids using the seed-mediated growth method. Besides the primary spheres, gold nano-rods (GNRs) are another important formation for delivery. Niikura et al. [131] demonstrated that compared to spheres and cubes, rods were the most efficiently internalized into cells and induced the secretion of inflammasome related cytokines, and thus could be used as an effective vaccine platform.

The most common way to produce GNRs is the seed-mediated method [132,133]. Cetyltrimethylammonium bromide (CTAB) is usually used as the capping reagent for GNRs [134] (Figure 1.8).
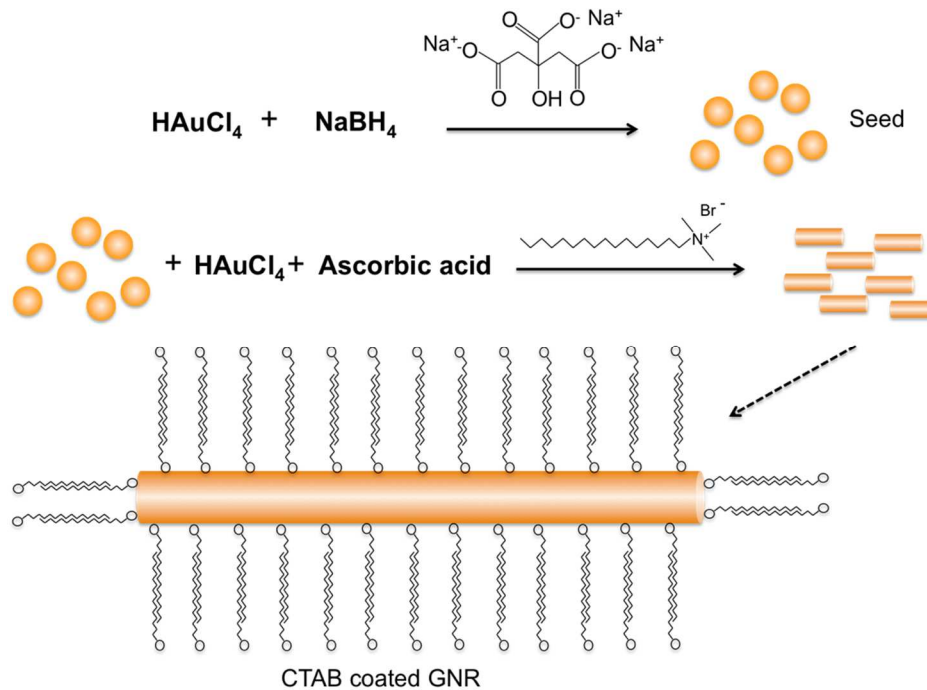
Figure 1.8: Making GNRs

Seed-mediated growth method for making GNRs. Instead of citrate, a strong reducing agent like $NaBH_4$ is used for the reduction of gold salt. Citrate or CTAB is used to cap the seed particles. Those seeds can grow into a larger, rod-like shape by using more gold salt, a weak reducing agent (usually ascorbic acid), and more CTAB (rod-like micelle template).

1.3.2.3 Linking biomolecules on GNPs

Capping ligands like citrate or CTAB serve as stabilizers for the newly synthesized GNPs. However, the surface ligands can be displaced by thiols through the ligand exchange reaction [135,136]. The strong binding of thiol to gold (~50 kcal/mol [137]) is the foundation to link the protein-based vaccine or other therapeutic molecules on GNPs for delivery. The thiol bond can be either provided by the protein/peptide itself or through a linker with a thiol end. Cysteine is the only amino acid that has a thiol group on its side chain, and it is usually used to link GNPs. Studies have either introduced cysteine mutations or directly synthesized the cysteine into the small peptides, which may not have cysteine naturally [138,139].

Another way of loading antigens on GNPs is to use a linker with one thiol at the end. 4-aminothiolphenol (4-ATP) can be used to cap the GNP surface [140,141].
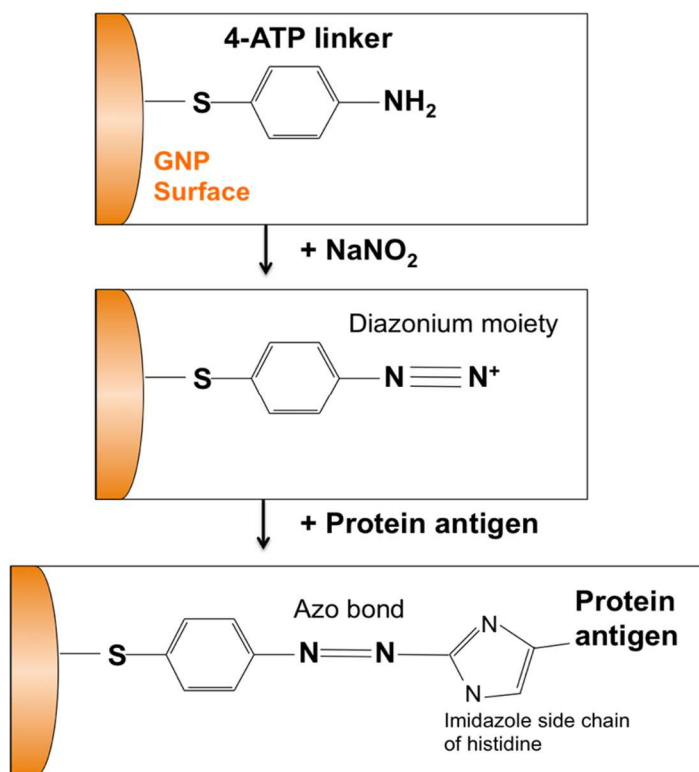
Figure 1.9: 4-ATP linker

A schematic graph showing how to load protein antigens on GNPs through the 4-ATP linker: the thiol end of 4-ATP provides binding with GNPs, and the primary amine end will form an Azo bond with the imidazole side chain of the histidine inside the protein after sodium nitrite treatment.

The thiol end of 4-ATP can attach to GNPs while the amine group can be modified into a diazonium group, which will form the azo bond with the aromatic side chain of histidine [142-144]. Since the his-tag is widely used in recombinant proteins and is quite easy to incorporate into protein antigens, 4-ATP has great potential to be used as an alternate linker.

The most commonly used chemical to bind his-tag is the nitrilotiracetic acid (NTA), which is commercially available for purification of his-tagged proteins. Linker N-[Nα,Nα-Bis(carboxymethyl)-L-lysine]-12-mercaptododecanamide (SH-

NTA) has both a thiol end and a NTA end, therefore, it can be a perfect linker between the GNPs and antigens. Additionally, the bond between NTA and histidine is not stable in a low pH environment, which means that after the protein-loaded GNPs are taken up by antigen presenting cells (APCs), the antigen will be released for further processing, since the acidification inside the endosomes can break the bond between NTA and his-tag.

1.3.2.4   Biocompatibility and in vivo delivery

Mammalian cells can easily take up GNPs. Chithrani et al. [145] tested the uptake efficiency of different sizes and shapes of GNPs using Hela cells. They found the cells could most efficiently take up spherical GNPs with diameters of 50nm, reaching $6*10^3$ particles in one cell within 6 hrs. In another study [146], these researchers revealed the mechanism of cell entrance is via the receptor-mediated endocytosis pathway (RME). In this pathway, the ligand on a surface coated protein binds onto a receptor on the cell surface, and then the cell will engulf the whole GNP through endocytosis. Besides high tissue permeability without hampering cell functionality, GNPs are also well known for their biocompatibility, such as non-toxicity and non-immunogenicity to mammalian cells [147]. *In vitro* studies have shown that, in varying sizes, gold spheres [148] and gold rods [149] are non-toxic to mammalian cells even at very high concentrations (150~250µM, around 10^{10} particles/ml). Chen et al. [150] performed further toxicity tests *in vivo* using BALB/c mice. They tested GNPs of varying diameters. The mice were injected intraperitoneally (IP) at a dose of 8 mg/kg/week (four times more than the dosage used for mice immunization in

Chapter 3). Their results showed that GNPs with sizes of 3, 5, 50, and 100nm were safe through the experimental period (more than 50 days). However, mice injected with other sizes (8, 12, 17 and 38 nm) exhibited symptoms of toxicity, and the length of time until half mortality was 21 days. They also found that coating the toxic GNPs (e.g. 17nm) with protein antigens could prolong lifespan to more than 50 days. Along with the reduction of toxicity, strong antibody responses were induced.

The bio-distribution of GNPs following administration has also been analyzed. De Jong et al. [151] examined the bio-distribution of GNPs of varying sizes in rats 24 hours after intravenous administration. They found the 10nm particles had spread into many different systems such as the blood, liver, spleen, kidney, heart, lung and brain. In contrast, the 50nm and larger particles were only detected in the blood, liver and spleen. Elsewhere, it has been shown that GNPs smaller than 20nm can cross the blood-brain barrier (BBB) [152] and the blood-retinal barrier (BRB) [153] for therapeutic applications. Simpson et al. [154] monitored the bio-distribution of glutathione coated GNPs (~2nm) in mice for 6 weeks. They found that 30% of the GNPs were excreted though the renal system within one hour, and 80% of what remained was voided within hours. The distribution pattern for what remained was correlated with the injection dose, and the kidneys, spleen and liver were the main organs that accumulated GNPs. Those GNPs located in the liver and spleen were excreted after 3 to 4 months [155]. Most of these particles can be excreted through the hepato-biliary or renal clearance [156,157].

1.3.2.5   Applications for vaccine delivery

GNPs have been widely used in vaccine development as a delivery platform to boost both B cell and T cell responses [158]. This platform has been used against many bacteria pathogens including *Escherichia coli (E. coli)* [159], *Listeria moncytogenes* (listeria) [160], *Burkholderia mallei* (causative agent of glanders) [161,162], and *Clostridium tetani* (causative agent of tetanus) [163] to induce higher antibody titers as compared to other platforms or no platforms, as well as to help elicit many T cell activation cytokines including interferon gamma (INFγ) and interleukin-17 (IL-17).

GNPs can also target many viruses. Chen et al. [138] investigated the antibody response elicited in mice by a synthetic peptide, which resembles a foot-and mouth disease virus (FMDV) protein, loaded on GNPs of different sizes. They found that 8nm GNPs elicited the highest antibody titer (6×10^4) at week 6, which is three times higher than the keyhole limpet hemocyanin (KLH) platform when tested under parallel conditions. Furthermore, GNPs did not induce any detectable immune response against the platform, while KLH induced a strong antibody response against itself, which was even higher than the response against the loaded antigen. Niikura et al. [131] also evaluated the immune responses of the West Nile virus (WNV) envelope protein loaded on GNPs of different sizes and shapes. Compared to cube (40x40x40 nm) and rod (40x10nm) shapes, they found that the 40nm spherical GNPs elicited the highest immune response in mice. Their *in vitro* study revealed that rods could induce inflammasome-related cytokines such as IL-1β and IL-18, while spheres and

cubes induced the pro-inflammatory cytokines such as TNF-α, IL-6, IL-12 and GM-CSF. The high antibody production was speculated to correlate with these inflammatory cytokines, whereas rods acted via the inflammasome activation. There are also reports using GNPs to carry anti-HIV drugs [164-166]; however, the application of GNPs in HIV-1 vaccines is limited. One group used GNPs to deliver a DNA-based vaccine against HIV-1 [167]. They modified the surface of GNRs with three different chemicals to load HIV-1 Env plasmid DNA for vaccination in mice: CTAB, poly (diallydimethylammonium chloride) (PDDAC), and polyethyleneimine (PEI). Compared to the naked DNA plasmid, the PDDAC or PEI modified GNRs significantly promoted both humoral and cellular immunity. Apart from this study, we are not aware of any literature discussing the delivery of protein-based antigens for HIV-1 vaccine study.

To apply this novel platform in HIV-1 subunit vaccine development, we started the original research first in gp41-based antigens by loading directly on GNPs though the introduced cysteine mutations (Chapter 2). By introducing cysteine at different part of the antigen, we tend to obtain different antigen orientations on the GNP surface to better present the critical epitopes. The result indicated that a linker might be helpful to improve the antibody response rather than direct linking. Therefore, we further performed a study for a gp120-based antigen delivered on GNPs using the SH-NTA linker (Chapter 3). Strong antibody responses were elicited in both mice and rabbits. We also obtained neutralizing activity in the rabbit sera. Additionally, there is also an immune response assessment in mice by using the GNR-4ATP delivery platform (Appendix).

CHAPTER 2 ASSESSING THE IMMUNE RESPONSES OF HIV-1 GP41-BASED ANTIGENS DELIVERED ON GOLD NANOPARTICLES

Feng Lin[1,2], Habtom H. Habte[1,2], Keiji Takamoto[3], and Michael W. Cho[1,2,*]

[1]Department of Biomedical Sciences, [2]Center for Advanced Host Defenses, Immunobiotics and Translational Comparative Medicine, Iowa State University, Ames, IA 50011, USA

[3]Department of Biochemistry, Albert Einstein College of Medicine, New York, NY 10461, USA

*Corresponding Author.

Email addresses:

FL: fenglin@iastate.edu

HHH: hhhabte@gmail.com

KT: kgtakamoto@gmail.com

MWC: mcho@iastate.edu

2.1 Abstract

Inducing a high neutralizing antibody response is of crucial importance for the success of a subunit vaccine. In this study, we utilized gold nanoparticles (GNPs) to deliver HIV-1 gp41-based antigens, hypothesizing this platform could enhance the observed immune response as well as present the critical epitopes to immune cells. To link the antigen to the GNP, we first introduced a cysteine mutation at either terminal. Both variants elicited strong immune responses in rabbits, but no neutralizing antibodies were elicited. Next we introduced three separate internal cysteine mutations to block a nearby immune-dominant region by steric hindrance via protein-GNP attachment. In contrast to our first results, the immune responses from these variants were very low when compared to the original terminal variants. This study indicates that the location of antigen-GNP linkage might be critical to elicit high immune response and provides insights for vaccine development using GNPs as a vaccine delivery platform.

2.2 Introduction

Choosing a proper antigen delivery platform is essential for the success of a vaccine [168]. Gold nanoparticles (GNPs) have been used as non-toxic carriers for drug and gene delivery applications [169-171], and more recently have also been applied as a platform to deliver vaccines [131,138]. Studies have shown that GNPs can greatly improve the immune response of an attached antigen [158] without producing detectable toxicity and physiological damage [154,172]. Additionally, the self-assembly reaction of organo-thiol compounds onto the gold

surface allows covalent linkage of antigens containing cysteine with a free thiol to GNP without having to use harsh chemicals that could potentially alter epitope structure [173]. We are unaware of any other groups using GNPs to deliver a HIV-based subunit immunogen, so it is important to test this novel delivery platform for this purpose.

When using antigen delivery platforms, the attached antigen must still interact well with the B cell receptors [174]. We speculated that exposing the broadly neutralizing antibodies (bnAbs) epitopes in the antigen on delivery platform could facilitate this interaction. Because these epitopes are known, our strategy is to generate GNP bound antigens, which present the bnAbs epitopes to immune cells. Those epitopes suitable for B cell activation are located on the envelope glycoprotein of HIV [47]. The two HIV glycoproteins are gp120 and gp41 [175]. A small, highly conserved domain located in gp41, the membrane proximal external region (MPER) [176], is targeted by four previously isolated bnAbs; namely, 2F5 [177-179], 4E10 [180], Z13e1 [63,65], and 10E8 [66]. Thus, this region is an attractive target for HIV vaccine development.

However, short MPER-based peptides are weakly immunogenic [176,181,182], thus requiring potent adjuvants or delivery platforms to increase their immunogenicity. Additionally, optimizing the presentation of the MPER may also be crucial for eliciting nAbs with potencies equal to or exceeding those of currently isolated ones [65,183]. Thus, a delivery platform, which could adopt different MPER orientations on its surface, could be helpful to present the critical epitopes, depending on how the antigen is attached on the platform.

GNPs present many benefits as vaccine carriers by serving as delivery systems that facilitate targeting to antigen-presenting cells and induce strong immune responses [84]. Thus, we hypothesized that GNPs could enhance the effectiveness of MPER-based antigens as well as present the critical MPER epitope to the immune system. We therefore designed several gp41-derived antigens capable of using GNPs as the delivery platform.

2.3 Results

2.3.1 Construction of The Terminal Cysteine Variants

The original antigen gp41-54Q contained the gp41 heptad repeat 2 (HR2) and MPER. To link this gp41-based antigen on GNPs, we introduced cysteine mutation in the constructs through site-directed mutagenesis. Mutations were first introduced in the original antigen at the N or C terminus to ensure peptide conjugation to GNPs (Figure 2.1, A). Highly pure proteins were obtained (Figure 2.1, B). The purified proteins are around 9kDa.
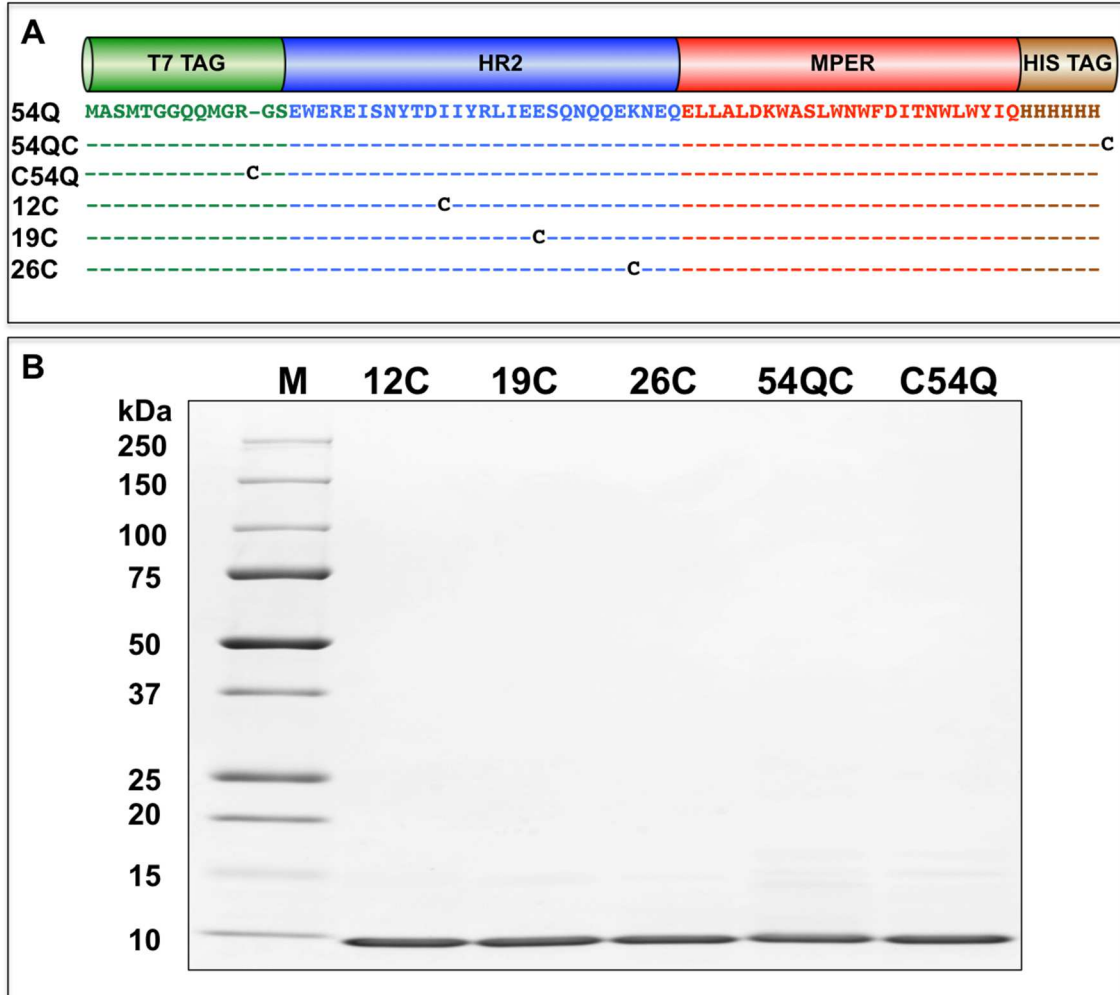
Figure 2.1: Schematic diagram, construct sequence, and purification of the cysteine variants.

(A) Construct map for the cysteine variants. The T7 protein expression tag is removed from the 54QC and C54Q constructs after protein purification by trypsin. HR2 and MPER from HIV-1 gp41 are the main antigen parts. The C-terminal his-tag is used for protein purification. (B) Purified 12C, 19C, 26C, 54QC and C54Q on SDS-PAGE.

2.3.2 Terminal Variants Loading on GNPs

We tested whether the cysteine variants could bind the GNPs. The newly introduced cysteine residue can provide a sulfhydryl group as a conjugating site

for attachment to the GNPs. Conjugation of cysteine variants to GNPs was optimized by adding different concentrations of the antigens to 1 ml suspensions of 50 nm GNPs (4.5×10^{10} particles). For all the cysteine variants, 8 μg was the maximum amount that could be loaded onto 1 ml suspension of the 50 nm GNPs, which means around 10^4 antigen molecules, can be loaded on a single GNP. Conjugations of cysteine variants to GNPs were analyzed by 0.8% agarose gel electrophoresis. GNPs alone do not move in the agarose gel, but after protein binding, they are negatively charged and can migrate (Figure 2.2, A).
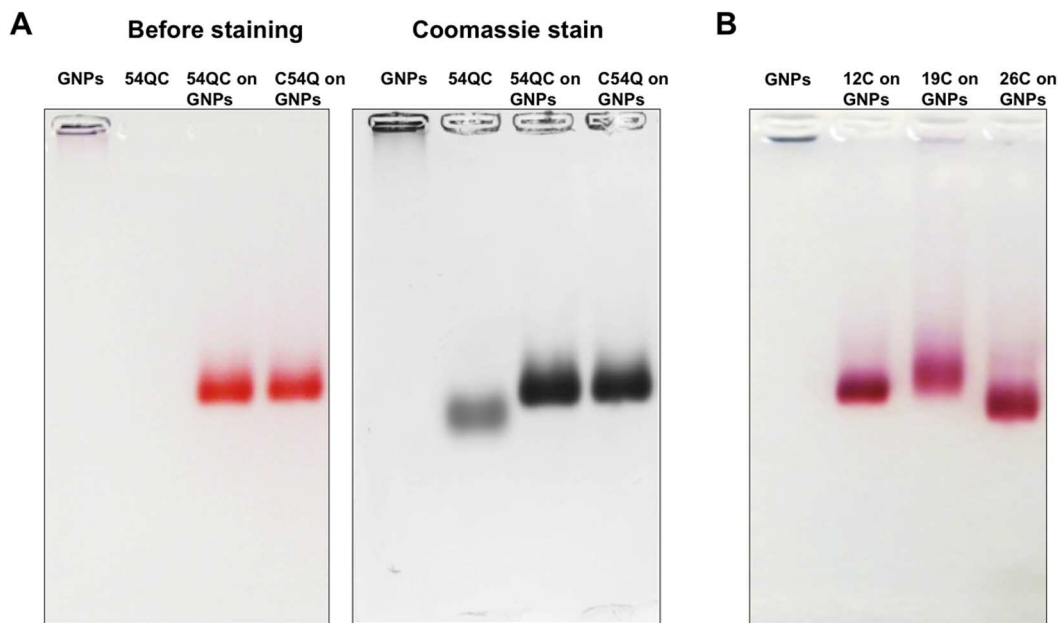
Figure 2.2: Characterization of antigens loading onto GNPs

(A) Agarose gel analysis of the terminal cysteine variants 54QC and C54Q, The right gel is the same gel stained with Coomassie Blue. (B) Gel analysis done for the internal cysteine variants 12C, 19C and 26C.

2.3.3 Antigenicity Test of The Terminal Variants

An ELISA test was done to determine if the bnAb epitope in the MPER region is still exposed when the variants are bound to GNPs (Figure 2.3). Compared to the ELISA results from the free antigen coated plates, the results from the GNP ELISA indicate that C54Q and 54QC could still be strongly recognized by 2F5 even after loaded on GNPs. However, the binding with 4E10 and Z13e1 were significantly reduced after loading antigens on the GNPs. We did not include 10E8, because the K683Q mutation disrupts a crucial amino acid for 10E8 binding.
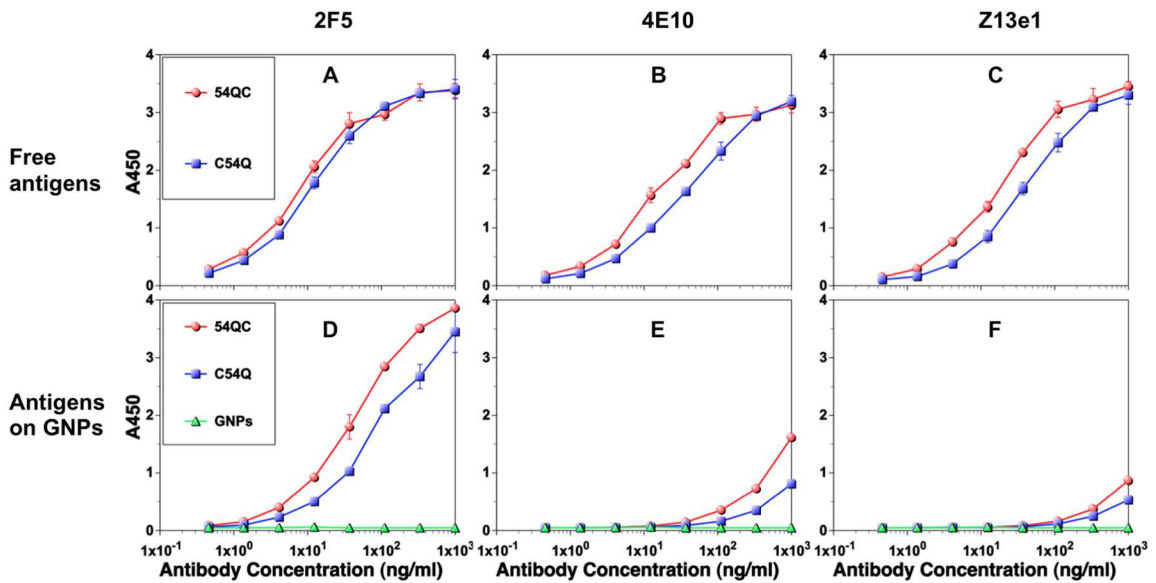
Figure 2.3: Antigenic properties of 54QC and C54Q.

(A-C) Antibodies recognition of the free antigens (D-F) Same analysis for the cysteine variants loaded on GNPs

2.3.4 Immunization Study of The Terminal Variants

To assess the immunogenicity of C54Q and 54QC, two groups of three rabbits each were immunized with either antigen loaded onto 50 nm GNPs. Sera were drawn two weeks after each immunization, and antibody titer was determined using ELISA (Figure 2.4). A low antibody titer of around 10^3 was recorded after the first immunization in both groups. The antibody response continued to increase significantly after the second and third immunizations. Rabbits immunized with 54QC induced antibody titers up to 10^6. Rabbits immunized with C54Q induced slightly lower antibody titers, which were less than 10^6. Overall, no major differences in antibody titers were seen among rabbits within each group (unpaired t test, P=0.37). To determine whether antibodies against GNPs were elicited, ELISA was done with just GNPs as a coating antigen. No antibody response specific to the GNPs was elicited.
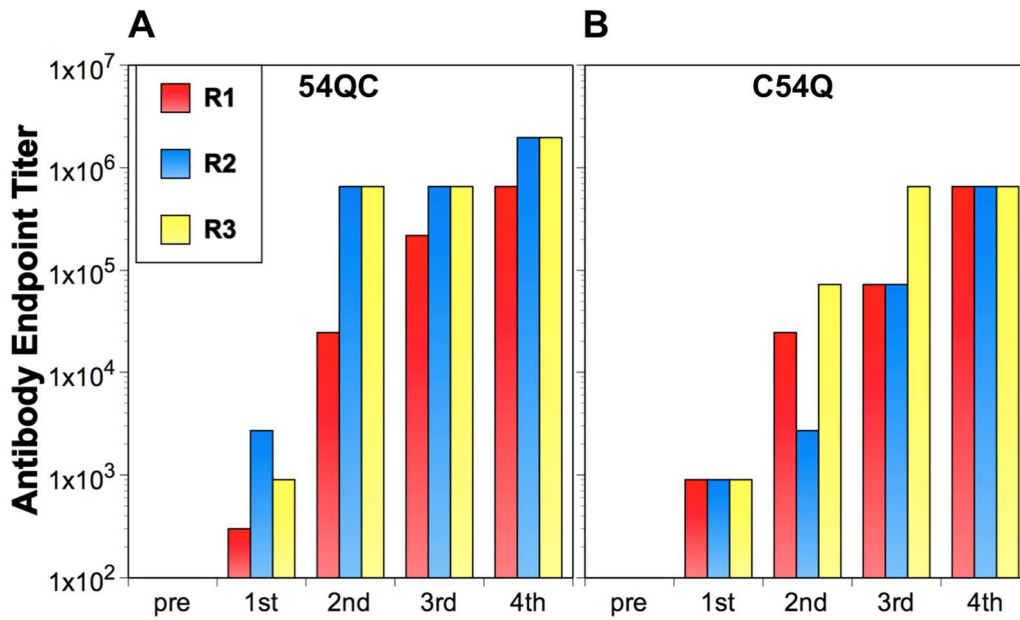
Figure 2.4: Immunogenicity of 54QC and C54Q immunized rabbits.

(A) End-point antibody titers of 54QC in immunized rabbits measured by ELISA. Sera from pre-immune (pre) and those collected two weeks after 1st, 2nd, 3rd, and 4th immunization were analyzed. (B) Same analysis for C54Q. Rabbit numbers are indicated by R1, R2 and R3.

2.3.5 Epitope Mapping of The Terminal Variants

Since no neutralizing activity was detected in the rabbit sera from these two terminal variants, we want to determine from which regions of 54QC and C54Q the antibodies were raised. The peptide ELISA test with overlapping biotinylated peptides (10-mer) was then performed. The majority of the antibody responses were targeting linear epitopes within the HR2 region (Figure 2.5). Specifically, antibodies from all rabbits recognized peptides 638 to 656, with the peptide 641 inducing the highest immune response. This region has been classified as the non-neutralizing cluster II immune-dominant region [184], while the neutralizing epitopes of gp41 are located in the MPER region (peptide 659 to 674) [185], which is at the C terminal end of our antigens.
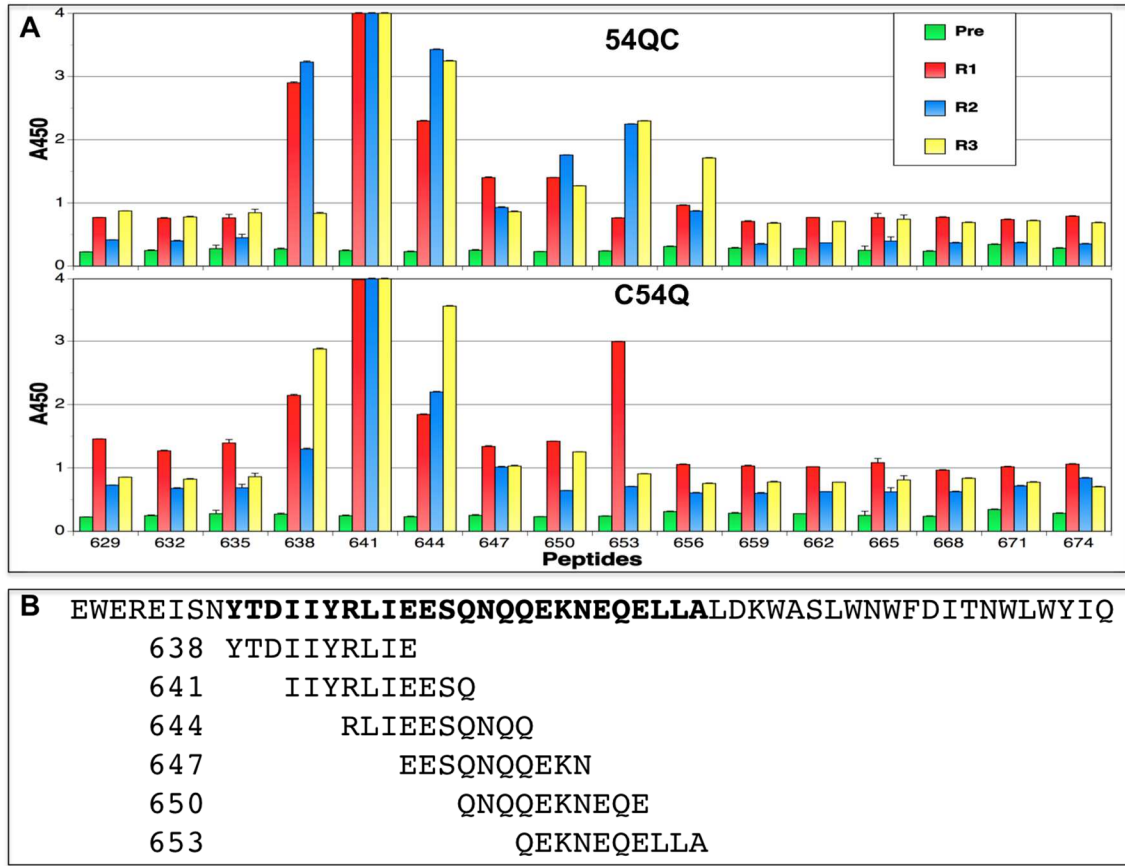
Figure 2.5: Identification of immunogenic linear epitopes.

(A) ELISA was performed using 10-mer biotinylated overlapping peptides that cover the entire length of gp41-54Q. On the top panel, the data is for 54QC-immunized rabbits, and the bottom panel shows the data for C54Q immunized rabbits. Data points represent serum samples (1:100 dilution) from the three rabbits collected two weeks after the fourth immunization. (B) List of immunogenic linear peptides epitopes.

2.3.6 Introducing The Internal Cysteine Variants

To direct the immune response away from the non-neutralizing epitopes and towards the neutralizing epitopes found in the MPER, we tried to minimize immune responses toward non-neutralizing epitopes present in the HR2 by using steric hindrance introduced by GNPs surface linkage. We therefore made three

more variants containing a cysteine mutation inside the HR2 domain to replace

the amino acids L12, E19 and K26 (counted from the beginning of HR2) to make

the 12C, 19C and 26C variants (Figure 2.1, A). Because cysteine can directly

bind to the surface of GNPs, the opposite protein side should be exposed to the

immune system. We hypothesized that attaching the protein through the non-

neutralizing immune-dominant region to the GNPs could block immune

responses to this region and better expose the MPER neutralizing epitopes after

GNP loading.

2.3.7 Internal Variants Loading on GNPs

We can see internal variants can also bind well on GNPs (Figure 2.2, B).

The variants' different speeds on the agarose gel is most likely due to their

charge difference in the running buffer. For 19C, the original negatively charged

glutamic acid was replaced by the neutral cysteine, so 19C had a slower

migration than 12C. On the contrary, in 26C, the original amino acid lysine was

positively charged, which resulted in a faster migration than 12C.

2.3.8 Antigenicity Test of The Internal Variants

The internal variants could bind to 2F5 as strongly as the original two

terminal variants. And for 4E10, unlike the terminal variants, even after loaded on

GNPs, these internal variants still showed similar binding patterns with the free

antigens. Even for Z13e1, while the gold-loaded internal variants also showed

weaker binding than the free antigens, their binding signals were still higher than

the gold-loaded terminal variants (Figure 2.3 and Figure 2.6). These results may indicate that the epitopes on MPER have the potential for better exposure when alternate GNP attachment sites are introduced. Additionally, 4E10 has a much higher signal than Z13e1, which suggests the C-terminal of the antigens are well exposed on GNPs, as the 4E10 epitope is at the very C-terminal end while Z13e1 is more inside.
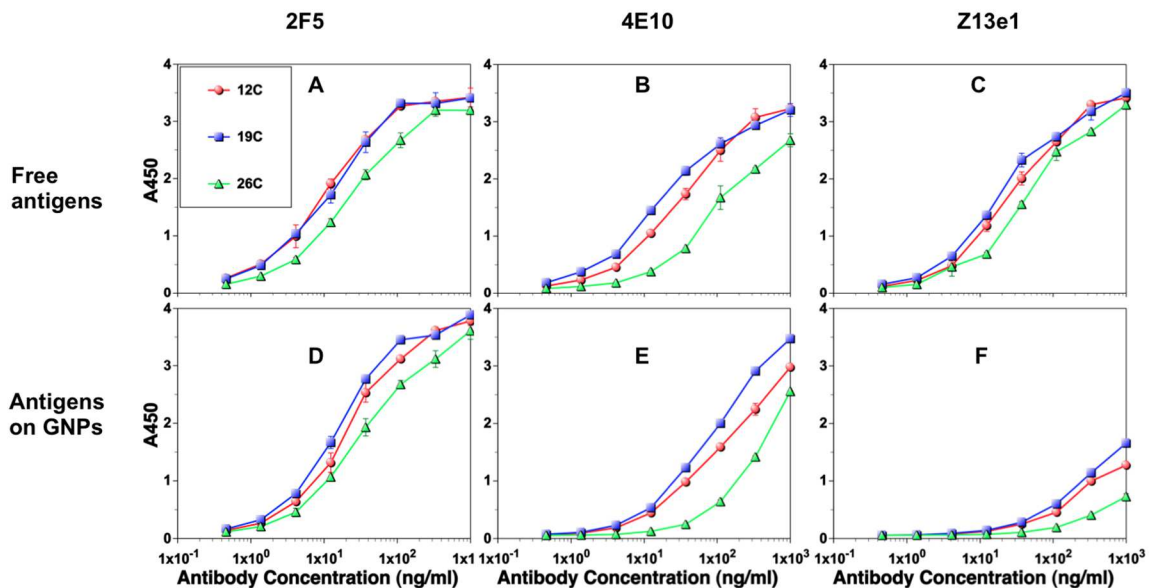
Figure 2.6: Antigenic properties of 12C, 19C and 26C.

(A-C) Antibodies recognition of the free antigens (D-F) Same analysis for the cysteine variants loaded on GNPs

2.3.9 Immunization Study of Internal Variants

We immunized additional rabbits using the 12C, 19C and 26C constructs, hypothesizing that the internal mutation would block antibody responses against undesired epitopes and redirect immune responses toward the more desirable

bnAb epitopes in peptides 665 (2F5) and 671 (4E10 and Z13e1) [186]. Three groups of two rabbits each were immunized with the cysteine variants bound to 50 nm GNPs. Surprisingly, the immune responses elicited by 12C, 19C and 26C were very low (most up to 10^3, Figure 2.7, A-C), compared to that of 54QC and C54Q (Figure 2.4). Additionally, the peptide ELISA did not detect antibody responses directed toward the MPER (data not shown). However, for another variant 28C (E657C), we found higher antibody responses (up to 10^5) after the 3rd immunization using Zinc chitosan (ZNC) instead of GNPs (data not shown).

We suspected that the very low antibody response was more likely due to the close binding of the internal region of the antigen onto the GNPs rather than the influence brought by the mutation itself. Because even if the cysteine mutation incorporated within the antigen disturbed the T helper cell epitope, the antibody response should not be severely reduced, since multivalent presentation of antigens can activate B cell through the T cell independent pathway [187,188]. To test our hypothesis, we immunized rabbits with the alternate ZNC adjuvant. As the antigens bind ZNC through their C-terminal 6xHis-tag, we hypothesized that these variants would now have a conformation similar to 54QC bound to GNP. This time, we elicited a stronger immune response, with most reaching up to 10^5 (Figure 2.7, D-F), which suggested the mutations inside may not harm the antibody response, but the way of binding the antigen on the platform could affect the response greatly. And again, neutralizing activity was not detected in any of the sera samples (data not shown)
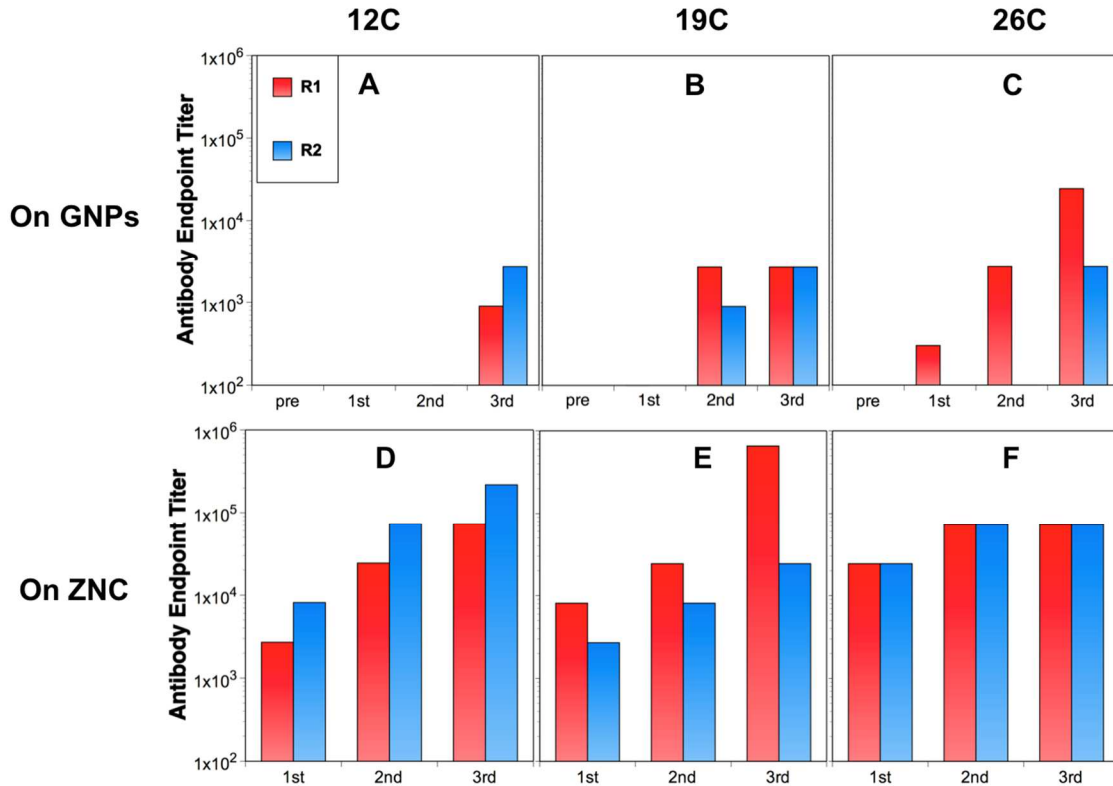
Figure 2.7: Immunogenicity of 12C, 19C and 26C immunized rabbits

(A-C) ELISA end point titer of cysteine mutants immunized using GNPs as delivery platform.

(D-F) Same analysis for the internal cysteine variants immunized with ZNC.

2.4   Discussion

Recently, many studies have focused their research on the optimization of delivery platforms for vaccines to enhance their efficiency [124,131,163,173,189]. Gold nanoparticles are certainly a strong potential platform. There are also reports showing that using GNPs can achieve higher titer compared to using other adjuvants [138,158,172,190]. The objective of this study was to test the immunogenicity of our M group consensus sequence based gp41-54Q antigen (unpublished data) by using a GNP delivery platform to conjugate antigens in a

site-directed manner while maintaining their conformation. To this end, we initially constructed variants 54QC and C54Q, which includes a N-terminal or C-terminal cysteine for site-directed GNPs attachment.

Although we obtained antibody titers up to 10^6, we did not observe neutralizing activity in the sera of immunized rabbits. Interestingly, the immune responses were mostly targeting outside the MPER and towards non-neutralizing epitopes condensed in the HR2 area. However, we did see strong 2F5 binding of 54QC and C54Q even after loading GNPs, which indicate that after GNP attachment, the variants still retain the functional conformation required for presenting the epitope for 2F5. Nevertheless, we did not observe strong binding of the 4E10 and Z13e1 with these two antigens on GNP. Therefore, the reason why all the antibody responses are diverted to HR2 could indicate that the immuno-dominant epitope in the HR2 region may misdirect the immune system response away from the neutralizing epitope. One possibility, specific to 54QC, is that the 4E10 and Z13e1 epitopes are close to the GNP and thus less accessible to antibody binding. This, however, does not explain the same observance with C54Q, as the region that contains the bnAbs epitopes should be well exposed. It is possible that the 6xHis-tag, which is known to adsorb on gold [191-193], may have also bound the GNPs. Therefore, with two ends of the antigen binding on GNP, the bending antigen would most likely not present the bnAb epitopes well because of their proximity to the surface of GNPs.

Based on the data of the epitope mapping of 54QC and C54Q immunized rabbits sera (Figure 2.5), we attempted to expose the bnAb epitopes and

disguise the non-neutralizing epitopes by linking the antigens on the GNPs through the HR2 region. However, the whole antibody responses for these internal cysteine variants were considerably lower than our earlier tests. Besides, the antibody responses were low against all the 10-mer peptides covering the HR2 and MPER in gp41 with no sign of immune focusing in the MPER (data not shown). Nevertheless, all rabbits induced a better immune response against the internal cysteine variants when paired with ZNC rather than GNPs, indicating that the very low antibody titers may have resulted from how the antigens were conjugated or oriented on the surface of the GNPs. Although the way these internal cysteine variants could bind on the ZNC through the C-terminal his-tag is quite similar to the way 54QC bind on GNPs through the C-terminal cysteine, their antibody titers using the ZNC were still lower than that of 54QC on GNPs. This small difference in antibody titers was probably because of the effect of GNPs, which can elicit a higher immune response [138,158,172,190]. Additionally, the cysteine replacement of the internal amino acid might change the antigen conformation, which could also affect the immune response. However, we want to emphasize here, even these two factors could result a lower antibody response of those internal cysteine variants on ZNC than 54QC on GNP, we still obtained much higher titer than these variants on GNP, which suggested that the linking site on the antigen to GNP might be of crucial importance to affect the antibody response.

From the results of the antigenicity tests, we know that when using GNPs as the delivery platform, introducing cysteine inside of the antigen assists MPER

epitopes exposing *in vitro*. However, the *in vivo* immunization studies gave us the opposite result; internal insertions of cysteine did not provide neutralizing activity but blocked overall immune response. Our hypothesis is that the steric hindrance prevented effective protease cleavage within antigen-presenting cells. The immune system exposure of the internal cysteine variants may have been drastically impaired because the proteinase cleavage site was located too close to the GNPs' surface. Thus, they may have been poorly accessible to the proteinase, which ultimately resulted in less overall epitope exposure and lower overall antibody titers.

These results indicate that the problem might not be the immunogenicity of the variants but perhaps how they were conjugated or oriented on the surface of the GNPs. These experiments highlight the need for a linker to better expose antigens and epitopes of interests. Therefore, while choosing the appropriate antigen delivery platform is important, the placement of antigen to platform linkage is also crucial. Eliciting a higher immune response may require a spacer between the antigen and the GNPs. To this end, we are developing a new construct that includes this modification to better expose the antigen to the immune cells and enhance responses.

2.5　Materials and Methods

2.5.1　Construction of Cysteine Variants

We introduced five cysteine variants to the original gp41-based antigen, gp41-54Q (unpublished data), which encode 54 amino acids of the HR2 and

MPER of HIV-1 gp41 (based on MCON6 sequence [194]) (Figure 2.1). Two contained mutations at the C-terminal and N-terminal ends, called 54QC and C54Q, respectively. The other three constructs (12C, 19C, and 26C) contain internal gp41-54Q mutations at the indicated positions. Cysteine mutations were introduced to the pUC57 vector by site directed mutagenesis using the QuickChange XL II Site-Directed Mutagenesis Kit (Agilent). Primers for the cysteine variants were designed using the QuickChange Primer Design Application. Primer pairs are shown in table 2.1.

Table 2.1: Primer sets for the cysteine variants

Variant names	Sense	Anti-sense
54QC	5'-gcaaatgggtcgctgcggatccgagtggg-3'	5'-cccactcggatccgcagcgacccatttgc-3'
C54Q	5'-catcaccatcatcaccattgctaagaattcgagctccgt-3'	5'-acggagctcgaattcttagcaatggtgatgatggtgatg-3'
12C	5'-tctccaactacaccgactgcatctaccgcctgatcg-3'	5'-cgatcaggcggtagatgcagtcggtgtagttggaga-3'
19C	5'-ctaccgcctgatcgagtgctcccagaaccagcagg-3'	5'-cctgctggttctgggagcactcgatcaggcggtag-3'
26C	5'-ccagaaccagcaggagtgcaacgagcaggagctgc-3'	5'-gcagctcctgctcgttgcactcctgctggttctgg-3'

PCR was performed at 95°C for 1 min for the initial denaturation, followed by 18 cycles of 95°C for 50 s, 60°C for 50 s, and 68°C for 6 min, with a final extension step at 68°C for 7 min. 1 µl of DpnI was added to the application reaction and incubated at 37 °C for another 1hr; products were then transformed into XL-10 Gold competent cells to obtain the final variant constructs. BamHI and EcoRI were used as the digestion site to insert the constructs into pET-21a. All constructs were confirmed by DNA sequencing.

2.5.2 Expression and Purification of Cysteine Variants

Expression and purification of the variants were performed based on the method from Penn-Nicholson et al. [195] with a few modifications. For the expression of cysteine variants, the plasmid transformed *E. coli* T7 Express lysY/lq (NEB) was cultured to OD_{600}=1.0 at 37°C. 1 mM isopropyl-beta-D-thiogalactopyranoside (IPTG) was added in to the culture till OD_{600} reached 5.0 at 31°C. The bacteria pellet was span down by centrifugation at 5000 rpm for 20 min and washed in PBS (pH 7.4) and then lysed through sonication with Branson Digital Sonifier. The sonicated sample was centrifuged at 10,000 rpm for 20 min. And the pellet went through sonication for two more times, before we dissolve the inclusion bodies in the pellet in 8 M urea (PBS, pH 7.4). After removing the Insoluble debris by centrifugation at 10,000 rpm for 20 min, Ni-NTA resin (QIAGEN) was added into the soluble supernatant and mixing on a shaker overnight at 4°C. The whole mixture was loaded into a column, and the bound protein was re-natured through slow washing the column with decreased concentration of urea (8 M, 6 M, 4 M, 3 M, 2 M, 1 M, and 0 M). The column was then washed by 20 mM imidazole in PBS, and eluted with 250 mM imidazole in PBS. The final protein product was dialyzed in PBS (pH 8).

2.5.3 Loading Cysteine Variants onto 50 nm GNPs

50 nm GNPs were purchased from NANOCS™. Conjugation of cysteine variants to 50 nm GNPs was performed according to the method of Chen et al. [138]. Antigen-GNP conjugation was achieved by titrating the antigens into a

GNP's suspension. After reaching the saturation point, the antigen-GNP complexes were pelleted by centrifugation at 6000×g for 60 min at 4°C, and the supernatant was removed and saved for protein analysis. The antigen-GNP pellet was then re-suspended in PBS and used for rabbit immunization. The amount of antigen loaded onto GNPs was calculated as the amount of antigen initially added minus the amount of antigen in the supernatant after centrifugation.

2.5.4 Gel Electrophoresis

Gel analysis was done according to the method from Chen et al. [138] with slight modifications. The antigen-GNP pellet was re-suspended in 10 µl of 1% tris-buffered saline (TBS) and loaded onto a 0.8% agarose gel. Gel separation was performed using an electrophoresis unit running at 80 V for 1 hr at room temperature. Gels were stained with 0.5% Coomassie Brilliant Blue R-250 in 50% methanol and 10% acetic acid and destained in 40 % methanol and 10 % acetic acid to view the protein bands.

2.5.5 Rabbit Immunization

New Zealand white female rabbits (2 kg) were purchased from Charles River (USA) and housed under specific-pathogen-free environments following the animal protocol guidelines of the Committee on Animal Care of Iowa State University. For 54QC and C54Q we subcutaneously immunized 3 rabbits each on weeks 0, 4, 9 and 15. For 12C, 19C and 26C, we immunized 2 rabbits each

on weeks 0, 4, 9 loaded on GNPs and 13, 17, 22 loaded on ZNC. The immunizations were performed with a dose of 50μg for antigens loaded on GNPs and 200μg for antigens loaded on ZNC per immunization, and blood was collected 2 weeks after each immunization.

2.5.6 Enzyme-linked Immunosorbent Assay (ELISA)

Blood was drawn from the central ear artery at two weeks after each injection, and antibody titer was determined using ELISA. Briefly, 30 ng of cysteine variants protein were added onto each well of the 96-well Nunc-Immuno Plates in coating buffer (15 mM Na_2CO_3, 35 mM $NaHCO_3$, 3 mM NaN_3, pH 9.6) overnight at $4\,^{\circ}C$. 200 μl of blocking buffer containing 2.5% skim milk and 5% calf serum in PBS was added into each well and incubated at $37\,^{\circ}C$ for 1hr to block the non-specific binding of antibodies, and the plates were washed 5 times with 0.1% Tween 20 in PBS. Rabbit serum (anti-cysteine variant) was diluted 1:1000 in blocking buffer, and 100 μl of serial 3-fold dilutions were added to each well and incubated for 2 hrs at $37\,^{\circ}C$. Wells were washed five times, and horseradish peroxidase (HRP)-linked secondary antibody (goat anti-rabbit, 1:3000 dilution) (Thermo Scientific; Cat #31430) was added to each well and incubated (100 μl, 1 hr at $37\,^{\circ}C$). Each well was washed five times before adding 100 μl of TMB HRP-substrate (Bio-Rad) for 10 min developing. 50 μl of 2 N H_2SO_4 was then added to each well to stop the reaction. The 450 nm value was read on a microplate reader (Versamax by Molecular Devices). Experiments were performed in duplicate.

2.5.7 GNP ELISA

Also to determine if GNP-bound cysteine variants were recognized by 2F5, 4E10, and Z13, ELISA was done mainly according to the methods of Chen et al [138]. Briefly, to coat plates with protein loaded GNPs, each well was pretreated with 200 µl of 1 mM 3-aminopropyl-triethoxysilane (APTES) in ethanol at room temperature for 40 min. According to the authors, APTES encourages optimal crosslinking of GNPs to plastic wells, allowing an effective ELISA to be conducted. The activated wells were washed with ethanol twice, followed by distilled water twice. Antigen-loaded GNPs were coated at 30ng/well onto 96-well Nunc-Immuno plates using a coating buffer (150mM Na_2CO_3, 350mM $NaHCO_3$, 30 mM NaN_3, pH9.6), and they were incubated at room temperature for 2 hrs. This was followed by three distilled water washes and three washes with 0.5% Triton X-100 in PBS. The assay proceeded with the conventional ELISA steps as above. Human monoclonal antibodies (2F5 [177-179], 4E10 [180] and Z13e1 [63,65] and goat anti-human (Thermo-Scientific; Cat# 31430) were used as primary and secondary antibodies respectively.

2.5.8 Peptide ELISA

Peptide ELISA with overlapping biotinylated peptides (10-mer, mixture of both N and C terminally biotinylated peptides) was also performed as described, except that 10-mer peptides (200 ng/well, 100 ng of N terminal plus 100 ng C terminal biotinylated peptides) covering the entire length of the original gp41-54Q

antigen were coated onto a streptavidin-coated plate instead of the whole antigens. The rest of the test followed conventional ELISA steps as previously outlined.

2.5.9 Neutralization Assays

Single round HIV-1 pseudovirus infection assays in TZM-bl cells were measured by a luciferase-based assay as previously described [196,197]. Briefly, heat inactivated (56°C for 1h) rabbit sera were diluted in Dulbecco's modified Eagle's medium (DMEM) with 10% heat inactivated FBS and incubated for 1 hr in the presence of 200 50% tissue culture infective doses (TCID50) of virus at 37°C. $1*10^4$ TZM-bl cells were then added into the mixtures with DEAE-dextran (Sigma) added at a final concentration of 10 µg/ml. Plates were incubated at 37°C for 48 hrs, developed with Bright-Glo Luciferase (Promega, Madison, WI) and analyzed for luciferase activity using a luminometer (Synergy 2, BioTek). The 50% inhibitory dose (ID50) or concentration (IC50) was defined as either the sera dilution or purified IgG concentration at which relative luminescence units (RLU) were reduced 50% compared to virus control wells after subtraction of background RLU in cell control wells.

Viruses tested were SF162 (tier 1A, clade B), MW965.26 (tier 1A, clade C), and MN.3 (tier 1A, clade B). Murine leukemia virus Env plasmid was used as a negative control. Sera were heat inactivated (60 min, 56°C) before use.

2.6   Acknowledgments

CHAPTER 3   DEVELOPMENT OF A NOVEL ANTIGEN DELIVERY PLATFORM BASED ON GOLD NANOPARTICLES TO INDUCE POTENT ANTIBODY RESPONSES

Feng Lin[1, 2], Habtom H. Habte[1, 2], Yali Qin[1, 2], Kari L. Rohl[1, 2], Feng Jiao[1, 2], Keiji Takamoto[3] and Michael W. Cho[1, 2, *]

[1]Department of Biomedical Sciences, [2]Center for Advanced Host Defenses, Immunobiotics and Translational Comparative Medicine, Iowa State University, Ames, IA 50011, USA.

[3]Department of Biochemistry, Albert Einstein College of Medicine, New York, NY 10461, USA

*Corresponding Author.

Email addresses:

FL: fenglin@iastate.edu

HHH: hhhabte@gmail.com

YQ: yaliq@hotmail.com

KLR: klrohl@iastate.edu

FJ: fjiao@iastate.edu

KT: kgtakamoto@gmail.com

MWC: mcho@iastate.edu

3.1   Abstract

Inducing high titers of broadly neutralizing antibodies (bnAbs) against HIV-1 is a critical step towards developing a protective vaccine against the virus. Although subunit protein immunizations can induce high antibody titers, they often utilize lipid-based adjuvants that could potentially denature protein immunogens, which would likely result in the loss of conformational epitope structures targeted by bnAbs. Hence, development of an antigen delivery platform that could induce strong antibody responses without using lipid-based adjuvants is much needed. In this study, we describe the establishment of an antigen delivery platform based on gold nanoparticles (GNP) that uses N-[Nα,Nα-Bis(carboxymethyl)-L-lysine]-12-mercaptododecanamide for loading any proteins with a 6xHis tag. This antigen loading strategy was used for efficient release of antigens in endosomes upon acidification, which would facilitate antigen processing and presentation. Our platform allows display of polyvalent forms of antigens for efficient B cell receptor crosslinking and B cell activation. Furthermore, the platform is modular and could allow the use of different antigens as well as co-stimulatory molecules. To demonstrate its potential, gp120-ODx3 was used as a model antigen that consists of three tandem repeats of the HIV-1 gp120 outer domain. The antigenic properties of the protein bound to GNP were well preserved. The protein was highly immunogenic in both mice and rabbits, inducing antibody titers up to 10^7 after three immunizations without any adjuvants. Neutralizing assays demonstrated induction of nAbs against tier 1

HIV-1 isolates from multiple clades. Results thus far demonstrate that our GNP-based antigen delivery platform has great potential.

3.2 Introduction

An effective HIV-1 vaccine that can stop the AIDS pandemic has yet to be developed. While many efforts have been made in developing immunogens, many researchers are working towards the development of a delivery platform that will enhance the effectiveness of the vaccine candidates as well [163,198-201]. GNPs are one of the most popular delivery platforms. They have been widely used and studied in different areas like bio-imaging [202], biosensor [203], and delivery platform for drugs [204-208] and vaccines [131,161,167,209].

The GNP delivery platform can present the antigen to the immune system in a multivalent manner, which has the potential to greatly enhance immune response [173,210,211]. GNPs can attach to the antigen either directly or with a linker. For small peptide antigens, the best way to link the antigen to GNPs is through a cysteine amino acid [212,213]. An introduced linker can also be used to attach the target antigen onto the GNPs [161,207,208,214,215]. In this paper we chose to study the linker SH-NTA.

When nitrilotriacetic acid (NTA) is coupled with a metal ion (Co^{2+}, Ni^{2+}, Cu^{2+}, Zn^{2+}), it has high affinity to the histidine imidazole ring [216]. Therefore, Ni-NTA resin/columns have been widely used for his-tagged protein purification. The NTA linker on GNP can also be useful in labeling [217,218] different his-tagged proteins. In the early 1990s, Hainfeld et al. [219] used a similar linker,

NTA-dipeptide-thiol, for a His-tagged adenovirus "knob" protein on 1.8 nm GNP as a probe for cell receptors. Later, Brinas et al. [220] tried to apply the same NTA linker on size–controlled GNPs (2 to 6 nm). Cho et al. [221] used MutS on a Ni-NTA coated gold electrode to detect the DNA mismatches. NTA linkers can also be used to bind an enzyme on the gold surface. SH-NTA linker [222] is used to bind the silicatein on the gold surface without disturbing its biocatalytic activity. Nakamura et al. [223] used three different NTA linkers to immobilize his-tagged endoglucanase on the gold surface, the enzyme still retained its inherent hydrolytic activity. Although the NTA linker has many different uses and applications, we are unaware of any publication that has the NTA linker on GNPs to deliver vaccines.

We choose Cu^{2+} over other metal ions, like the Ni^{2+}, because it will couple to NTA in a more stable manner [224], and it has stronger binding with the protein antigens [225] on GNPs. Thus, in our linker system, the thiol group of the SH-NTA is bound at one end to the GNP, while the other end has the NTA, which can bind to the histidine in the protein antigen. The thiol-gold bond is very strong, on the order of 50 kcal/mol [137], while the bind between Cu-NTA and histidine will break under acidic conditions (Figure 3.1). Therefore, after the antigen-presenting cell (APC) has taken up the GNPs, the protein antigens on the GNP surface will be released in the endosome. This allows the proteinase to easily degrade the antigen for later processing.
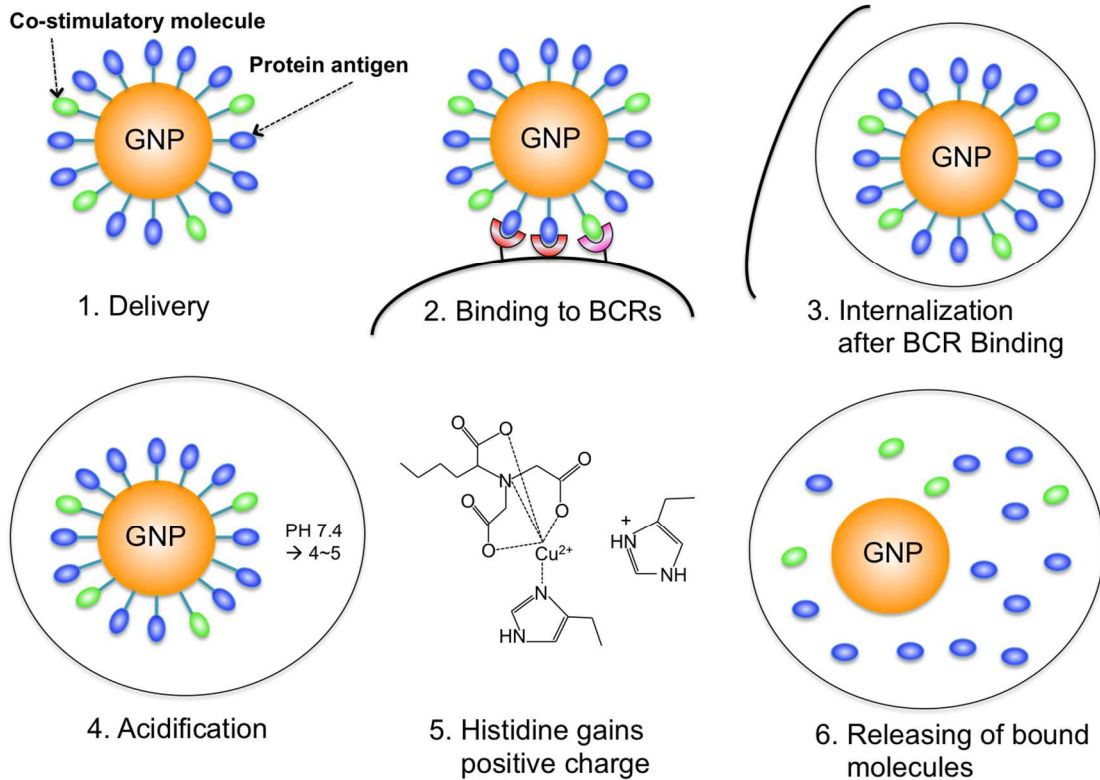
Figure 3.1: Proposed mechanism of antigen delivery in vivo through GNPs

The antigen loaded GNPs can be engulfed by APC. Inside the endosome of APC, the pH in the environment will reduce, which will then facilitate the breakage of the binding between the protein antigens with the GNPs. The released antigens are subjected for down-stream processing of the immune cells.

Previously, we reported using a protein-based antigen derived from gp120 outer domain (OD) as a vaccine candidate [80]. In that study, we found that ODx3 is potentially better than gp120. Since we are unaware of any studies using GNPs to deliver a HIV-based subunit immunogen, it is important to test this novel delivery platform for this purpose. We use SH-NTA as a linker to bridge the GNP and our protein antigen ODx3 and test its immunogenicity in both mice and rabbits.

3.3   Results

3.3.1   Loading Antigen on GNPs

The protein antigen ODx3 can be easily attached to the GNP through the SH-NTA linker (Figure 3.2, A). The binding capacity was measured by loading different amounts of antigen on the GNPs, and then measuring the unbound protein remaining in the supernatant after spinning down the particles. We found that 1ml of GNPs (4.5×10^{10} particles) can bind up to 20µg of ODx3. The conjugation of ODx3 to GNPs was analyzed by 1% agarose gel electrophoresis (Figure 3.2, B). GNPs alone cannot move on the gel, but after coupled to SH-NTA, the particles become negatively charged and are able to migrate. When ODx3 is loaded on the particles, the pKa of ODx3 (9.6) is higher than the pH of the TAE (pH 8.0), they will be retained more than the SH-NTA particles alone because of the added molecules and the positive charge of the protein in the running buffer.
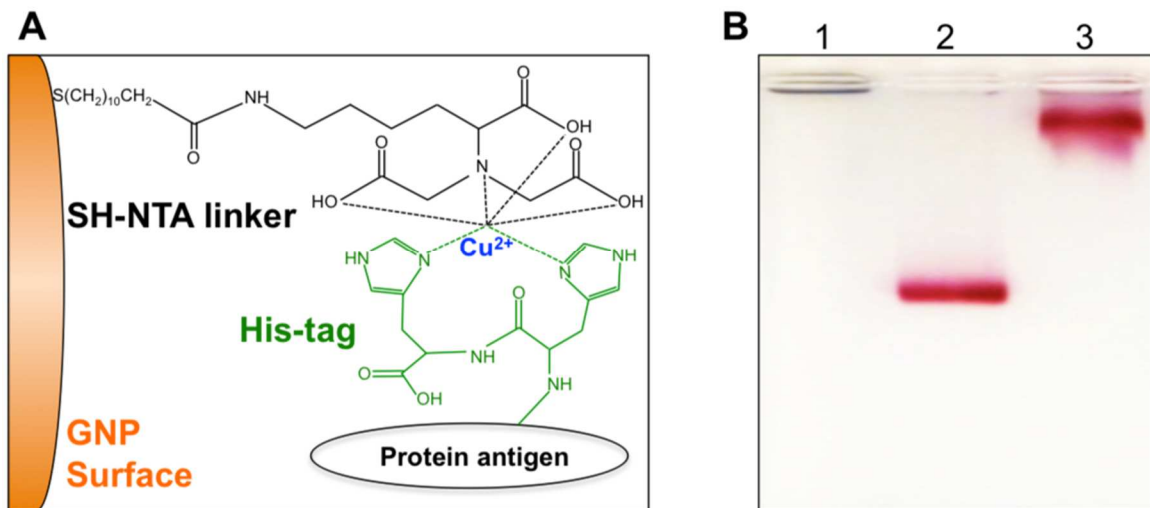
Figure 3.2: Gold binding diagram and agarose gel analysis

(A) Schematic diagram showing how ODx3 is linked on GNPs. (B) GNPs and antigen running on 1% agarose gel under 80V for 1 hr. Lane 1: GNPs only; Lane 2: GNPs coated with the SH-NTA linker; Lane 3: ODx3 loaded GNP-NTA particles.

3.3.2 Antigenicity Test

To test whether the epitopes of common gp120 neutralizing antibodies are still exposed after ODx3 was loaded on the GNPs, we used both the enzyme-linked immunosorbent assay (ELISA) (Figure 3.3, A) and Immunoprecipitation (IP) (Figure 3.3, B). For the ELISA, we coated a 96-well plate with the protein-linked particles and tested the binding with the antibodies. For IP, different antibodies were used to test whether they could pull down the antigen-coated particles. 10A3 is one monoclonal antibody we isolated from a gp120-immunized rabbit that targets the gp120 V3 loop (unpublished data). 257-D IV [53,226] and 447-52D [227,228] are also V3 loop targeting antibodies. PGT 121 [229,230] binds to the N332 glycan-V3 loop. The epitope of 2G12 [54,177,231-233] is glycan dependent. 2C2 was used as a negative control, a non-neutralizing monoclonal antibody we isolated from a gp41-based antigen immunized rabbit that targets the heptad repeat 2 (HR2) and membrane proximal external region (MPER) (unpublished data). Thus, as we can see from Figure 3.3, even after attachment to the GNPs, ODx3 can still display the epitopes of the neutralizing antibodies well, especially for the V3 loop and the glycan epitopes. There is also a small amount of signal for VRC01 [234], even though its epitope is the CD4 binding site.
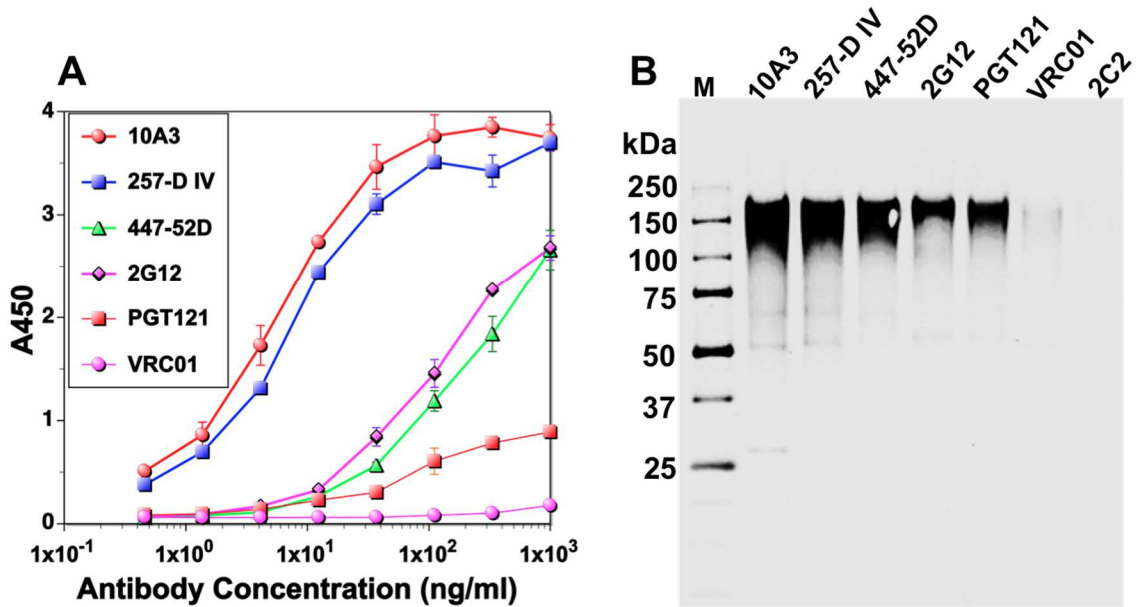
Figure 3.3: Antibodies detection of ODx3 conjugated to GNP-NTA

(A) Plate coated with ODx3 loaded GNPs tested with different antibodies using ELISA. (B) Gel shows western blot result of IP assay using ODx3 on GNPs to pull out different antibodies.

3.3.3 Immunogenicity Responses in Mice

We initially tested the immunogenicity of the GNP-linked antigen in mice. The mice immunization was conducted first by comparing the ODx3 loaded on GNP group, the ODx3-only immunization group, and the GNPs-only immunization group. The GNPs-only immunization group did not show any immune response (data not shown). For the other two groups, we collected the serum samples two weeks after the second and third immunization, and then tested the antibody titer using ELISA. From the ELISA data we can see a major difference in the titer between the two groups after both the 2nd and 3rd

immunizations (Figure 3.4). Following the second immunization, there is a five-fold increase between ODx3-GNP and ODx3 alone, and an even larger increase of close to ten-fold after the 3rd immunization. The fact that the antibody titer of ODx3 on GNP can reach 10^7 after only three immunizations is quite significant, especially since no adjuvant was used. This shows that the GNP-NTA delivery platform was a great benefit to the immune system.
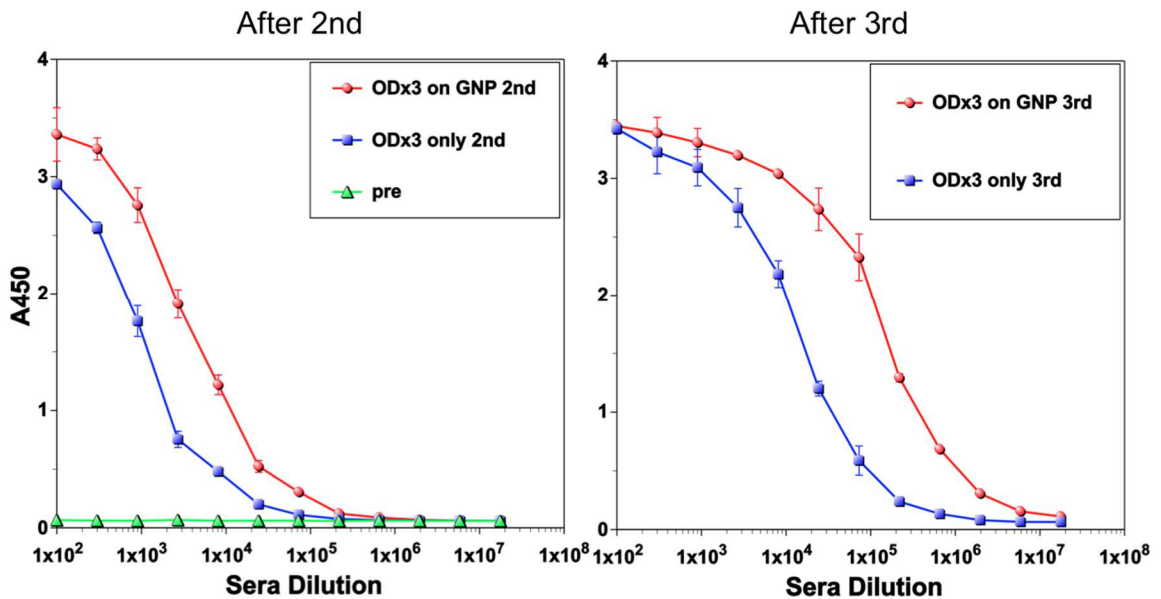
Figure 3.4: Serum immunogenicity in mice

Antibody responses elicited in mice using only ODx3 protein and ODx3 loaded GNPs. Pre is a negative control that means before immunization; 2nd and 3rd indicate the sera withdraw from after 2nd and 3rd immunizations.

3.3.4 Immunogenicity Responses in Rabbits

The rabbit serum samples were also collected two weeks after each immunization. Figure 3.5 shows how the titer gradually increases after each immunization; after the third immunization, the titer also reached to 10^7. Therefore, the GNP-NTA platform successfully enhanced the immune response in both mice and rabbits. We also looked into the specific binding pattern of the immune response using linear epitope mapping. This showed us where the immune response was focused in the rabbit serum. In Figure 3.6, we can see that the strongest signal is in the V3 and C4 regions. This result is consistent with our previous study using zinc chitosan (ZNC) to deliver ODx3 in rabbits [80]. The V3 loop is known to play a key role in HIV entry by binding to the co-receptor CXCR4 and CCR5 [235]. We can see in all the rabbits immunized, the serum antibodies from all the rabbits immunized showed an affinity for the linear epitopes in the V3 region (Figure 3.7). As mentioned earlier, even after loading ODx3 on the GNP, the epitopes are still preserved and accessible for neutralizing antibodies, exhibiting strong affinity to antibodies targeting the V3 loop (Figure 3.3). Therefore, this GNP-NTA platform will preserve the epitopes of the antigen we loaded. Peptide ELISA was also performed using the MCON6 variable region peptides, because the ODx3 was originally generated based on MCON6 sequence [80]. We can also see strong binding in V3 and C4 region.
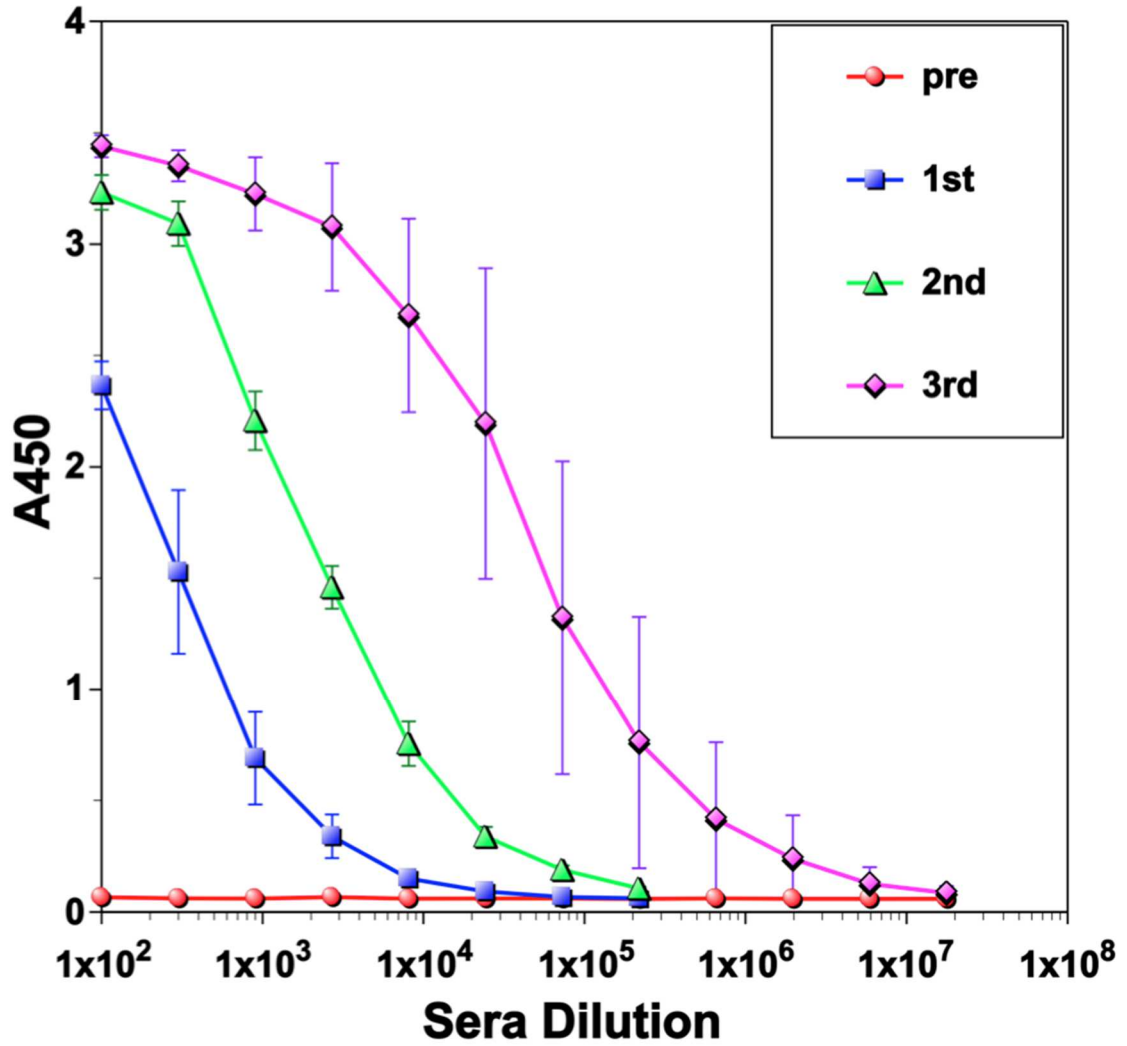
Figure 3.5: Serum immunogenicity in rabbits

Antibody responses elicited in rabbits using ODx3 loaded GNPs. Pre means before immunization;

2nd and 3rd indicate the sera withdraw from after 2nd and 3rd immunizations
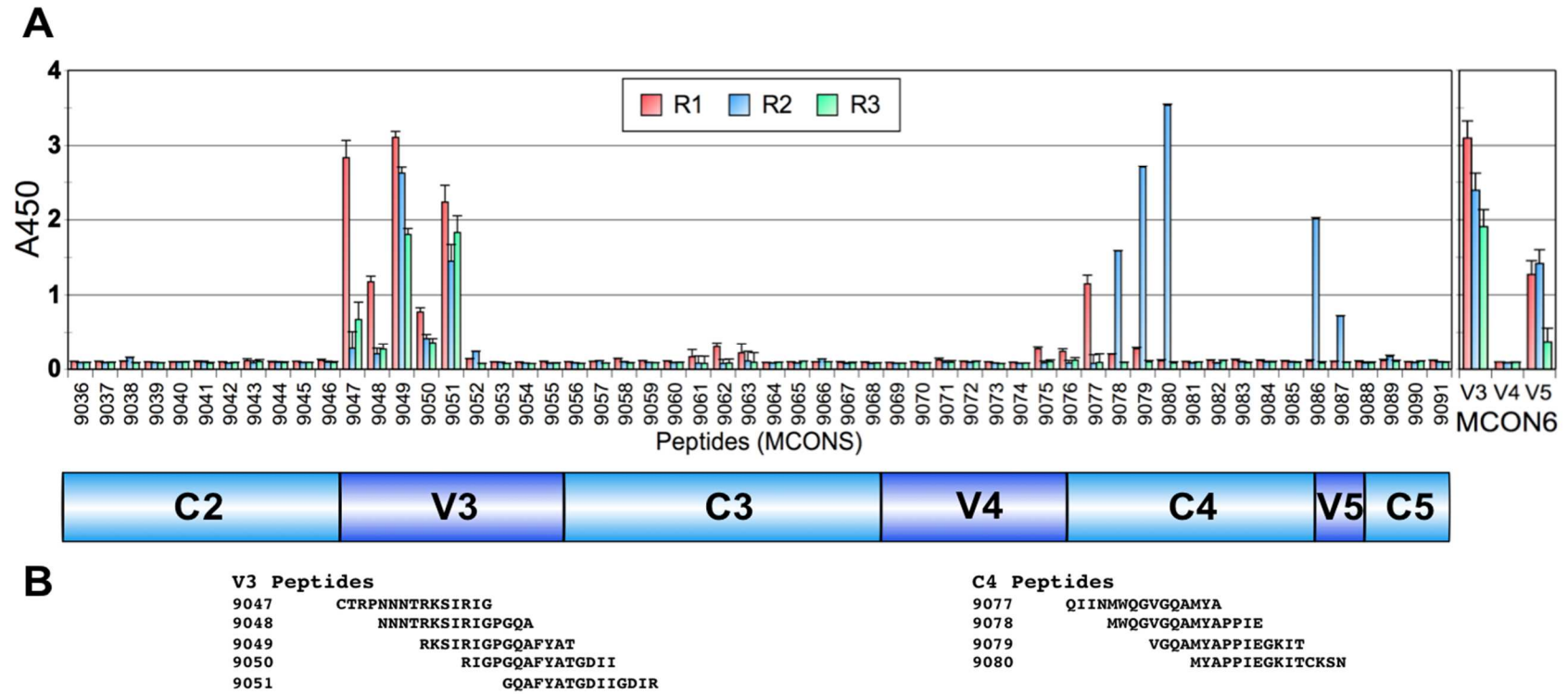
Figure 3.6: Linear epitopes identification

15-mer overlapping peptides covering the whole gp120 outer domain region was used. (A) Linear epitope of different rabbit serum sample. R1, R2, R3 are rabbit numbers. The serum is from the ODx3 loaded on GNP-NTA post-third immunization. (B) List of immunogenic epitopes in V3 and C4 region.

3.3.5 Neutralizing Activity

Pseudovirus neutralization assay was performed to test the anti-HIV-1 activity of the immunized rabbit sera from all groups in TZM-bl cells. Several viruses from Clade B and C were tested. We did not detect any neutralizing activity in mouse sera; however, the rabbit sera (Table 3.1, A), had potent neutralizing activity against tier 1A viruses. For the tier 1B viruses BaL.26, SS1196.1 and 6535.3, there was little or no neutralizing activity within the sera. To eliminate other factors in the serum as the cause of the neutralization, we purified the serum IgG and repeated the assay. With the purified IgG, these tier 1B viruses can now be neutralized (Table 3.1, B).

Table 3.1: TZM-bl assay tested using HIV-1 pseudo-viruses with serum (A) and purified IgG (B) from after third immunization.

A (ID$_{50}$, dilution)	SF162.LS (B, Tier 1A)	MN.3 (B, Tier 1A)	MW965.26 (C, Tier 1A)	BaL.26 (B, Tier 1B)	SS1196.1 (B, Tier 1B)	6535.3 (B, Tier 2)	MuLV
R1	806.7	163.8	411.4	32.98	<20	<20	<20
R2	277.9	101.4	73.92	<20	<20	<20	<20
R3	262.5	38.65	257.2	<20	<20	<20	<20

B (IC$_{50}$, µg/ml)	SF162.LS (B, Tier 1A)	MN.3 (B, Tier 1A)	MW965.26 (C, Tier 1A)	BaL.26 (B, Tier 1B)	SS1196.1 (B, Tier 1B)	6535.3 (B, Tier 2)
R1	2.559	8.989	5.890	36.86	407.5	408
R2	5.870	7.442	26.05	66.12	406.1	>500
R3	9.918	56.95	15.12	>500	>500	>500
VRC01	0.2153	0.03087	0.04167	0.04394	0.1578	1.156

ID$_{50}$	IC$_{50}$
<20	<1
<50	<10
<100	<50
<200	<100
<500	<500
>500	>500

3.3.6 Inhibition Assay

We further conducted a neutralization inhibition assay using the MCON6 V3 loop peptide (TRPNNNTRKSIHIGPGQAFYATGEIIGDIRQAH) to assess if the V3 loop is crucial for neutralization activity or not. For this analysis, we used the purified IgG (100 mg/ml) from rabbits in the presence of various concentrations of the peptide. VRC01 (10 mg/ml) was used as a negative control. As shown in Figure 3.7, neutralization of both MN.3 and MW965.26 viruses by ODx3 induced nAbs was efficiently inhibited by the peptide. As expected, the neutralizing activity of VRC01 was not affected. The peptide affected the neutralizing activity of MN.3 more than it did MW965.26. This could be that the IC_{50} of the purified IgG against MN.3 is higher than it is against of MW965.26. Especially for the IgG from R3, the IC_{50} is 56.95 µg/ml against MN.3, which may explain why the peptide can inhibit neutralizing activity even at low concentrations.
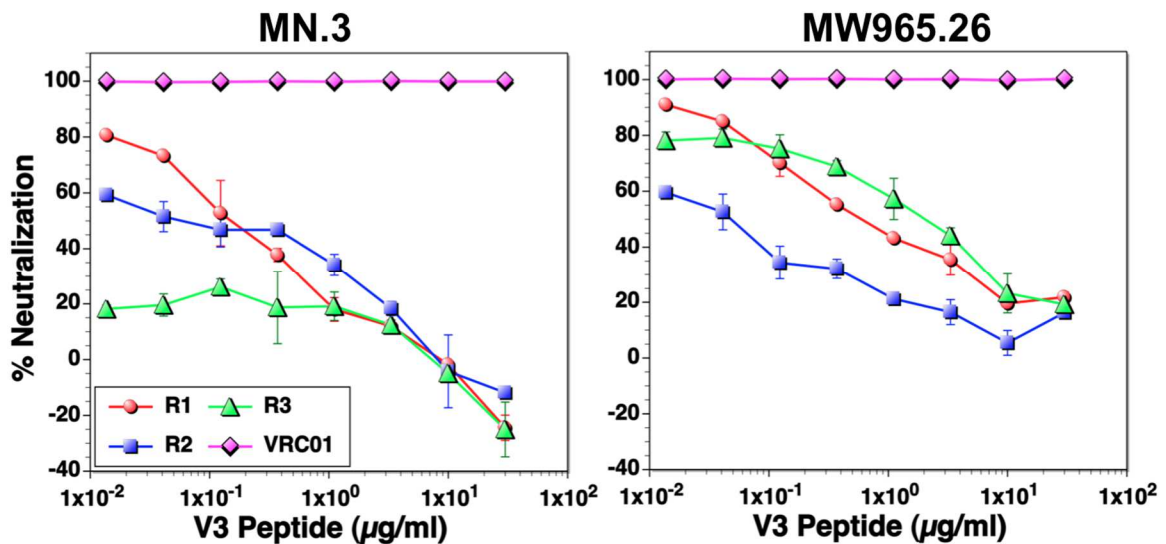
Figure 3.7: Inhibition of neutralizing activity by V3 loop peptide

Neutralizing activity of purified IgG (100 µg/ml) from rabbits immunized with ODx3 on GNPs in the presence of various concentrations of MCON6 V3 peptide (TRPNNNTRKSIHIGPGQAFYATGEIIGDIRQAH). VRC01 bnAb (10 mg/ml) that targets the CD4bs was used as a negative control.

3.4   Discussion

A good delivery platform is crucial for enhancing the effectiveness of a vaccine candidate. GNPs have many advantages when used as a delivery platform for vaccines. They are stable [236], biocompatible [147], and have a variety of sizes and shapes [131,237]. Additionally, the natural bond between gold and the thiol group is quite stable and this reaction does not alter the epitope structure [238,239]. This makes it easy to attach any compound to the GNPs using the thiol group. We introduced a linker called SH-NTA. This linker has a thiol group at one end to attach to the GNPs, and on the other end, the NTA portion has a very strong affinity to the imidazole ring of histidine that can be used to attach the protein antigen. The bond between NTA and histidine is not stable in a low pH environment, which means that after the protein-loaded GNPs are taken up by APCs, the antigen or other activating factor (described in Chapter 4) can be released for further processing because of the acidification inside the endosomes (Figure 3.1). Additionally, a high density of antigens can be loaded onto a single GNP. From our binding test, 1 ml of GNPs (4.5×10^{10} particles) can bind with 20µg of ODx3 without showing aggregation. This means that around 1500 molecules of ODx3 could be loaded onto a single 50nm GNP.

The results from the ELISA and IP assay demonstrated that even after binding to GNPs, the antigen ODx3 still preserved the epitope of commonly used bnAbs. Those epitopes are mostly in the V3 loops, as confirmed later by the epitope mapping and inhibition assay. However, our previous study showed that ODx3 could also bind with VRC01 in the IP assay although the signal is weaker than the V3-loop targeting antibody 447-52D [80]. The weaker binding of VRC01 compared to 447-52D was also observed in this study. But binding of VRC01 is very weak, that we can barely see the signal. This is most likely because compared to normal IP assay, our newly developed IP assay specifically for antigens already loaded on GNPs is more complicated and requires more steps. Therefore, the loss of some of the antibodies or proteins during the washing is a possible contributing factor to the loss of the final signal. It is also possible that after loading on GNPs, CD4bs could be less accessible compared to the V3 loop on ODx3 to the bnAbs. Additionally, the strong binding results of ODx3 with these V3 loop targeted bnAbs from our IP assay are also consistent with those from the ELISA technique designed for antigens loaded on GNPs used previously by other study [138].

We hypothesized that a multivalent antigen would be better at stimulating the immune system to induce high immune responses. We achieved much higher antibody titers from the ODx3 on GNPs than the ODx3 only group in mice. Consistently, there was also a very high immune response from rabbits, with the antibody titer reaching 10^7 (Figure 3.5). The high titer elicited in both mice and rabbits is quite significant. Researchers have been using adjuvants to boost the

immune responses from mice and rabbit for HIV envelope antigens to reach a titer of around 10^5 to 10^6 [240-242]. In our previous study with ODx3, we also observed a titer of 10^7 using zinc-chitosan as an adjuvant with 200 μg of ODx3 [80]. Therefore, the GNPs helped us obtain the same high titer as we obtained from using a potent adjuvant with only half doses, which makes this platform effective in boosting the immune response in two different animal models.

Unfortunately, we did not see neutralizing activity from the mice sera. One possible reason is that mice do not make antibodies with long HCDR3s [243], while most HIV bnAbs have long HCDR3 [244,245]. Therefore, mice may not be a suitable animal model for eliciting HIV nAbs. Law et al. [183] also did not obtain nAbs response from the mice they immunized with HIV envelope based antigen. However, they were able to observe neutralizing activity from the rabbits with the same antigen. Besides, for our study, there were not enough mice sera left for IgG purification or epitope mapping. Therefore, we continued our study further in rabbits, since more blood samples can be collected for further experiments and they possess long HCDR3s [246]. As expected, neutralizing activity was detected from the rabbit serum against several tier 1A viruses (Table 3.1, A). Purified IgG also demonstrated neutralizing activity against several viruses from clade B and clade C. Since the purified IgG is still polyclonal, we suspect that the actual neutralizing antibodies in the serum could probably neutralize these viruses at a much lower concentration.

This study demonstrated that our platform could significantly elevate the immune responses of the loaded antigen in two different animal models.

Although no nAbs were elicited against tier 2 viruses, we can always use this platform to carry other protein antigens that have better antigenicity and immunogenicity to elicit nAbs against tier 2 viruses and further amplify their immune responses. This delivery platform can be applied to any protein-based therapeutic molecules beyond the HIV vaccine development field as described in this study.

In sum, we were able to induce a strong immune response in both mice and rabbits due to the presentation and multivalent coating of epitopes in this novel GNP delivery platform. This platform has great potential for future protein-based biomolecule delivery.

3.5   Materials and Methods

3.5.1 Loading ODx3 onto 50 nm GNPs

1ml of 50nm GNPs were incubated and mixed with 2.5 µl of SH-NTA (1mg/ml freshly prepared in DMSO before use) for 1 hr at room temperature (RT). Then, 67µl of 0.3M Copper (II) sulfate pentahydrate was added to the solution to make the final concentration 20mM. After another 1 hr incubation, 8 µg of ODx3 (diluted in 160µl of PBS, pH 8.0) was added and allowed to mixed for 1 hr at RT. The whole mixture was pelleted by centrifugation at 6000g for 1 hr at 4°C. The pellet was washed 1x with PBS (pH 8.0) before immunization study.

3.5.2 Gel Electrophoresis

Agarose gel analysis method was modified from Chen et al. [138]. The ODx3-GNP pellet was re-suspended in 20 µl of 1% tris-buffered saline (TBS) and loaded onto a 1% agarose gel. Gel separation was performed at 80V for 1 hr at RT.

3.5.3 Immunoprecipitation Assay (IP)

The ODx3 loaded GNP was added to 1mL Odyssey Blocking Buffer (LI-COR) and rocked for 1hr at RT. Antibody (1 µg) was mixed with 60µL Protein A beads in 1mL IP buffer (10mM Tris pH 7.5, 200mM NaCl, 1mM EDTA, 0.5% Triton X-100, filter sterilized) for 2hrs at RT. The GNP/NTA/$CuSO_4.5H_2O$/ODx3 mixture was centrifuged (6000g, 1hr, 4°C) to remove the blocking supernatant. The Antibody/Protein A mixture was centrifuged at 200g for 5min and the supernatant was removed. The pellet was re-suspended in 1ml IP buffer. The mixture was then added to the GNP/NTA/ $CuSO_4.5H_2O$ /ODx3 pellet and rocked overnight at 4°C. The mixture was centrifuged at 200g for 3min. The supernatant was removed and pellet washed 2x with 1mL IP buffer. After the supernatant was removed, a SDS sample buffer was added to all samples and boiled for 10 min. Sample (20 µl) was loaded on a 4-20% Tris-glycine gel, and ran at 120V for 2 hrs. The gel was then transferred to a nitrocellulose membrane at 250 Amps for 70 min. Western was performed according to Odyssey protocol. Briefly, the membrane was blocked at 4°C overnight. The primary antibody was a monoclonal mouse antibody specific for ODx3 (S7.5.14) at a 1:2500 dilution,

rocked for 1 hr at RT. The secondary antibody, anti-mouse (OD_{680}) from Odyssey, was utilized in a dilution of 1:10,000 and incubated for 1 hr at RT. The membrane was read using an imaging machine (ODYSSEY CLx, LI-COR).

3.5.4 Mice and Rabbit Immunization

Female BALB/CJ mice (Jackson Lab) were immunized intraperitoneally with 10 µg of protein, either alone or loaded on the GNPs, at weeks 0, 3, and 7. Blood was collected at weeks 5 and 9 through the lateral tail vein.

Female New Zealand white rabbits (Charles River) were immunized subcutaneously with 100 µg of protein loading on GNPs at weeks 0, 4, and 9. Blood was collected from the central ear artery two weeks after each immunization. All animal studies were conducted with the approval of IACUC.

3.5.5 Enzyme-linked Immunosorbent Assay (ELISA)

ELISA was used to monitor the immune responses of the antigen. Antigen (30 ng) was coated onto 96-well Nunc-Immuno plates overnight at 4 °C (coating buffer: 15 mM Na_2CO_3, 35 mM $NaHCO_3$, 3 mM NaN_3, pH 9.6). The following morning, 200 µl of blocking buffer (1xPBS, pH 7.4, with 2.5% skim milk and 5% Calf Serum) was added to each well to block the uncoated surface and incubate at 37 °C for 1 hr. After discarding the coating buffer, wells were then washed 10x using washing buffer (PBS containing 0.1% Tween 20). Animal sera samples were diluted in blocking buffer, and 100 µl of 3-fold serial dilutions was added to each well and incubated for 2 hrs at 37 °C. The wells were washed 10x, and

horseradish peroxidase (HRP)-linked secondary antibody (goat anti-rabbit, 1:3000 dilution) was added to each well and incubated for 1 hr at 37 °C. Wells were washed 10x and developed by adding 100 µl TMB HRP-substrate (Bio-Rad) for 10 min. Reactions were stopped with 50 µl of 2 N H_2SO_4. Plates were read on a micro-plate reader (Versamax by Molecular Devices) at 450 nm. Experiments were performed in duplicate.

3.5.6 GNP ELISA

GNP ELISA was done according to the methods from Chen et al [138]. Briefly, to coat plates with protein loaded GNPs, 200 µl of 1 mM 3-aminopropyl-triethoxysilane (APTES) in ethanol was added to each well and incubating 40 min at room temperature. According to the authors, APTES facilitate the crosslinking of GNPs to plastic wells. The pretreated wells were washed with ethanol twice, and then distilled water twice. Antigen loaded GNP were coated at 30 ng/well onto 96-well Nunc-Immuno Plates using coating buffer (150mM Na_2CO_3, 350mM $NaHCO_3$, 30 mM NaN_3, pH9.6), and they were incubated at room temperature for 2 hrs. Then, the wells will be wash with distilled water three times and 0.5% Triton X-100 in PBS three times. The assay proceeded with the conventional ELISA steps as stated above.

3.5.7 Peptide ELISA

Peptide ELISA with overlapping peptides (15-mer) was also performed. 15-mer peptides (100 ng/well) covering the entire length of the OD region of

gp120 were coated onto a streptavidin-coated plate instead of the whole antigens. The rest was the conventional ELISA steps as stated above.

3.5.8 Neutralization Assays

HIV-1 pseudovirus infection assays in TZM-bl cells were carried out as previously described [196]. Briefly, heat inactivated (56°C for 1 hr) rabbit sera or purified IgG were diluted in Dulbecco's modified Eagle's medium (DMEM) with 10% heat inactivated FBS and incubated for 1 hr in the presence of viruses at 37°C. TZM-bl cells (1×10^4) were then added to the mixtures in medium containing DEAE-dextran (Sigma) at a final concentration of 10 µg/ml. Plates were incubated at 37°C for 48 hrs, developed with Bright-Glo Luciferase Assay kit (Promega, Madison, WI) and immediately analyzed for luciferase activity with an illuminometer (Synergy 2, BioTek). The 50% inhibitory dose (ID_{50}) or concentration (IC_{50}) were defined as the sera dilution or purified IgG concentration at which relative luminescence units (RLU) were reduced 50% compared to virus control wells after subtraction of background RLU in cell control wells. For the peptide inhibition neutralizing assays, the same procedure was followed except that antibodies were pre-incubated with V3 peptide (in varying concentrations) for 1 hr at 37°C.

Viruses tested were SF162.LS (tier 1A, Clade B), MW965.26 (tier 1A, Clade C), MN.3 (tier 1A, Clade B), BaL.26 (tier 1B, Clade B), SS1196.1 (tier 1B, Clade B), and 6535.3 (tier 1B, Clade B). Also murine leukemia virus Env-pseudotyped virus (MuLv) was used as a negative control.

3.6   Acknowledgments

CHAPTER 4   GENERAL CONCLUSIONS

GNPs as a promising delivery platform have already been used for human clinical trials in cancer research [247,248]. There is also an explosion of applications of GNPs in drug and vaccine delivery recently as described in Chapter 1. However, we are not aware of any studies using GNPs to deliver protein-based HIV antigens. Since HIV vaccine development is still moving slowly, with limited success during the past 30 years, we decided to include GNPs in our research to explore their potential to accelerate HIV vaccine research.

4.1   Conclusions

4.1.1 Linking HIV-1 Envelope Antigens Directly on GNPs

As we know from Chapter 1, thiol can form a strong bond with GNP. The only amino acid that has thiol group is cysteine; therefore, we introduced cysteine mutations into the original gp41-54Q antigen to make several cysteine variants by site-directed mutagenesis. All these cysteine variants can successfully bind to GNPs and expose the epitope to several common bnAbs after binding to the GNPs. However, while the two terminal variants (54QC and C54Q) can elicit strong immune responses with the antibody titer reaching 10^6, we did not detect any neutralizing antibody elicited in the immunized rabbits. Epitope mapping further demonstrated that most antibody responses target the middle of the

antigens, where many non-neutralizing epitopes located. Therefore, we further introduced three other cysteine mutations to make 12C, 19C and 26C, to investigate whether attaching the antigens to GNPs through the middle cysteine could help to block those non-neutralizing epitopes. Unfortunately, we found almost no immune response after the second immunization, and the after third immunization, antibody tiers were around 10^3, which were significantly lower than results from the other two terminal cysteine variants. We supposed that it might because those internal variants cannot be well processed *in vivo* by binding in their middle sections on GNPs. To make sure those antigens are still immunogenic, we further immunized them using ZNC which bind the c-terminal of the antigens through his-tag. This time, we got higher antibody responses; most titers were above 10^5 after the third immunization. This is the first study that reported the eligibility of loading protein antigens from HIV-1 on GNPs to induce antibody responses from rabbits. The results of internal variants suggested that the linking site of antigen to GNPs is crucial and can influence immune responses. A space linker between the antigen and GNPs may be necessary to improve immune responses, this possibility was explored in Chapter 3.

4.1.2 Linking Antigen to GNPs Using The SH-NTA Linker

Linking HIV-1 antigens directly to GNPs may result in inducing low antibody responses as described in Chapter 2. Therefore, we designed two linkers to attach our antigens to GNPs (4-ATP and SH-NTA). The immunogenicity result by using the 4ATP linker is described in the Appendix. We

found that the SH-NTA is potentially better than the 4-ATP linker, so we continued our studies using the SH-NTA linker. The antigen we used for this study is ODx3, a promising protein antigen that consists of three tandem repeats of HIV-1 gp120 outer domain gp120 [80]. Again, the *in vitro* tests demonstrated that ODx3 could be successfully loaded on GNPs through the linker and its epitopes for the V3 targeted bnAbs were still properly exposed after loaded. We compared immune responses of the protein-on-GNP and the protein-only group in mice. From Chapter 3, we can see the protein-on-GNP group clearly gave us stronger titer than the protein-only group. Unfortunately, we did not detect any neutralizing activity in the mice sera. Given the limited mice sera are not enough for detailed epitope mapping and purification of the serum IgG, we continued our study in rabbits. Again, we obtained antibody tier up to 10^7, which was similar to that observed in mice. Those antibody responses were mostly towards the V3 and C4 region in the outer domain, which was also consistent with our published data of ODx3 [80]. Furthermore, nAbs were also elicited against several tier 1 HIV-1 isolates. This platform has demonstrated its capability to delivery HIV Env based antigens with their antigenic properties preserved and immunogenicity enhanced. The results from Chapters 2 and 3 together demonstrate our GNP-based antigen delivery platform has great potential for further development.

4.2   Future directions

4.2.1   Co-stimulatory Molecules

Besides the immunized antigen, there are many other effectors that could contribute to polyclonal B cell activation [249]. One famous stimulator, BlyS (B Lymphocyte Stimulator [250]; also known as BAFF, B-cell activating factor [251]; THANK, TNF Homologue That Activates Apoptosis, Nuclear Factor-κB, and c-Jun NH2-Terminal Kinase [252]; TALL-1, TNF- and ApoL-related leukocyte-expressed ligand 1 [253]; and zTNF4 [254]), a member of the tumor necrosis factor (TNF) family that stimulates B cell growth and immunoglobulin secretion. As a costimulator of B cell proliferation and function, BlyS has been widely used as an adjuvant in vaccine research. Gor et al. [255] fused the human BLyS with Pneumococcal Surface Adhesin A (PsaA), and found that the fusion protein elicited significantly higher serum antibody responses as well as cell-mediated immune responses compared to the Psa A alone in mice. Dosenovic et al. [256] injected BLyS into mice before they immunized their gp140 antigen. Their results also indicated that the pre-injection of BLyS led to a great improvement of the neutralizing antibody responses induced by the antigen against HIV-1. Another commonly used co-stimulator is the CD40 ligand (CD40L, or CD154) [257,258]. CD40L on a T cell surface is known to bind the CD40 molecule on a B cell and cooperates with BLyS in B cell activation [259]. This co-stimulator has also been applied as an adjuvant in vaccine research against viruses including HIV-1 [260,261]. Melchers et al. [262] fused APRIL (A Proliferation–Inducing Ligand, shared two receptors with BLyS [263]), BLyS, and CD40L with gp140 protein and

reported improvement of the induction of humoral immunity against HIV-1 from all the three fusion antigens. Since all these co-stimulatory molecules are proteins, therefore, by introducing his-tag, we can link them together with our antigens on the GNP surface through the SH-NTA linker to facilitate eliciting stronger immune responses.

4.2.2 Gold Nano-cages

Apart from antigens present solely on the surface of GNPs, we can also load antigens inside GNPs by using gold nano-cages (GNCs). The principle of making GNCs is based on galvanic replacement reaction. The driving force of this reaction is the electrical potential difference between two different metals; one acts as anode and the other as cathode. The high potential cathode metallic ions are reduced into metal and accumulate on the anode, while the anode metal dissolves into the electrolyte. To make GNCs, we need sliver nano-cubes, which can be easily synthesized by reducing silver nitrate with ethylene glycol in the presence of poly (vinyl pyrrolidone) (PVP) as the capping reagent [264]. Silver serves as the anode, since Ag (Ag^+/Ag, 0.8V) can be oxidized by $HAuCl_4$ ($AuCl_4^-/Au$, 0.99V).

$$3Ag_{(s)} + AuCl_4^-{}_{(aq)} \rightarrow Au_{(s)} + 3Ag^+{}_{(aq)} + 4Cl^-{}_{(aq)}$$

From the formula, we know that one gold atom can replace three silver atoms; therefore, empty spaces continue to grow inside the cube while the reaction continues, and when all the silver atoms are replaced by gold, GNCs are formed (Figure 4.1).
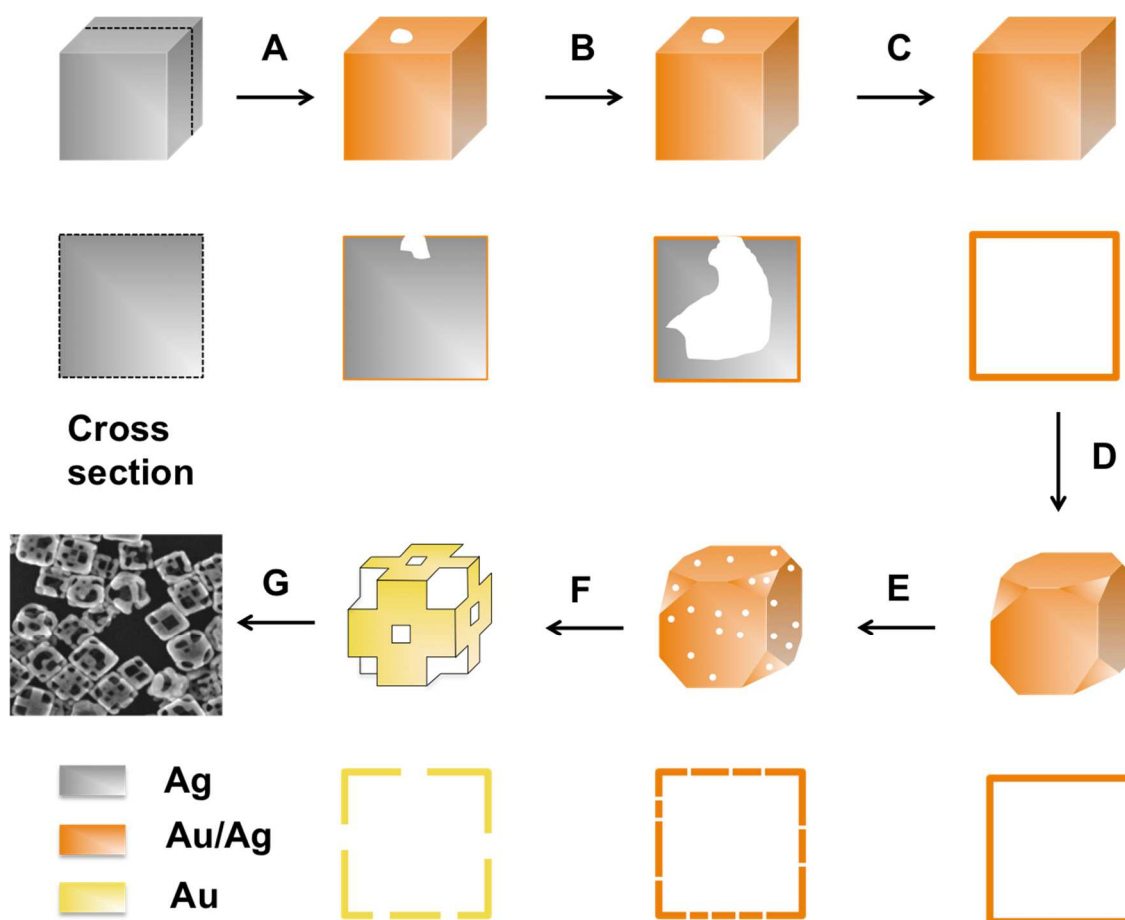
Figure 4.1: Making GNCs through galvanic replacement reaction

(A) Initiation at a spot with high surface energy; (B) Partially hollow nanostructure; (C) Nano-boxes with Au/Ag alloy homogeneous wall; (D) Dealloying and morphological reconstruction; (E) Continuation of dealloying, formation of pores; (F) Gold nano-cage (G) Scanning electron microscopy (SEM) image for the gold nano-cages. Adapted from [265].

To further control the cage wall thickness and nano-cage porosity, we can use $Fe(NO_3)_3$.

$$Ag_{(s)} + Fe(NO_3)_3 \rightarrow AgNO_{3(aq)} + Fe(NO_3)_{2(aq)}$$

This process is called wet chemical etching [266]. Depending on the amount of etchant used, we can control our gold nano-cage with different size of surface pores and internal spaces.

A GNC surface can be used to coat biological molecules for delivery purpose. Chen et al. [267] found that GNC could deliver antibodies on the surface to target cancer cells, and the efficiency for delivery was similar to commercial GNPs (same size spheres). For our vaccine delivery, we can link protein antigens like ODx3 to the surface of GNCs to stimulate the B-cell immune response as we did in Chapter 3.

The inside space of GNCs can also be used for delivery and controlled release of the contained molecules. Yavuz et al. [268] coated a GNC with polymers based on poly (N-isopropylacrylamide) (pNIPAAm) and its derivatives. This kind of polymer can change conformation and uncover the pores on the GNC surface to allow the release of the inside drugs in response to heat. A laser beam can be used to generate heat when its wavelength matches the absorption peak of the GNC through photothermal effect [269]. For our study, the surfaced coated antigens could block the release of the inside antigens. However, when the whole antigen-loaded GNC is engulfed by APCs in the endosomes, the reduction of pH will lead to the release of the surface antigens (see mechanism in Chapter 3), thus, the inside antigen can be released gradually afterwards.

Since the antigen inside the GNC cannot directly contact BCRs to elicit humoral responses, we will select antigens that specifically stimulate the other arm of the immune response, the cell-mediated immunity [270]. In HIV vaccine

research, Gag protein as an essential part of the virus [271] is well known to elicit T cells responses, which correlated with delayed progression [272]. Kiepiela et al. [273] found that from 160 dominant CD8 T-cell responses, only Gag-specific responses were associated with lowering viremia. The CD8 cells from those high Gag responders demonstrated a more significant suppression of the virus replication *in vitro* as well than did low Gag responders [274]. The enhanced CD8 T cell activity from these studies highlighted the usage of the Gag protein or its components as vaccine candidates. The T cell epitopes on Gag has already been identified [275], with one study reporting that patients whose immune responses targeted the conserved HIV-Gag-epitopes had significantly lower viral load compared to those targeting variable epitopes [276]. For our study, the conserved T cell epitope of Gag protein will be selected to load inside the GNCs to eliciting cell-mediated immunity.

APPENDIX   IMMUNIZATION STUDY USING GNR-4ATP PLATFORM

In this study, we investigated the immunogenicity of ODx3 loaded on GNR-4ATP delivery platform. Dr. Chenxu Yu's lab in Iowa State University developed the GNR-4ATP platform and has been using it to load antibodies for bacteria detection[141,142]. With the help from his lab, we decided to test their platform together with our GNP-NTA platform for HIV-1 vaccine delivery research. The producing process of GNRs and the conjunction with protein through the linker 4-ATP on GNRs was elaborated in Chapter 1 (section 1.3.2.2 and 1.3.2.3), and the immunogenicity data of ODx3 loaded on GNP-NTA platform was described in Chapter 3.

ODx3 was intraperitoneally administrated to BALB/c mice at a dose of 10μg per mice either alone or conjugated with GNR-4ATP. The mice were immunized three times at weeks 0, 3, and 7. The presence of anti-ODx3 antibodies was assessed in the sera collected two weeks after the second and third immunizations (Figure Appendix 1). In the GNR-4ATP group, an increased trend of the antibody titer was observed from the second to third administrations, which suggested that the retaining effect of the antigen in the GNR cluster nano-carriers was relatively high due to the strong and stable covalent bonding between ODx3 and diazonium moiety in 4-ATP. Especially for one mouse, the serum titer can reach up to 10^6 after the third boost. However, comparing with the protein-only group, we did not see stronger antibody response brought by this

GNR-4ATP delivery platform. In contrast, the GNP-NTA complex showed much better antibody responses (Chapter 3, Figure 3.4) compared with the results we got from this study. Thus, the results indicated that this GNR-4ATP platform might not be suitable for stimulating strong immune response of the loaded antigen. Therefore, we continued our study using the GNP-NTA platform as described in Chapter 3.
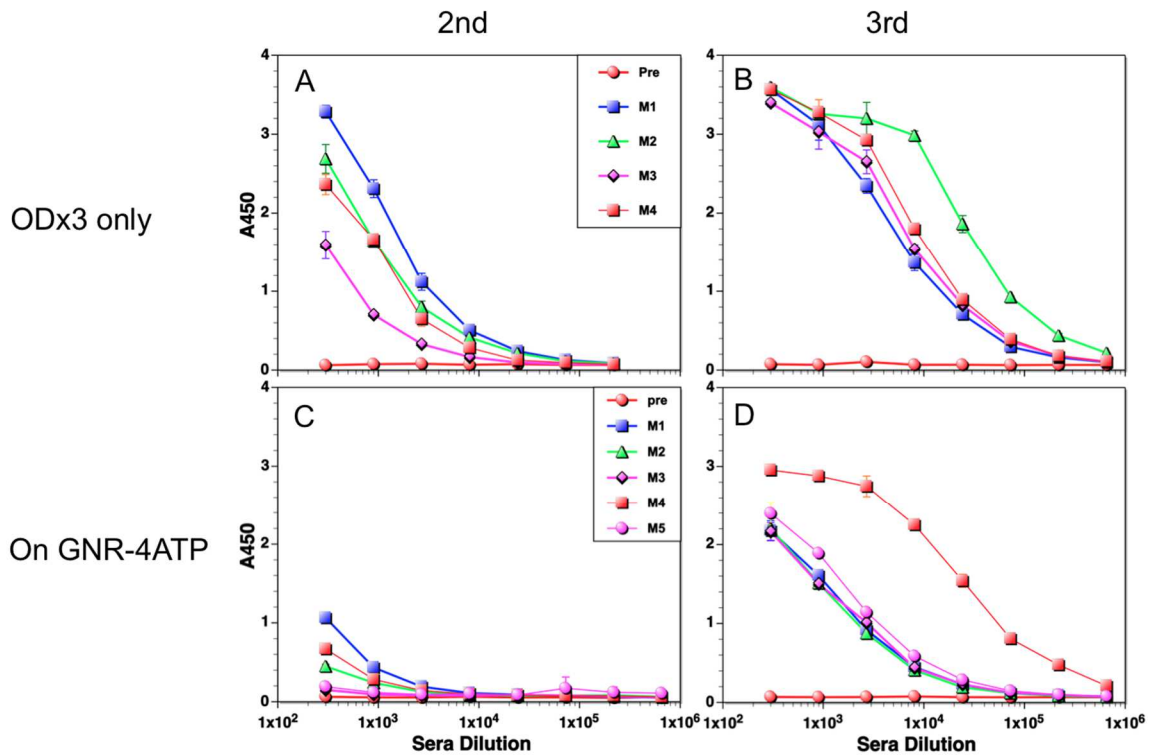
Figure Appendix: Antibody titers of the ODx3 only group and the GNR-4ATP group

(A, C) Sera antibody titer of mice immunized with ODx3 only and delivered on GNR-4ATP after 2nd immunization. (B, D) Same analysis for mice sera after 3rd immunization. Pre is the pre-immunization serum; Mice serum numbers are indicated by M1, M2, M3, M4, and M5.

REFERENCES

1.   Centers for Disease Control. Pneumocystis pneumonia--Los Angeles. *MMWR Morb. Mortal. Wkly. Rep.* 30(21), 250–252 (1981).

2.   Centers for Disease Control. First report of AIDS. *MMWR Morb. Mortal. Wkly. Rep*. 50(21) (2001).

3.   Barré-Sinoussi F, Chermann JC, Rey F, *et al.* Isolation of a T-lymphotropic retrovirus from a patient at risk for acquired immune deficiency syndrome (AIDS). *Science*. 220(4599), 868–871 (1983).

4.   Coffin J, Haase A, Levy JA, *et al.* What to call the AIDS virus? *Nature*. 321(6065), 10 (1986).

5.   Marlink R, Kanki P, Thior I, *et al.* Reduced rate of disease development after HIV-2 infection as compared to HIV-1. *Science*. 265(5178), 1587–1590 (1994).

6.   De Cock KM. Epidemiology and Transmission of HIV-2. *JAMA*. 270(17), 2083 (1993).

7.   Simon F, Mauclère P, Roques P, *et al.* Identification of a new human immunodeficiency virus type 1 distinct from group M and group O. *Nat Med*. 4(9), 1032–1037 (1998).

8.   Plantier J-C, Leoz M, Dickerson JE, *et al.* A new human immunodeficiency virus derived from gorillas. *Nat Med*. 15(8), 871–872 (2009).

9.   Vallari A, Holzmayer V, Harris B, *et al.* Confirmation of Putative HIV-1 Group P in Cameroon. *J Virol*. 85(3), 1403–1407 (2011).

10.   Ward MJ, Lycett SJ, Kalish ML, Rambaut A, Leigh Brown AJ. Estimating the Rate of Intersubtype Recombination in Early HIV-1 Group M Strains. *J Virol*. 87(4), 1967–1973 (2013).

11.   Kiwelu IE, Novitsky V, Margolin L, *et al.* HIV-1 subtypes and recombinants in Northern Tanzania: distribution of viral quasispecies. *PLoS ONE*. 7(10), e47605 (2012).

12.   Buonaguro L, Tornesello ML, Buonaguro FM. Human Immunodeficiency Virus Type 1 Subtype Distribution in the Worldwide Epidemic: Pathogenetic and Therapeutic Implications. *J Virol*. 81(19), 10209–10219 (2007).

13. Hemelaar J, Gouws E, Ghys PD, Osmanov S. Global trends in molecular epidemiology of HIV-1 during 2000–2007. *AIDS*. 25(5), 679–689 (2011).

14. Connors M, Kovacs JA, Krevat S, *et al.* HIV infection induces changes in CD4+ T-cell phenotype and depletions within the CD4+ T-cell repertoire that are not immediately restored by antiviral or immune-based therapies. *Nat Med*. 3(5), 533–540 (1997).

15. Pelchen-Matthews A, Pelchen-Matthews A. Infectious HIV-1 assembles in late endosomes in primary macrophages. *The Journal of Cell Biology*. 162(3), 443–455 (2003).

16. Cunningham AL, Donaghy H, Harman AN, Kim M, Turville SG. Manipulation of dendritic cell function by viruses. *Curr. Opin. Microbiol.* 13(4), 524–529 (2010).

17. Epstein FH, Pantaleo G, Graziosi C, Fauci AS. The Immunopathogenesis of Human Immunodeficiency Virus Infection. *N. Engl. J. Med.* 328(5), 327–335 (1993).

18. Luckheeram RV, Zhou R, Verma AD, Xia B. CD4+T Cells: Differentiation and Functions. *Clinical and Developmental Immunology*. 2012(12), 1–12 (2012).

19. Hogg RS, Hogg RS, Yip B, *et al.* Rates of disease progression by baseline CD4 cell count and viral load after initiating triple-drug therapy. *JAMA*. 286(20), 2568–2577 (2001).

20. Lucas S, Nelson AM. HIV and the spectrum of human disease. *J. Pathol.* 235(2), 229–241 (2015).

21. Fauci AS, Pantaleo G, Stanley S, Weissman D. Immunopathogenic mechanisms of HIV infection. *N. Engl. J. Med.* 328(5). 654–663 (1996).

22. Frankel AD, Young JAT. HIV-1: Fifteen Proteins and an RNA. *Annu. Rev. Biochem.* 67(1), 1–25 (1998).

23. Peterlin BM, Trono D. Hide, shield and strike back: how HIV-infected cells avoid immune eradication. *Nat Rev Immunol*. 3(2), 97–107 (2003).

24. Gallay P, Swingler S, Song J, Bushman F, Trono D. HIV nuclear import is governed by the phosphotyrosine-mediated binding of matrix to the core domain of integrase. *Cell*. 83(4), 569–576 (1995).

25. Franke EK, Franke EK, Luban J, Luban J. Inhibition of HIV-1 Replication by Cyclosporine A or Related Compounds Correlates with the Ability to Disrupt the Gag–Cyclophilin A Interaction. *Virology*. 222(1), 279–282 (1996).

26. Harrison GP, Lever AM. The human immunodeficiency virus type 1 packaging signal and major splice donor region have a conserved stable secondary structure. *J Virol*. 66(7), 4144–4153 (1992).

27. Lapadat-Tapolsky M, Rocquigny HD, Gent DV, Roques B, Plasterk R, Darlix JL. Interactions between HIV-1 nucleocapsid protein and viral DNA may have important functions in the viral life cycle. *Nucleic Acids Res.* 21(4), 831–839 (1993).

28. Paxton W, Connor RI, Landau NR. Incorporation of Vpr into human immunodeficiency virus type 1 virions: requirement for the p6 region of gag and mutational analysis. *J Virol*. 67(12), 7229–7237 (1993).

29. Navia MA, Navia MA, Fitzgerald PMD, *et al.* Three-dimensional structure of aspartyl protease from human immunodeficiency virus HIV-1. *Nature*. 337(6208), 615–620 (1989).

30. Ashorn P, McQuade TJ, Thaisrivongs S, Tomasselli AG, Tarpley WG, Moss B. An inhibitor of the protease blocks maturation of human and simian immunodeficiency viruses and spread of infection. *Proc. Natl. Acad. Sci. U.S.A.* 87(19), 7472–7476 (1990).

31. Kohlstaedt L, Kohlstaedt L, Wang J, *et al.* Crystal structure at 3.5 A resolution of HIV-1 reverse transcriptase complexed with an inhibitor. *Science*. 256(5065), 1783–1790 (1992).

32. Beilhartz GL, Götte M. HIV-1 Ribonuclease H: Structure, Catalytic Mechanism and Inhibitors. *Viruses*. 2(4), 900–926 (2010).

33. Bushman F, Bushman F, Fujiwara T, Fujiwara T, Craigie R, Craigie R. Retroviral DNA integration directed by HIV integration protein in vitro. *Science*. 249(4976), 1555–1558 (1990).

34. Ruben S, Perkins A, Purcell R, *et al.* Structural and functional characterization of human immunodeficiency virus tat protein. *J Virol*. 63(1), 1–8 (1989).

35. Kim SY, Byrn R, Groopman J, Baltimore D. Temporal aspects of DNA and RNA synthesis during human immunodeficiency virus infection: evidence for differential gene expression. *J Virol*. 63(9), 3708–3713 (1989).

36.   Aiken C, Konner J, Landau NR, Lenburg ME, Trono D. Nef induces CD4 endocytosis: Requirement for a critical dileucine motif in the membrane-proximal CD4 cytoplasmic domain. *Cell*. 76(5), 853–864 (1994).

37.   Schwartz O, Marechal V, Le Gall S, Lemonnier F, Heard JM. Endocytosis of major histocompatibility complex class I molecules is induced by the HIV-1 Nef protein. *Nat Med*. 2(3), 338–342 (1996).

38.   Strebel K, Daugherty D, Clouse K, Cohen D, Folks T, Martin MA. The HIV A (sor) gene product is essential for virus infectivity. *Nature*. 328(6132), 728–730 (1987).

39.   Heinzinger NK, Bukrinsky MI, Haggerty SA, *et al.* The Vpr protein of human immunodeficiency virus type 1 influences nuclear localization of viral nucleic acids in nondividing host cells. *Proc. Natl. Acad. Sci. U.S.A.* 91(15), 7311–7315 (1994).

40.   Rogel ME, Wu LI, Emerman M. The human immunodeficiency virus type 1 vpr gene prevents cell proliferation during chronic infection. *J Virol.* 69(2), 882–888 (1995).

41.   Schubert U, Schubert U, Bour S, *et al.* The two biological activities of human immunodeficiency virus type 1 Vpu protein involve two separable structural domains. *J Virol.* 70(2), 809–819 (1996).

42.   Veillette M, Désormeaux A, Medjahed H, *et al.* Interaction with Cellular CD4 Exposes HIV-1 Envelope Epitopes Targeted by Antibody-Dependent Cell-Mediated Cytotoxicity. *J Virol.* 88(5), 2633–2644 (2014).

43.   Ye L, Bu Z, Vzorov A, Taylor D, Compans RW, Yang C. Surface Stability and Immunogenicity of the Human Immunodeficiency Virus Envelope Glycoprotein: Role of the Cytoplasmic Domain. *J Virol.* 78(24), 13409–13419 (2004).

44.   Berger EA, Murphy PM, Farber JM. CHEMOKINE RECEPTORS AS HIV-1 CORECEPTORS: Roles in Viral Entry, Tropism, and Disease. *Annu. Rev. Immunol.* 17(1), 657–700 (1999).

45.   Leonard CK, Spellman MW, Riddle L, Harris RJ, Thomas JN, Gregory TJ. Assignment of intrachain disulfide bonds and characterization of potential glycosylation sites of the type 1 recombinant human immunodeficiency virus envelope glycoprotein (gp120) expressed in Chinese hamster ovary cells. *J. Biol. Chem.* 265(18), 10373–10382 (1990).

46. Wibmer CK, Moore PL, Morris L. HIV broadly neutralizing antibody targets. *Curr Opin HIV AIDS*. 10(3), 135–143 (2015).

47. McCoy LE, Weiss RA. Neutralizing antibodies to HIV-1 induced by immunization. *J. Exp. Med.* 210(2), 209–223 (2013).

48. Zolla-Pazner S. Identifying epitopes of HIV-1 that induce protective antibodies. *Nat Rev Immunol*. 4(3), 199–210 (2004).

49. Burton D, Pyati J, Koduri R, *et al.* Efficient neutralization of primary isolates of HIV-1 by a recombinant human monoclonal antibody. *Science*. 266(5187), 1024–1027 (1994).

50. Klein F, Gaebler C, Mouquet H, *et al.* Broad neutralization by a combination of antibodies recognizing the CD4 binding site and a new conformational epitope on the HIV-1 envelope protein. *J. Exp. Med.* 209(8), 1469–1479 (2012).

51. Thali M, Moore JP, Furman C, *et al.* Characterization of conserved human immunodeficiency virus type 1 gp120 neutralization epitopes exposed upon gp120-CD4 binding. *J Virol*. 67(7), 3978–3988 (1993).

52. Walker LM, Phogat SK, Chan-Hui PY, *et al.* Broad and Potent Neutralizing Antibodies from an African Donor Reveal a New HIV-1 Vaccine Target. *Science*. 326(5950), 285–289 (2009).

53. Gorny MK, Xu JY, Karwowska S, Buchbinder A, Zolla-Pazner S. Repertoire of neutralizing human monoclonal antibodies specific for the V3 domain of HIV-1 gp120. *The Journal of Immunology*. 150(2), 635–643 (1993).

54. Trkola A, Purtscher M, Muster T, *et al.* Human monoclonal antibody 2G12 defines a distinctive neutralization epitope on the gp120 glycoprotein of human immunodeficiency virus type 1. *J Virol*. 70(2), 1100–1108 (1996).

55. Julien J-P, Sok D, Khayat R, *et al.* Broadly Neutralizing Antibody PGT121 Allosterically Modulates CD4 Binding via Recognition of the HIV-1 gp120 V3 Base and Multiple Surrounding Glycans. *PLoS Pathog*. 9(5), e1003342 (2013).

56. Kong L, Lee JH, Doores KJ, *et al.* Supersite of immune vulnerability on the glycosylated face of HIV-1 envelope glycoprotein gp120. *Nat Struct Mol Biol*. 20(7), 796–803 (2013).

57. Scharf L, Scheid JF, Lee JH, *et al.* Antibody 8ANC195 Reveals a Site of Broad Vulnerability on the HIV-1 Envelope Spike. *Cell Reports*. 7(3), 785–795 (2014).

58. Huang J, Kang BH, Pancera M, *et al.* Broad and potent HIV-1 neutralization by a human antibody that binds the gp41–gp120 interface. *Nature*. 515(7525), 138–142 (2014).

59. Weissenhorn W, Dessen A, Harrison SC, Skehel JJ, Wiley DC. Atomic structure of the ectodomain from HIV-1 gp41. *Nature*. 387(6631), 426–430 (1997).

60. Chan DC, Fass D, Berger JM, Kim PS. Core Structure of gp41 from the HIV Envelope Glycoprotein. *Cell*. 89(2), 263–273 (1997).

61. Fujii G, Horvath S, Woodward S, Eiserling F, Eisenberg D. A molecular model for membrane fusion based on solution studies of an amphiphilic peptide from HIV gp41. *Protein Sci.* 1(11), 1454–1464 (1992).

62. Frey G, Peng H, Rits-Volloch S, Morelli M, Cheng Y, Chen B. A fusion-intermediate state of HIV-1 gp41 targeted by broadly neutralizing antibodies. *Proc. Natl. Acad. Sci. U.S.A.* 105(10), 3739–3744 (2008).

63. Zwick MB, Labrijn AF, Wang M, *et al.* Broadly neutralizing antibodies targeted to the membrane-proximal external region of human immunodeficiency virus type 1 glycoprotein gp41. *J Virol*. 75(22), 10892–10905 (2001).

64. Muster T, Steindl F, Purtscher M, *et al.* A conserved neutralizing epitope on gp41 of human immunodeficiency virus type 1. *J Virol*. 67(11), 6642–6647 (1993).

65. Nelson JD, Brunel FM, Jensen R, *et al.* An affinity-enhanced neutralizing antibody against the membrane-proximal external region of human immunodeficiency virus type 1 gp41 recognizes an epitope between those of 2F5 and 4E10. *J Virol*. 81(8), 4033–4043 (2007).

66. Huang J, Huang J, Ofek G, *et al.* Broad and potent neutralization of HIV-1 by a gp41-specific human antibody. *Nature*. 491(7424), 406–412 (2012).

67. Melikyan GB, Melikyan GB, Markosyan RM, *et al.* Evidence That the Transition of HIV-1 Gp41 into a Six-Helix Bundle, Not the Bundle Configuration, Induces Membrane Fusion. *The Journal of Cell Biology*. 151(2), 413–423 (2000).

68. Welch BD, VanDemark AP, Heroux A, Hill CP, Kay MS. Potent D-peptide inhibitors of HIV-1 entry. *Proc. Natl. Acad. Sci. U.S.A.* 104(43), 16828–16833 (2007).

69.   Mansky LM, Mansky LM, Temin HM, Temin HM. Lower in vivo mutation rate of human immunodeficiency virus type 1 than that predicted from the fidelity of purified reverse transcriptase. *J Virol.* 69(8), 5087–5094 (1995).

70.   Barré-Sinoussi F, Ross AL, Delfraissy J-F. Past, present and future: 30 years of HIV research. *Nat Rev Micro.* 11(12), 877–883 (2013).

71.   Mutimura E, Stewart A, Crowther NJ. Assessment of quality of life in HAART-treated HIV-positive subjects with body fat redistribution in Rwanda. *AIDS Res Ther.* 4(19) (2007).

72.   Dore GJ, Cooper DA. HAART's first decade: success brings further challenges. *Lancet.* 368(9534), 427–428 (2006).

73.   Demirjian A, Levy O. Novel vaccines: bridging research, development and production. *Expert Rev Vaccines.* 7(9), 1321–1324 (2008).

74.   Minor PD. Eradication and cessation of programmes. *Br. Med. Bull.* 62, 213–224 (2002).

75.   Esparza J. A brief history of the global effort to develop a preventive HIV vaccine. *Vaccines.* 31(35), 3502–3518 (2013).

76.   Bevan MJ. Understand memory, design better vaccines. *Nat Immunol.* 12(6), 463–465 (2011).

77.   Yang X, Lee J, Mahony EM, Kwong PD, Wyatt R, Sodroski J. Highly Stable Trimers Formed by Human Immunodeficiency Virus Type 1 Envelope Glycoproteins Fused with the Trimeric Motif of T4 Bacteriophage Fibritin. *J Virol.* 76(9), 4634–4642 (2002).

78.   Zhang L, Miao L, Gong X, *et al.* Multiple antigen peptide mimetics containing gp41 membrane-proximal external region elicit broad neutralizing antibodies against human immunodeficiency virus type 1 in guinea pigs. *J. Pept. Sci.* 19(8), 491–498 (2013).

79.   Bhattacharyya S, Singh P, Rathore U, *et al.* Design of an Escherichia coli expressed HIV-1 gp120 fragment immunogen that binds to b12 and induces broad and potent neutralizing antibodies. *Journal of Biological Chemistry.* 288(14), 9815–9825 (2013).

80.   Qin Y, Banasik M, Kim S, *et al.* Eliciting neutralizing antibodies with gp120 outer domain constructs based on M-group consensus sequence. *Virology.* 462-463, 363–376 (2014).

81.   Bricault CA, Kovacs JM, Nkolola JP, *et al.* A Multivalent Clade C HIV-1 Env Trimer Cocktail Elicits a Higher Magnitude of Neutralizing

Antibodies than Any Individual Component. *J Virol*. 89(5), 2507–2519 (2015).

82.   Mann JK, Ndung U T. HIV-1 vaccine immunogen design strategies. *Virol. J.* 12(1), (2015).

83.   Rerks-Ngarm S, Pitisuttithum P, Nitayaphan S, *et al.* Vaccination with ALVAC and AIDSVAX to prevent HIV-1 infection in Thailand. *N. Engl. J. Med.* 361(23), 2209–2220 (2009).

84.   Gregory AE, Titball R, Williamson D. Vaccine delivery using nanoparticles. *Frontiers in Cellular and Infection Microbiology*. 3(13), 1–13 (2013).

85.   Tang DC, DeVit M, Johnston SA. Genetic immunization is a simple method for eliciting an immune response. *Nature*. 356(6365), 152–154 (1992).

86.   Giri M, Ugen KE, Weiner DB. DNA vaccines against human immunodeficiency virus type 1 in the past decade. *Clin. Microbiol. Rev.* 17(2), 370–389 (2004).

87.   Kutzler MA, Weiner DB. DNA vaccines: ready for prime time? *Nat Rev Genet*. 9(10), 776–788 (2008).

88.   Cao Y, Zhao B, Han Y, *et al.* Gene gun bombardment with DNA-coated golden particles enhanced the protective effect of a DNA vaccine based on thioredoxin glutathione reductase of Schistosoma japonicum. *Biomed Res Int*. 2013, 952416 (2013).

89.   Kopycinski J, Cheeseman H, Ashraf A, *et al.* A DNA-based candidate HIV vaccine delivered via in vivo electroporation induces CD4 responses toward the α4β7-binding V2 loop of HIV gp120 in healthy volunteers. *Clin. Vaccine Immunol.* 19(9), 1557–1559 (2012).

90.   Wang Q, Jiang W, Chen Y, *et al.* In Vivo Electroporation of Minicircle DNA as a Novel Method of Vaccine Delivery to Enhance HIV-1-Specific Immune Responses. *J Virol*. (2013).

91.   Borhani K, Ajorloo M, Bamdad T, Mozhgani SHR, Ghaderi M, Gholami AR. A Comparative Approach between Heterologous Prime-Boost Vaccination Strategy and DNA Vaccinations for Rabies. *Arch Iran Med*. 18(4), 223–227 (2015).

92.   A prime/boost strategy using DNA/fowlpox recombinants expressing the genetically attenuated E6 protein as a putative vaccine against HPV-16-associated cancers. 13(1), 80 (2015).

93.   Kianmehr Z, Ardestani SK, Soleimanjahi H, *et al.* An effective DNA priming-protein boosting approach for the cervical cancer vaccination. *Pathog Dis*. 73(2), 1–8 (2015).

94.   Jackson DA, Symons RH, Berg P. Biochemical method for inserting new genetic information into DNA of Simian Virus 40: circular SV40 DNA molecules containing lambda phage genes and the galactose operon of Escherichia coli. *Proc. Natl. Acad. Sci. U.S.A.* 69(10), 2904–2909 (1972).

95.   Ura T, Okuda K, Shimada. Developments in Viral Vector-Based Vaccines. Vaccines. 2, 624–641 (2014).

96.   Shiver JW, Shiver JW, Emini EA, Emini EA. Recent advances in the development of HIV-1 vaccines using replication-incompetent adenovirus vectors. *Annu. Rev. Med.* 55, 355–372 (2004).

97.   Mwau M, Mwau M, Cebere I, *et al.* A human immunodeficiency virus 1 (HIV-1) clade A vaccine in clinical trials: stimulation of HIV-specific T-cell responses by DNA and recombinant modified vaccinia virus Ankara (MVA) vaccines in humans. *J. Gen. Virol.* 85(Pt 4), 911–919 (2004).

98.   de Bruyn G, Rossini AJ, Chiu Y-L, *et al.* Safety profile of recombinant canarypox HIV vaccines. *Vaccines*. 22(5-6), 704–713 (2004).

99.   Pitisuttithum P, Rerks-Ngarm S, Bussaratid V, *et al.* Safety and Reactogenicity of Canarypox ALVAC-HIV (vCP1521) and HIV-1 gp120 AIDSVAX B/E Vaccination in an Efficacy Trial in Thailand. *PLoS ONE*. 6(12), e27837 (2011).

100.   Mingozzi F, High KA. Immune responses to AAV vectors: overcoming barriers to successful gene therapy. *Blood*. 122(1), 23–36 (2013).

101.   Thomas CE, Ehrhardt A, Kay MA. Progress and problems with the use of viral vectors for gene therapy. *Nat Rev Genet*. 4(5), 346–358 (2003).

102.   Pearse MJ, Drane D. ISCOMATRIX adjuvant for antigen delivery. *Advanced Drug Delivery Reviews*. 57(3), 465–474 (2005).

103.   Sanders MT, Brown LE, Deliyannis G, Pearse MJ. ISCOMTM-based vaccines: The second decade. *Immunol Cell Biol*. 83(2), 119–128 (2005).

104.   Sun H-X, Xie Y, Ye Y-P. ISCOMs and ISCOMATRIX. *Vaccines*. 27(33), 4388–4401 (2009).

105.   Correia-Pinto JF, Csaba N, Alonso MJ. Vaccine delivery carriers: Insights and future perspectives. *Int J Pharm*. 440(1), 27–38 (2013).

106.   Nkolola JP, Cheung A, Perry JR, *et al.* Comparison of multiple adjuvants on the stability and immunogenicity of a clade C HIV-1 gp140 trimer. *Vaccines*. 32(18), 2109–2116 (2014).

107.   Santos LG, Oliveira DC, Santos MSL, *et al.* Electrospun Membranes of Poly(Lactic Acid) (PLA) Used as Scaffold in Drug Delivery of Extract of Sedum Dendroideum. *j. nanosci. nanotech.* 13(7), 4694–4702 (2013).

108.   Immich APS, Immich APS, Arias ML, *et al.* Drug delivery systems using sandwich configurations of electrospun poly(lactic acid) nanofiber membranes and ibuprofen. *Mater Sci Eng C Mater Biol Appl*. 33(7), 4002–4008 (2013).

109.   Makadia HK, Siegel SJ. Poly Lactic-co-Glycolic Acid (PLGA) as Biodegradable Controlled Drug Delivery Carrier. *Polymers*. 3(4), 1377–1397 (2011).

110.   Silva AL, Rosalia RA, Varypataki E, Sibuea S, Ossendorp F, Jiskoot W. Poly-(lactic-co-glycolic-acid)-based particulate vaccines: Particle uptake by dendritic cells is a key parameter for immune activation. *Vaccines*. (2015).

111.   Rosalia RA, Cruz LJ, van Duikeren S, *et al.* CD40-targeted dendritic cell delivery of PLGA-nanoparticle vaccines induce potent anti-tumor responses. *Biomaterials*. 40, 88–97 (2015).

112.   Ayre AP, Pawar HA, Khutle NM, Lalitha KG. POLYMERIC NANOPARTICLES IN DRUG DELIVERY SYSTEMS CRITICAL REVIEW AND CONCEPTS. *International Journal Of Pharmacy&Technology*. 5(4), 2809–2823 (2014).

113.   Read RC, Naylor SC, Potter CW, *et al.* Effective nasal influenza vaccine delivery using chitosan. *Vaccines*. 23, 4367–4374 (2005).

114.   Luo Y, Wang Q. Recent development of chitosan-based polyelectrolyte complexes with natural polysaccharides for drug delivery. *Int. J. Biol. Macromol.* 64, 353–367 (2014).

115.   Harde H, Agrawal AK, Jain S. Tetanus toxoids loaded glucomannosylated chitosan based nanohoming vaccine adjuvant with improved oral stability and immunostimulatory response. *Pharm Res*. 32(1), 122–134 (2015).

116. Tran DL, Tran DL, Pham GD, *et al.* Some biomedical applications of chitosan-based hybrid nanomaterials. *Adv. Nat. Sci: Nanosci. Nanotechnol.* 2(4), 045004 (2011).

117. Bangham AD, Horne RW. Negative staining of phospholipids and their structural modification by surface-active agents as observed in the electron microscope. *J. Mol. Biol.* 8(5), 660–IN10 (1964).

118. Huynh HT, Passirani C, Saulnier P, Benoit JP. Lipid based nanocapsules: A multitude of biomedical applications. *Int J Pharm*. 379, 201–209 (2009).

119. Al-Jamal WT, Kostarelos K. Liposomes: From a Clinically Established Drug Delivery System to a Nanoparticle Platform for Theranostic Nanomedicine. *Acc. Chem. Res.* 44(10), 1094–1104 (2011).

120. Zelphati O, Zelphati O, Wang Y, *et al.* Intracellular Delivery of Proteins with a New Lipid-mediated Delivery System. *Journal of Biological Chemistry*. 276(37), 35103–35110 (2001).

121. Nair R, Kumar K, Priya KV, Sevukarajan M. Recent Advances in Solid Lipid Nanoparticle Based Drug Delivery Systems. *J Biomed Sci and Res*. 3(2), 368–384 (2011).

122. Torchilin VP. Recent advances with liposomes as pharmaceutical carriers. *Nat Rev Drug Discov*. 4(2), 145–160 (2005).

123. Akbarzadeh A, Rezaei-Sadabady R, Davaran S, *et al.* Liposome: classification, preparation, and applications. *Nanoscale Res Lett*. 8(1), 102 (2013).

124. Hadinoto K, Sundaresan A, Cheow WS. Lipid-polymer hybrid nanoparticles as a new generation therapeutic delivery platform: a review. *Eur J Pharm Biopharm*. 85, 427–443 (2013).

125. Bansal A, Zhang Y. Photocontrolled nanoparticle delivery systems for biomedical applications. *Acc. Chem. Res.* 47(10), 3052–3060 (2014).

126. Turkevich J, Turkevich J, Stevenson PC, Stevenson PC, Hillier J, Hillier J. A study of the nucleation and growth processes in the synthesis of colloidal gold. *Discussions of the Faraday Society*. 11, 55–75 (1951).

127. Verma HN, Singh P, Chavan RM. Gold nanoparticle: synthesis and characterization. Veterinary World. 7(2), 72–77 (2014).

128.   Frens G. Controlled Nucleation for the Regulation of the Particle Size in Monodisperse Gold Suspensions. *Nat Phys Sci.* 241(105), 20–22 (1973).

129.   Ghosh D, Chattopadhyay N. Gold Nanoparticles: Acceptors for Efficient Energy Transfer from the Photoexcited Fluorophores. *Optics and Photonics Journal.* 3, 18–26 (2013).

130.   Chen H, Kou X, Yang Z, Ni W, Wang J. Shape- and size-dependent refractive index sensitivity of gold nanoparticles. *Langmuir.* 24(10), 5233–5237 (2008).

131.   Niikura K, Matsunaga T, Suzuki T, *et al.* Gold Nanoparticles as a Vaccine Platform: Influence of Size and Shape on Immunological Responses in Vitroand in Vivo. *ACS Nano.* 7(5), 3926–3938 (2013).

132.   Nikoobakht B, El-Sayed MA. Preparation and Growth Mechanism of Gold Nanorods (NRs) Using Seed-Mediated Growth Method. *Chem. Mater.* 15(10), 1957–1962 (2003).

133.   Jana NR, Gearheart L, Murphy CJ. Seed-mediated growth approach for shape-controlled synthesis of spheroidal and rod-like gold nanoparticles using a surfactant template. *Adv. Mater.* 13(18), 1389–1398 (2001).

134.   Murphy CJ, Jana NR. Controlling the aspect ratio of inorganic nanorods and nanowires. *Adv. Mater.* 14(1), 80–82 (2002).

135.   Khoury El JM, Zhou X, Qu L, Dai L, Urbas A, Li Q. Organo-soluble photoresponsive azo thiol monolayer-protected gold nanorods. *Chem. Commun.* 1, 2109–2111 (2009).

136.   Dahl JA, Maddux B, Hutchison JE. Toward greener nanosynthesis. *Chem. Rev.* 107(6), 2228–2269 (2007).

137.   Love JC, Estroff LA, Kriebel JK, Nuzzo RG, Whitesides GM. Self-assembled monolayers of thiolates on metals as a form of nanotechnology. *Chem. Rev.* 105(4), 1103–1169 (2005).

138.   Chen Y-S, Hung Y-C, Lin W-H, Huang GS. Assessment of gold nanoparticles as a size-dependent vaccine carrier for enhancing the antibody response against synthetic foot-and-mouth disease virus peptide. *Nanotechnology.* 21(19), 195101 (2010).

139.   Cruz LJ, Rueda F, Cordobilla B, *et al.* Targeting nanosystems to human DCs via Fc receptor as an effective strategy to deliver antigen for immunotherapy. *Mol. Pharm.* 8(1), 104–116 (2011).

140. Sharma J, Mahima S, Kakade BA, Pasricha R, Mandale AB, Vijayamohanan K. Solvent-Assisted One-Pot Synthesis and Self-Assembly of 4-Aminothiophenol-Capped Gold Nanoparticles. *J Phys Chem B*. 108(35), 13280–13286 (2004).

141. Xiao N, Yu C. Rapid-Response and Highly Sensitive Noncross-Linking Colorimetric Nitrite Sensor Using 4-Aminothiophenol Modified Gold Nanorods. *Anal. Chem.* 82(9), 3659–3663 (2010).

142. Xiao N, Wang C, Yu C. A Self-Referencing Detection of Microorganisms Using Surface Enhanced Raman Scattering Nanoprobes in a Test-in-a-Tube Platform. *Biosensors*. 3(3), 312–326 (2013).

143. Bizzarri AR, Cannistraro S. SERS detection of thrombin by protein recognition using functionalized gold nanoparticles. *Nanomedicine*. 3(4), 306–310 (2007).

144. Wu Y, Buranda T, Metzenberg RL, Sklar LA, Lopez GP. Diazo coupling method for covalent attachment of proteins to solid substrates. *Bioconjug. Chem.* 17(2), 359–365 (2006).

145. Chithrani BD, Chithrani BD, Ghazani AA, Ghazani AA, Chan WCW, Chan WCW. Determining the size and shape dependence of gold nanoparticle uptake into mammalian cells. *Nano Lett.* 6(4), 662–668 (2006).

146. Chithrani BD, Chan WCW. Elucidating the mechanism of cellular uptake and removal of protein-coated gold nanoparticles of different sizes and shapes. *Nano Lett.* 7(6), 1542–1550 (2007).

147. Shukla R, Shukla R, Bansal V, *et al.* Biocompatibility of gold nanoparticles and their endocytotic fate inside the cellular compartment: a microscopic overview. *Langmuir*. 21(23), 10644–10654 (2005).

148. Connor EE, Mwamuka J, Gole A, Murphy CJ, Wyatt MD. Gold Nanoparticles Are Taken Up by Human Cells but Do Not Cause Acute Cytotoxicity. *Small*. 1(3), 325–327 (2005).

149. Hauck TS, Ghazani AA, Chan WCW. Assessing the Effect of Surface Chemistry on Gold Nanorod Uptake, Toxicity, and Gene Expression in Mammalian Cells. *Small*. 4(1), 153–159 (2008).

150. Chen Y-S, Hung Y-C, Liau I, Huang GS. Assessment of the In Vivo Toxicity of Gold Nanoparticles. *Nanoscale Res Lett*. 4(8), 858–864 (2009).

151. De Jong WH, Hagens WI, Krystek P, Burger MC, Sips AJAM, Geertsma RE. Particle size-dependent organ distribution of gold nanoparticles after intravenous administration. *Biomaterials*. 29(12), 1912–1919 (2008).

152. Shilo M, Motiei M, Hana P, Popovtzer R. Transport of nanoparticles through the blood-brain barrier for imaging and therapeutic applications. *Nanoscale*. 6(4), 2146–2152 (2014).

153. Kim JH, Kim JH, Kim K-W, Kim MH, Yu YS. Intravenously administered gold nanoparticles pass through the blood–retinal barrier depending on the particle size, and induce no retinal toxicity. *Nanotechnology*. 20(50), 505101 (2009).

154. Simpson CA, Salleng KJ, Cliffel DE, Feldheim DL. In vivo toxicity, biodistribution, and clearance of glutathione-coated gold nanoparticles. *Nanomedicine*. 9(2), 257–263 (2013).

155. Khlebtsov N, Dykman L. Biodistribution and toxicity of engineered gold nanoparticles: a review of in vitro and in vivo studies. *Chem Soc Rev*. 40(3), 1647–1671 (2011).

156. Hirn S, Hirn S, Semmler-Behnke M, *et al.* Particle size-dependent and surface charge-dependent biodistribution of gold nanoparticles after intravenous administration. *Eur J Pharm Biopharm*. 77(3), 407–416 (2011).

157. Lasagna-Reeves C, Gonzalez-Romero D, Barria MA, *et al.* Bioaccumulation and toxicity of gold nanoparticles after repeated administration in mice. *Biochemical and Biophysical Research Communications*. 393(4), 649–655 (2010).

158. Dykman L, Khlebtsov N. Gold nanoparticles in biomedical applications: recent advances and perspectives. *Chem Soc Rev*. 41(6), 2256–2282 (2012).

159. Gao W, Fang RH, Thamphiwatana S, *et al.* Modulating Antibacterial Immunity via Bacterial Membrane-Coated Nanoparticles. *Nano Lett.* 15(2), 1403–1409 (2015).

160. Rodriguez-Del Rio E, Marradi M, Calderon-Gonzalez R, *et al.* A gold glyco-nanoparticle carrying a listeriolysin O peptide and formulated with Advax™ delta inulin adjuvant induces robust T-cell protection against listeria infection. *Vaccines*. 33(12), 1465–1473 (2015).

161. Gregory AE, Judy BM, Qazi O, *et al.* A gold nanoparticle-linked glycoconjugate vaccine against Burkholderia mallei. *Nanomedicine*. (2014).

162.   Torres AG, Gregory AE, Hatcher CL, *et al.* Protection of non-human primates against glanders with a gold nanoparticle glycoconjugate vaccine. *Vaccines*. 33(5), 686–692 (2015).

163.   Barhate G, Gautam M, Gairola S, Jadhav S, Pokharkar V. Enhanced Mucosal Immune Responses Against Tetanus Toxoid Using Novel Delivery System Comprised of Chitosan-Functionalized Gold Nanoparticles and Botanical Adjuvant: Characterization, Immunogenicity, and Stability Assessment. *J Pharm Sci*. 103, 3448–3456 (2014).

164.   Martínez-Ávila O, Hijazi K, Marradi M, *et al.* Gold Manno-Glyconanoparticles: Multivalent Systems to Block HIV-1 gp120 Binding to the Lectin DC-SIGN. *Chem. Eur. J.* 15(38), 9874–9888 (2009).

165.   Martínez-Ávila O, Bedoya LM, Marradi M, Clavel C, Alcamí J, Penadés S. Multivalent Manno-Glyconanoparticles Inhibit DC-SIGN-Mediated HIV-1 Trans-Infection of Human T Cells. *Chem. Eur. J. of Chem. Bio.* 10(11), 1806–1809 (2009).

166.   Chiodo F, Marradi M, Calvo J, Yuste E, Penadés S. Glycosystems in nanotechnology: Gold glyconanoparticles as carrier for anti-HIV prodrugs. *Beilstein J Org Chem*. 10, 1339–1346 (2014).

167.   Xu L, Liu Y, Chen Z, *et al.* Surface-engineered gold nanorods: promising DNA vaccine adjuvant for HIV-1 treatment. *Nano Lett.* 12(4), 2003–2012 (2012).

168.   Reed SG, Bertholet S, Coler RN, Friede M. New horizons in adjuvants for vaccine development. *Trends in Immunology*. 30(1), 23–32 (2009).

169.   Kim D-W, Kim J-H, Park M, *et al.* Modulation of biological processes in the nucleus by delivery of DNA oligonucleotides conjugated with gold nanoparticles. *Biomaterials*. 32(10), 2593–2604 (2011).

170.   Khandelia R, Jaiswal A, Ghosh SS, Chattopadhyay A. Gold nanoparticle-protein agglomerates as versatile nanocarriers for drug delivery. *Small*. 9(20), 3494–3505 (2013).

171.   Ghosh P, Han G, De M, KIM C, ROTELLO V. Gold nanoparticles in delivery applications. *Advanced Drug Delivery Reviews*. 60(11), 1307–1315 (2008).

172.   Wang Y-T, Lu X-M, Zhu F, *et al.* The use of a gold nanoparticle-based adjuvant to improve the therapeutic efficacy of hNgR-Fc protein

immunization in spinal cord-injured rats. *Biomaterials*. 32(31), 7988–7998 (2011).

173.   Fujita Y, Taguchi H. Current status of multiple antigen-presenting peptide vaccine systems: Application of organic and inorganic nanoparticles. *Chem Cent J*. 5(1), 48 (2011).

174.   Liu W, Liu W, Sohn HW, *et al.* It's All About Change: The Antigen-driven Initiation of B-Cell Receptor Signaling. *Cold Spring Harbor Perspectives in Biology*. 2(7), a002295 (2010).

175.   Mao Y, Mao Y, Wang L, *et al.* Molecular architecture of the uncleaved HIV-1 envelope glycoprotein trimer. *Proc. Natl. Acad. Sci. U.S.A.* 110(30), 12438–12443 (2013).

176.   Montero M, van Houten N, Wang X, Scott J. The membrane-proximal external region of the human immunodeficiency virus type 1 envelope: dominant site of antibody neutralization and target for vaccine design. *Microbiology and Molecular Biology Reviews*. 72(1), 54–84 (2008).

177.   Buchacher A, Predl R, Strutzenberger K, *et al.* Generation of Human Monoclonal Antibodies against HIV-1 Proteins; Electrofusion and Epstein-Barr Virus Transformation for Peripheral Blood Lymphocyte Immortalization. *AIDS Res. Hum. Retroviruses*. 10(4), 359–369 (1994).

178.   Purtscher M, Trkola A, Grassauer A, *et al.* Restricted antigenic variability of the epitope recognized by the neutralizing gp41 antibody 2F5. *AIDS*. 10(6), 587–593 (1996).

179.   Purtscher M, Trkola A, Gruber G, *et al.* A Broadly Neutralizing Human Monoclonal Antibody against gp41 of Human Immunodeficiency Virus Type 1. *AIDS Res. Hum. Retroviruses*. 10(12), 1651–1658 (1994).

180.   Stiegler G, Stiegler G, Kunert R, *et al.* A potent cross-clade neutralizing human monoclonal antibody against a novel epitope on gp41 of human immunodeficiency virus type 1. *AIDS Res. Hum. Retroviruses*. 17(18), 1757–1765 (2001).

181.   Kim M, Song L, Moon J, *et al.* Immunogenicity of Membrane-bound HIV-1 gp41 Membrane-proximal External Region (MPER) Segments Is Dominated by Residue Accessibility and Modulated by Stereochemistry. *Journal of Biological Chemistry*. 288(44), 31888–31901 (2013).

182.   Hanson MC, Abraham W, Crespo MP, *et al.* Liposomal vaccines incorporating molecular adjuvants and intrastructural T-cell help

promote the immunogenicity of HIV membrane-proximal external region peptides. *Vaccines*. 33(7), 861–868 (2015).

183.   Law M, Cardoso RMF, Wilson IA, Burton DR. Antigenic and Immunogenic Study of Membrane-Proximal External Region-Grafted gp120 Antigens by a DNA Prime-Protein Boost Immunization Strategy. *J Virol*. 81(8), 4272–4285 (2007).

184.   Dennison SM, Anasti K, Scearce RM, *et al.* Nonneutralizing HIV-1 gp41 envelope cluster II human monoclonal antibodies show polyreactivity for binding to phospholipids and protein autoantigens. *J Virol*. 85(3), 1340–1347 (2011).

185.   Sun Z-YJ, Oh KJ, Kim M, *et al.* HIV-1 broadly neutralizing antibody extracts its epitope from a kinked gp41 ectodomain region on the viral membrane. *Immunity*. 28(1), 52–63 (2008).

186.   Heuzenroeder MW, Barton MD, Vanniasinkam T, *et al.* Linear B-cell epitope mapping using enzyme-linked immunosorbent assay for libraries of overlapping synthetic peptides. *Methods Mol. Biol.* 524, 137–144 (2009).

187.   Sulzer B, Perelson AS. Immunons revisited: Binding of multivalent antigens to B cells. *Molecular Immunology*. 34(1), 63–74 (1997).

188.   Vos Q, Lees A, Wu Z, Snapper CM, Mond JJ. B-cell activation by T-cell-independent type 2 antigens as an integral part of the humoral immune response to pathogenic microorganisms. *Immunological Reviews*. 176(1), 154–170 (2000).

189.   Grenfell RFQ, Shollenberger LM, Samli EF, Harn DA. Vaccine Self-Assembling Immune Matrix Is a New Delivery Platform That Enhances Immune Responses to Recombinant HBsAg in Mice. *Clin. Vaccine Immunol.* 22(3), 336–343 (2015).

190.   Dykman LA, Bogatyrev VA. Gold nanoparticles: preparation, functionalisation and applications in biochemistry and immunochemistry. *Russ. Chem. Rev.* 76(2), 181–194 (2007).

191.   Feyer V, Feyer V, Plekan O, *et al.* Adsorption of histidine and histidine-containing peptides on Au(111). *Langmuir.* 26(11), 8606–8613 (2010).

192.   Lim JK, Kim Y, Lee SY, Joo S-W. Spectroscopic analysis of L-histidine adsorbed on gold and silver nanoparticle surfaces investigated by surface-enhanced Raman scattering. *Spectrochim Acta A Mol Biomol Spectrosc.* 69(1), 286–289 (2008).

193. Zhou JC, Wang X, Xue M, Xu Z, Hamasaki T. Characterization of gold nanoparticle binding to microtubule filaments. *Materials Science and Engineering C*. (30), 20–26 (2010).

194. Gao F, Weaver EA, Lu Z, *et al.* Antigenicity and immunogenicity of a synthetic human immunodeficiency virus type 1 group m consensus envelope glycoprotein. *J Virol*. 79(2), 1154–1163 (2005).

195. Penn-Nicholson AA, Han DPD, Kim SJS, *et al.* Assessment of antibody responses against gp41 in HIV-1-infected patients using soluble gp41 fusion proteins and peptides derived from M group consensus envelope. *Virology*. 372(2), 442–456 (2008).

196. Li M, Gao F, Mascola JR, *et al.* Human Immunodeficiency Virus Type 1 env Clones from Acute and Early Subtype B Infections for Standardized Assessments of Vaccine-Elicited Neutralizing Antibodies. *J Virol*. 79(16), 10108–10125 (2005).

197. Wei X, Decker JM, Liu H, *et al.* Emergence of resistant human immunodeficiency virus type 1 in patients receiving fusion inhibitor (T-20) monotherapy. *Antimicrob. Agents Chemother.* 46(6), 1896–1905 (2002).

198. Gupta PN, Gupta PN, Pattani A, *et al.* Development of liposome gel based formulations for intravaginal delivery of the recombinant HIV-1 envelope protein CN54gp140. *Eur J Pharm Sci*. 46(5), 315–322 (2012).

199. Pusic K, Aguilar Z, McLoughlin J, *et al.* Iron oxide nanoparticles as a clinically acceptable delivery platform for a recombinant blood-stage human malaria vaccine. *FASEB J.* 27(3), 1153–1166 (2013).

200. Huntimer L, Ramer-Tait AE, Petersen LK, *et al.* Evaluation of biocompatibility and administration site reactogenicity of polyanhydride-particle-based platform for vaccine delivery. *Adv Healthc Mater*. 2(2), 369–378 (2013).

201. Zhang L, Zhang L, Sinclair A, *et al.* Hydrolytic cationic ester microparticles for highly efficient DNA vaccine delivery. *Small*. 9(20), 3439–3444 (2013).

202. Büchel C, Büchel C, Morris E, *et al.* Localisation of the PsbH subunit in photosystem II: a new approach using labelling of His-tags with a Ni(2+)-NTA gold cluster and single particle analysis. *J. Mol. Biol.* 312(2), 371–379 (2001).

203. Chen X, Chen W, Mulchandani A. Application of displacement principle for detecting heavy metal ions and EDTA using

microcantilevers. *Sensors and Actuators B: Chemical*. 161, 203–208 (2012).

204.   Paciotti GF, Kingston DGI, Tamarkin L. Colloidal gold nanoparticles: a novel nanoparticle platform for developing multifunctional tumor-targeted drug delivery vectors. *Drug Dev. Res.* 67(1), 47–54 (2006).

205.   Cheng Y, C Samia A, Meyers JD, Panagopoulos I, Fei B, Burda C. Highly Efficient Drug Delivery with Gold Nanoparticle Vectors for in VivoPhotodynamic Therapy of Cancer. *J. Am. Chem. Soc.* 130(32), 10643–10647 (2008).

206.   Duncan B, Kim C, Rotello VM. Gold nanoparticle platforms as drug and biomacromolecule delivery systems. *Journal of Controlled Release*. 148(1), 122–127 (2010).

207.   Sun X, Zhang G, Keynton RS, O'Toole MG, Patel D, Gobin AM. Enhanced drug delivery via hyperthermal membrane disruption using targeted gold nanoparticles with PEGylated Protein-G as a cofactor. *Nanomedicine*. 9(8), 1214–1222 (2013).

208.   Dharmatti R, Phadke C, Mewada A, Thakur M, Pandey S, Sharon M. Biogenic gold nano-triangles: Cargos for anticancer drug delivery. *Mater Sci Eng C Mater Biol Appl*. 44, 92–98 (2014).

209.   Lee I-H, Kwon H-K, An S, *et al.* Imageable Antigen-Presenting Gold Nanoparticle Vaccines for Effective Cancer Immunotherapy In Vivo. *Angew. Chem.* 124(35), 8930–8935 (2012).

210.   Parry AL, Clemson NA, Ellis J, Bernhard SSR, Davis BG, Cameron NR. "Multicopy Multivalent" Glycopolymer-Stabilized Gold Nanoparticles as Potential Synthetic Cancer Vaccines. *J. Am. Chem. Soc.* 135(25), 9362–9365 (2013).

211.   Gu L, Li ZC, Krendelchtchikov A, Krendelchtchikova V, Wu H, Matthews QL. Using multivalent adenoviral vectors for HIV vaccination. *PLoS ONE*. 8(3), e60347 (2013).

212.   Guerrero AR, Caballero L, Adeva A, Melo F, Kogan MJ. Exploring the surface charge on peptide-gold nanoparticle conjugates by force spectroscopy. *Langmuir*. 26(14), 12026–12032 (2010).

213.   Nowinski AK, White AD, Keefe AJ, Jiang S. Biologically inspired stealth peptide-capped gold nanoparticles. *Langmuir*. 30(7), 1864–1870 (2014).

214. Lin AY, Lunsford J, Bear AS, *et al.* High-density sub-100-nm peptide-gold nanoparticle complexes improve vaccine presentation by dendritic cells in vitro. *Nanoscale Res Lett.* 8(1), 72 (2013).

215. Anthony KC, Anthony KC, You C, *et al.* High-affinity gold nanoparticle pin to label and localize histidine-tagged protein in macromolecular assemblies. *Structure.* 22(4), 628–635 (2014).

216. Joshua A Bornhorst JJF. Purification of Proteins Using Polyhistidine Affinity Tags. *Methods in enzymology.* 326, 245–254 (2000).

217. Dubendorff JW, Lymar E, Furuya FR, Hainfeld JF. Gold Labeling of Protein Fusion Tags for EM. *Microsc Microanal.* 16(S2), 866–867 (2010).

218. Ackerson CJ, Powell RD, Hainfeld JF. Site-Specific Biomolecule Labeling with Gold Clusters. *Methods Enzymol.* 481, 195–230 (2010).

219. Hainfeld JF, Hainfeld JF, Liu W, *et al.* Ni–NTA–Gold Clusters Target His-Tagged Proteins. *Journal of Structural Biology.* 127(2), 185–198 (1999).

220. Briñas RP, Hu M, Qian L, Lymar ES, Hainfeld JF. Gold Nanoparticle Size Controlled by Polymeric Au(I) Thiolate Precursor Size. *J. Am. Chem. Soc.* 130(3), 975–982 (2008).

221. Cho M, Lee S, Han S-Y, *et al.* Electrochemical detection of mismatched DNA using a MutS probe. *Nucleic Acids Res.* 34(10), e75 (2006).

222. Tahir MN, Th ato P, M ller WEG, *et al.* Monitoring the formation of biosilica catalysed by histidine-tagged silicatein. *Chem. Commun.*, 2848–2849 (2004).

223. Nakamura I, Nakamura I, Makino A, *et al.* Immobilization of His-tagged endoglucanase on gold via various Ni-NTA self-assembled monolayers and its hydrolytic activity. *Macromol Biosci.* 10(10), 1265–1272 (2010).

224. Hochuli E, Döbeli H, Schacher A. New metal chelate adsorbent selective for proteins and peptides containing neighbouring histidine residues. *Journal of Chromatography.* 411, 177–184 (1987).

225. Belew M, Yip TT, Andersson L, Ehrnström R. High-Performace Analytical Applications of Immobilized Metal Ion Affinity Chromatography. *Anal. Biochem.* 164(2), 457–465 (1987).

226. Gorny MK, Xu JY, Gianakakos V, *et al.* Production of site-selected neutralizing human monoclonal antibodies against the third variable domain of the human immunodeficiency virus type 1 envelope glycoprotein. *Proc. Natl. Acad. Sci. U.S.A.* 88(8), 3238–3242 (1991).

227. Conley AJ, Conley AJ, Gorny MK, *et al.* Neutralization of primary human immunodeficiency virus type 1 isolates by the broadly reactive anti-V3 monoclonal antibody, 447-52D. *J Virol.* 68(11), 6994–7000 (1994).

228. Nyambi PN, Gorny MK, Bastiani L, van der Groen G, Williams C, Zolla-Pazner S. Mapping of Epitopes Exposed on Intact Human Immunodeficiency Virus Type 1 (HIV-1) Virions: a New Strategy for Studying the Immunologic Relatedness of HIV-1. *J Virol.* 72(11), 9384–9391 (1998).

229. Walker LM, Walker LM, Huber M, *et al.* Broad neutralization coverage of HIV by multiple highly potent antibodies. *Nature.* 477(7365), 466–470 (2011).

230. Pejchal R, Pejchal R, Doores KJ, *et al.* A Potent and Broad Neutralizing Antibody Recognizes and Penetrates the HIV Glycan Shield. *Science.* 334(6059), 1097–1103 (2011).

231. Mascola JR, Lewis MG, Stiegler G, *et al.* Protection of Macaques against pathogenic simian/human immunodeficiency virus 89.6PD by passive transfer of neutralizing antibodies. *J Virol.* 73(5), 4009–4018 (1999).

232. Etemad-Moghadam B, Sun Y, Nicholson EK, Karlsson GB, Schenten D, Sodroski J. Determinants of neutralization resistance in the envelope glycoproteins of a simian-human immunodeficiency virus passaged in vivo. *J Virol.* 73(10), 8873–8879 (1999).

233. Crawford JM, Earl PL, Moss B, *et al.* Characterization of primary isolate-like variants of simian-human immunodeficiency virus. *J Virol.* 73(12), 10199–10207 (1999).

234. Wu X, Yang ZY, Li Y, *et al.* Rational Design of Envelope Identifies Broadly Neutralizing Human Monoclonal Antibodies to HIV-1. *Science.* 329(5993), 856–861 (2010).

235. Tamamis P, Floudas CA. Molecular Recognition of CCR5 by an HIV-1 gp120 V3 Loop. *PLoS ONE.* 9(4), e95767 (2014).

236. Daniel M-C, Astruc D. Gold nanoparticles: assembly, supramolecular chemistry, quantum-size-related properties, and applications toward

biology, catalysis, and nanotechnology. *Chem. Rev.* 104(1), 293–346 (2004).

237.   Perrault SD, Chan WCW. Synthesis and surface modification of highly monodispersed, spherical gold nanoparticles of 50-200 nm. *J. Am. Chem. Soc.* 131(47), 17042–17043 (2009).

238.   Grönbeck H, Curioni A, Andreoni W. Thiols and Disulfides on the Au(111) Surface: The Headgroup−Gold Interaction. *J. Am. Chem. Soc.* 122(16), 3839–3842 (2000).

239.   Yeh Y-C, Creran B, Rotello VM. Gold nanoparticles: preparation, properties, and applications in bionanotechnology. *Nanoscale*. 4(6), 1871–1880 (2012).

240.   Wang S, Arthos J, Lawrence JM, *et al.* Enhanced immunogenicity of gp120 protein when combined with recombinant DNA priming to generate antibodies that neutralize the JR-FL primary isolate of human immunodeficiency virus type 1. *J Virol*. 79(12), 7933–7937 (2005).

241.   Heyndrickx L, Stewart-Jones G, Jansson M, *et al.* Selected HIV-1 Env Trimeric Formulations Act as Potent Immunogens in a Rabbit Vaccination Model. *PLoS ONE*. 8(9), e74552 (2013).

242.   Sheppard NC, Brinckmann SA, Gartlan KH, *et al.* Polyethyleneimine is a potent systemic adjuvant for glycoprotein antigens. *International Immunology*. 26(10), 531–538 (2014).

243.   Schroeder HW. Similarity and divergence in the development and expression of the mouse and human antibody repertoires. *Dev. Comp. Immunol.* 30(1-2), 119–135 (2006).

244.   Zelda Euler HS. Cross-reactive broadly neutralizing antibodies: timing is everything. *Frontiers in Immunology*. 3 (2012).

245.   Briney BS, Willis JR, Crowe JE Jr. Human Peripheral Blood Antibodies with Long HCDR3s Are Established Primarily at Original Recombination Using a Limited Subset of Germline Genes. *PLoS ONE*. 7(5), e36750 (2012).

246.   Popkov M, Mage RG, Alexander CB, Thundivalappil S, Barbas CF, Rader C. Rabbit immune repertoires as sources for therapeutic monoclonal antibodies: the impact of kappa allotype-correlated variation in cysteine content on antibody libraries selected by phage display. *J. Mol. Biol.* 325(2), 325–335 (2003).

247. Libutti SK, Paciotti GF, Byrnes AA, *et al.* Phase I and Pharmacokinetic Studies of CYT-6091, a Novel PEGylated Colloidal Gold-rhTNF Nanomedicine. *Clinical Cancer Research*. 16(24), 6139–6149 (2010).

248. Jain S, Hirst DG, O'Sullivan JM. Gold nanoparticles as novel agents for cancer therapy. *BJR*. 85(1010), 101–113 (2012).

249. Haas A, Zimmermann K, Oxenius A. Antigen-Dependent and -Independent Mechanisms of T and B Cell Hyperactivation during Chronic HIV-1 Infection. *J Virol*. 85(23), 12102–12113 (2011).

250. Moore PA, Moore PA. BLyS: Member of the Tumor Necrosis Factor Family and B Lymphocyte Stimulator. *Science*. 285(5425), 260–263 (1999).

251. Schneider P, MacKay F, Steiner V, *et al.* BAFF, a Novel Ligand of the Tumor Necrosis Factor Family, Stimulates B Cell Growth. *J. Exp. Med.* 189(11), 1747–1756 (1999).

252. Mukhopadhyay A, Ni J, Zhai Y, Yu GL, Aggarwal BB. Identification and Characterization of a Novel Cytokine, THANK, aTNF Homologue That ActivatesApoptosis, Nuclear Factor- B, and c-Jun NH2-Terminal Kinase. *Journal of Biological Chemistry*. 274(23), 15978–15981 (1999).

253. Shu HB, Hu WH, Johnson H. TALL-1 is a novel member of the TNF family that is down-regulated by mitogens. *Journal of Leukocyte Biology*. 65, 680–683 (1999).

254. Gross JA, Johnston J, Mudri S, *et al.* TACI and BCMA are receptors for a TNF homologue implicated in B-cell autoimmune disease : Article : Nature. *Nature*. 404(6781), 995–999 (2000).

255. Gor DO, Ding X, Li Q, *et al.* Enhanced immunogenicity of pneumococcal surface adhesin A (PsaA) in mice via fusion to recombinant human B lymphocyte stimulator (BLyS). *Biol Direct*. 6(1), 9 (2011).

256. Dosenovic P, Soldemo M, Scholz JL, *et al.* BLyS-Mediated Modulation of Naive B Cell Subsets Impacts HIV Env-Induced Antibody Responses. *J. Immunol.* (188), 6018–6026 (2012).

257. Wykes M. Why do B cells produce CD40 ligand? *Immunol Cell Biol*. 81(4), 328–331 (2003).

258. Bishop GA, Hostager BS. The CD40–CD154 interaction in B cell–T cell liaisons. *Cytokine & Growth Factor Reviews*. 14(3-4), 297–309 (2003).

259. Do RKG, Hatada E, Lee H, Tourigny MR, Hilbert D, Chen-Kiang S. Attenuation of Apoptosis Underlies B Lymphocyte Stimulator Enhancement of Humoral Immune Response. *J. Exp. Med.* 192(7), 953–964 (2000).

260. Kwa S, Kwa S, Sadagopal S, *et al.* CD40L adjuvant for DNA/MVA vaccine: enhanced protection from acquisition of neutralization sensitive & neutralization resistant mucosal SIV infections. *Retrovirology*. 9(2), 365 (2012).

261. Kwa S, Lai L, Gangadhara S, *et al.* CD40L-Adjuvanted DNA/Modified Vaccinia Virus Ankara Simian Immunodeficiency Virus SIV239 Vaccine Enhances SIV-Specific Humoral and Cellular Immunity and Improves Protection against a Heterologous SIVE660 Mucosal Challenge. *J Virol*. 88(17), 9579–9589 (2014).

262. Melchers M, Bontjer I, Tong T, *et al.* Targeting HIV-1 Envelope Glycoprotein Trimers to B Cells by Using APRIL Improves Antibody Responses. *J Virol*. 86(5), 2488–2500 (2012).

263. Do RKG, Chen-Kiang S. Mechanism of BLyS action in B cell immunity. *Cytokine & Growth Factor Reviews*. 13(1), 19–25 (2002).

264. Sun Y. Shape-Controlled Synthesis of Gold and Silver Nanoparticles. *Science*. 298(5601), 2176–2179 (2002).

265. Lu X, Chen J, Skrabalak SE, Xia Y. Galvanic replacement reaction: a simple and powerful route to hollow and porous metal nanostructures. *Proceedings of the Institution of Mechanical Engineers, Part N: Journal of Nanoengineering and Nanosystems*. 221(1), 1–16 (2008).

266. Skrabalak SE, Skrabalak SE, Chen J, *et al.* Gold Nanocages: Synthesis, Properties, and Applications. *Acc. Chem. Res.* 41(12), 1587–1595 (2008).

267. Chen J, Chen J, Saeki F, *et al.* Gold nanocages: bioconjugation and their potential use as optical imaging contrast agents. *Nano Lett.* 5(3), 473–477 (2005).

268. Yavuz MS, Yavuz MS, Cheng Y, *et al.* Gold nanocages covered by smart polymers for controlled release with near-infrared light. *Nat Mater*. 8(12), 935–939 (2009).

269.   Au L, Zheng D, Zhou F, Li Z-Y, Li X, Xia Y. A quantitative study on the photothermal effect of immuno gold nanocages targeted to breast cancer cells. *ACS Nano*. 2(8), 1645–1652 (2008).

270.   Kumari J, Kumari J, Selvan SR, *et al.* Cell-Mediated Immunity and Vaccines. *Journal of Immunology Research*. 2014, 1–2 (2014).

271.   Freed EO. HIV-1 Gag Proteins: Diverse Functions in the Virus Life Cycle. *Virology*. 251(1), 1–15 (1998).

272.   Turk G, Turk G, Ghiglione Y, *et al.* Early Gag Immunodominance of the HIV-Specific T-Cell Response during Acute/Early Infection Is Associated with Higher CD8+ T-Cell Antiviral Activity and Correlates with Preservation of the CD4+ T-Cell Compartment. *J Virol*. 87(13), 7445–7462 (2013).

273.   Kiepiela P, Ngumbela K, Thobakgale C, *et al.* CD8+ T-cell responses to different HIV proteins have discordant associations with viral load. *Nat Med*. 13(1), 46–53 (2006).

274.   Julg B, Williams KL, Reddy S, *et al.* Enhanced anti-HIV functional activity associated with Gag-specific CD8 T-cell responses. *J Virol*. 84(11), 5540–5549 (2010).

275.   Levitz L, Koita OA, Sangare K, *et al.* Conservation of HIV-1 T cell epitopes across time and clades: Validation of immunogenic HLA-A2 epitopes selected for the GAIA HIV vaccine. *Vaccines*. 30(52), 7547–7560 (2012).

276.   Perez CL, Milush JM, Buggert M, *et al.* Targeting of Conserved Gag-Epitopes in Early HIV Infection Is Associated with Lower Plasma Viral Load and Slower CD4 +T Cell Depletion. *AIDS Res. Hum. Retroviruses*. 29(3), 602–612 (2013).